APPLICATION OF LIGNINOLYTIC ENZYMES IN THE PRODUCTION OF BIOFUELS FROM COTTON WASTES

A Dissertation

by

JERSSON EMIR PLACIDO ESCOBAR

Submitted to the Office of Graduate and Professional Studies of
Texas A&M University
in partial fulfillment of the requirements for the degree of

DOCTOR OF PHILOSOPHY

Chair of Committee,	Sergio Capareda
Committee Members,	Zivko Nikolov
	Raghuparty Karthikeyan
	Mark Holtzapple
Head of Department,	Stephen W. Searcy

December 2014

Major Subject: Biological and Agricultural Engineering

ABSTRACT

The application of ligninolytic fungi and enzymes is an option to overcome the issues related with the production of biofuels using cotton wastes. In this dissertation, the ligninolytic fungus and enzymes were evaluated as pretreatment for the biochemical conversion of Cotton Gin Trash (CGT) in ethanol and as a treatment for the transformation of cotton wastes biochar in other substances.

In biochemical conversion, seven combinations of three pretreatments (ultrasonication, liquid hot water and ligninolytic enzymes) were evaluated on CGT. The best results were achieved by the sequential combination of ultrasonication, hot water, and ligninolytic enzymes with an improvement of 10% in ethanol yield. To improve these results, alkaline-ultrasonication was evaluated. Additionally, Fourier Transform Infrared (FT-IR) and principal component analysis (PCA) were employed as fast methodology to identify structural differences in the biomass. The combination of ultrasonication-alkali hydrolysis, hot liquid water, and ligninolytic enzymes using 15% of NaOH improved 35% ethanol yield compared with the original treatment. Additionally, FT-IR and PCA identified modifications in the biomass structure after different types of pretreatments and conditions.

In thermal conversion, this study evaluated the biodepolymerization of cotton wastes biochar using chemical and biological treatments. The chemical depolymerization evaluated three chemical agents ($KMnO_4$, H_2SO_4, and NaOH), with three concentrations and two environmental conditions. The sulfuric acid treatments

performed the largest transformations of the biochar solid phase; whereas, the $KMnO_4$ treatments achieved the largest depolymerizations. The compounds released into the liquid phase were correlated with fulvic and humic acids and silicon compounds.

The biological depolymerization utilized four ligninolytic fungi *Phanerochaete chrysosporium*, *Ceriporiopsis subvermispora*, *Postia placenta*, and *Bjerkandera adusta*. The greatest depolymerization was obtained by *C. subvermispora*. The depolymerization kinetics of *C. subvermispora* evidenced the production of laccase and manganese peroxidase and a correlation between depolymerization and production of ligninolytic enzymes. The modifications obtained in the liquid and solid phases showed the production of humic and fulvic acids from the cultures with *C. subvermispora*.

The results of this research are the initial steps for the development of new processes using the ligninolytic fungus and their enzymes for the production of biofuels from cotton wastes.

DEDICATION

I am dedicating this dissertation to my parents, Blanca Luz and Hernando. Your support and company have been the base of all my accomplishments in life. I also dedicate this work to Sandra Catalina who has been by my side giving me love and support during all this process.

ACKNOWLEDGEMENTS

I would like to thank my mother and my father, who have supported me throughout my life and have always encouraged me to be a successful person. Thanks to my lovely girlfriend, Sandra, who has loved me and showed me things that I had never thought I would experience. I am thankful to my cousin, her husband and his family; they were always there making my days in the United States easier.

I would like to thank my committee chair, Dr. Sergio Capareda and his laboratory, The BioEnergy Testing and Analysis Laboratory. He has given me all the support and help to accomplish all the objectives during my stay at Texas A&M University. I am thankful to all my lab mates, Nam, Jinny, Amado, Monet, Bjorn, Tahmina, and Jewel. All of them were always ready to help me in my research and with my duties. Thanks also go to my friends here in the USA for making my time as an Aggie a great experience. Without you all these years, things would not have been the same.

Additionally, I want to thank my committee members, Dr. Nikolov, Dr. Holtzapple and Dr. Karthikeyan. Special thanks to Dr. Karthikeyan and the Water Quality Engineering Laboratory for their technical and methodological support. I would like to thank the Biological and Agricultural Department faculty and stuff for these years of learning and support.

Many thanks go to the Colombian government and the Fulbright organization who gave me financial support via the FULBRIGHT-COLCIENCIAS grant for my PhD

studies in the USA. Additionally, I would like to thank the LASPAU organization and the sponsored student program for make my life in the United States much easier. Finally, as Gustavo Cerati said

"¡No solo no hubiéramos sido nada sin ustedes, sino con toda la gente que estuvo a nuestro alrededor desde el comienzo; algunos siguen hasta hoy! ¡Gracias totales!"

"Not only we would not have been anything without you, but with all the people that were around us since the beginning; some continue until today! Many thanks!"

NOMENCLATURE

ABTS	2,2'-azino-bis(3-ethylbenzothiazoline-6-sulphonic acid)
AFEX	Ammonia Fiber Expansion
ANOVA	Analysis Of Variance
ASTM	American Society for Testing and Materials
ATC	Autoclave Conditions
C (%)	Carbon percentage
$CaCl_2$	Calcium Chloride
CGT	Cotton Gin Trash
CPT	Cotton Plant Trash
$CuSO_4$ $7H_2O$	Copper Sulphate
DMF	2,6-dimethoxypenol
E	Ligninolytic Enzyme
$Fe(SO_4)_3$	Ferric sulphate
FT-IR	Fourier Transform InfraRed
H (%)	Hydrogen
H_2MoO_4	Molybdic acid
H_2O	Water
H_2O_2	Hydrogen Peroxide
H_2SO_4	Sulfuric Acid
HBT	1-Hydroxybenzotriazole

HNO_3	Nitric Acid
HPLC	High Performance Liquid Chromatography
HW	Hot Water
HW+E	Hot Water+Ligninolytic Enzyme
IR	Infrared
$KMnO_4$	Potassium Permanganate
KH_2PO_4	Potassium Dihydrogen Phosphate
LiP	Lignin peroxidase
$MgSO_4.7H_2O$	Magnesium Sulfate Heptahydrate
Mn	Manganese
MnP	Manganese peroxidase
$MnSO_4$	Manganese sulphate
N (%)	Nitrogen
NaOH	Sodium Hydroxide
NREL	National Renewable Energy Laboratory
O (%)	Oxygen
O_3	Ozone
PAHs	Polycyclic Aromatic Hydrocarbons
PCA	Principal Component Analysis
PDA	Potato Dextrose Agar
PRIN	Principal Components
S (%)	Sulfur

TCI	Cellulose Total Crystallinity Index
U	Ultrasonication
U+E	Ultrasonication+ Ligninolytic Enzyme
U+HW	Ultrasonication+Hot Water
U+HW+E	Ultrasonication+Hot Water +Enzyme
U+HW+E	Ultrasonication + hot liquid water + Ligninolytic enzymes
U-NaOH5%+HW+E	Ultrasonication/NaOH5% + hot liquid water + enzymes
U-NaOH10%+HW+E	Ultrasonication/NaOH10% + hot liquid water + enzymes
U-NaOH15%+HW+E	Ultrasonication/NaOH15% + hot water + enzymes
UV-Vis	Ultraviolet Visible Spectrophotometry
VCM	Volatile Combustible Matter
Vmax	Maximum Velocity
$ZnSO_4.7H_2O$	Zinc sulphate

TABLE OF CONTENTS

Page

LIST OF FIGURES

Page

LIST OF TABLES

Page

CHAPTER I

INTRODUCTION AND LITERATURE REVIEW

INTRODUCTION

Cotton is the principal source of natural fibers for textile industries. It is one of the most abundant sources of agro-industrial biomass with global production of 24 million tonnes (2006−2007) and an annual increase of 2% (Sharma-Shivappa and Chen, 2008)**.** The high level of cotton production generates to the high production of wastes and residues. In the USA, nearly 2.5 million tonnes of waste is produced each year (White et al., 1996). The residues from cotton crop cultivation are of two types: the cotton plant trash (CPT) and the cotton gin trash (CGT). CPT is the residue that stays in the field after the harvest of cotton, whereas CGT is the residue that comes from the ginning process.

With this large quantity of wastes, final disposal is a major problem to the cotton industry, mainly during winter, when insects use these residues as survival sites (White et al., 1996). The conventional disposal method of cotton wastes was incineration which produced several health hazards (Aquino et al., 2010) and environmental pollution (Shen and Agblevor, 2008a). It was regulated by the federal law, making this disposal method economically unachievable. To provide a solution to this disposal problem, cotton wastes have been used in different ways: land filling (Smith et al., 1999), growth of edible fungus (Zervakis et al., 2001), activated carbons production (Klasson et al., 2009; Joan et al., 2007), animal bedding (Grimes et al., 2006 Mar), cellulase production (Tan and

Wahab, 1997), construction materials (Guler and Ozen, 2004), and bio-fuels production (Jeoh and Agblevor, 2001; Aquino et al., 2010).

The transformation of CGT to biofuels is done using thermal and biochemical conversion. Thermal conversion is defined as the biomass transformation in other chemical compounds using high temperatures and pressures at different oxygen conditions. Gasification and pyrolysis processes are the two most important processes inside the thermal conversion. Both processes generate synthesis gas, bio-oil, and biochar; however, the proportions of these three products are completely related with the conditions used. The syngas can be used directly to produce energy (combustion) or liquid fuels using the Fischer-Tropsch process (Leibbrandt et al., 2013). The bio-oil can be upgraded to generate liquid biofuels as gasoline, diesel, or JP8 (Butler et al., 2011). Different from these two is the biochar, which cannot be used to produce biofuels directly. Biochar principal uses are soil amendment (Wu et al., 2012; Mukome et al., 2013; Deal et al., 2012) and activated carbon (Angın et al., 2013; Park et al., 2013). To increase the use of thermal conversion as a competitive energy production strategy from cotton wastes, it is necessary to develop a strategy that transforms biochar in a valuable product.

On the other hand, biochemical conversion transforms using microorganisms or enzymes to produce liquid or gaseous fuels. The principal biofuel produced by biochemical conversion is ethanol; in general, the production of bio-ethanol from lignocellulosic material is based on three principal steps: 1) pretreatment, 2) saccharification, and 3) fermentation. To produce bioethanol from agro-industrial

feedstocks, different kinds of pretreatments have been evaluated. These are generally divided into physical, physicochemical, chemical, and biological (Sarkar et al., 2012). In Cotton wastes, the pretreatment principally used is physicochemical (steam explosion) followed by chemical (acid or basic hydrolysis) and biological (fungal or enzymatic) pretreatment (Shen and Agblevor, 2008b; Silverstein et al., 2007). Current biomass pretreatment processes utilize energy-intense methodologies (high pressures and temperatures) and harsh chemical compounds, which generates undesirable compounds and high cost.

The application of ligninolytic fungi and enzymes is an option to overcome the issues related with biomass pretreatment and biochar uses. In biofuels production, the ligninolytic enzymes have two principal purposes. First, delignification, fungus and enzymes are used alone or with other pretreatments to reduce the lignin content in several feedstocks (Li et al., 2008; Wan and Li, 2010; Lu et al., 2010; Salvachúa et al., 2011; Nigam et al., 2009). Second, the ligninolytic enzymes reduce the toxic compounds present in the biomass hydrolyzates after physicochemical pretreatments (Jönsson et al., 1998; Larsson et al., 1999; Kolb et al., 2012; Palmqvist and Hahn-Hägerdal, 2000; Martín et al., 2002; Chandel et al., 2007)**.** On the other hand, the ligninolytic enzymes and fungi can transform biochar through depolymerization. In this process, ligninolytic enzymes and fungi transform biochar in less recalcitrant compounds that can be consumed by themselves or other organisms. The depolymerization of any type of biochar has not been evaluated before; nevertheless, the depolymerization of low-rank coal has been evaluated using physical, chemical, and biological treatments (Huang et

al., 2013a; Huang et al., 2013b; Hofrichter et al., 1997). The use of an environmental and economically friendly option as the ligninolytic enzymes to replace or improve susceptible parts in the thermal and biochemical conversions can allow an increment in the feasibility and competitiveness of biofuels from biomass versus fossil fuels.

LITERATURE REVIEW

Ligninolytic enzymes

Laccases

The laccases (E.C 1.10.3.2) or benzenediol: oxygen oxidoreductase, *p*-diphenol oxidase belongs to the oxidoreductases class; the redox reaction in this enzyme has four copper molecules that participate in oxygen reduction to produce water (Dias et al., 2007). At the end of the 19th century, Yoshida was the first to extract laccases from exudates of the Japanese tree *Rhus venicifera.* Laccases are wide distributed in bacteria, fungi, insects, and plants, showing in each one a specific function. However, the most referenced and known laccases are from the white root fungi. These fungi use their enzymes to obtain the host nutrients, which are normally protected by the lignocellulosic wall. These fungal enzymes can degrade the complex polyphenol structure that constitutes lignin, the principal recalcitrant component in the lignocellulosic wall. Laccases have the advantages of being extracellular and inducible, they do not require

addition or synthesis of an expensive cofactor; in fact, the cofactor is oxygen which at the same time is the oxidize agent (Sergio, 2006; Couto, S., Toca-Herrera, J., 2006). Additionally, laccases have low substrate specificity, a characteristic that permits them to be used in several industrial and environmental recovery processes (Zouari-Mechichi et al., 2006). All of those characteristics have contributed to generate applications of these biocatalysts in several areas: bioremediation of aromatic recalcitrant compounds (Corvini et al., 2006), treatment of effluents polluted with lignin (Babot et al., 2011), chemical synthesis of compounds, degradation of a wide number of textile dyes (Robinson et al., 2001; Kirby et al., 2000), biomass pretreatment for biofuel production (Moreno et al., 2012), and low-rank coal depolymerization (Hofrichter et al., 1999).

Lignin peroxidase (LiP)

These enzymes were discovered in nitrogen and carbon-limited cultures of *Phanerochaete chrysosporium* (Dias et al., 2007). They belong to the peroxidases subclass (E.C 1.11.1.14), and can catalyze the degradation of a wide number of aromatic structures like veratryl alcohol (3,4-dimethoxybenzyl) and methoxybenzenes inter alia. LiP presents high redox potential (700–1400 mV) and a low optimum pH 3–4.5 (Dias et al., 2007; Piontek et al., 1993; Angel T., 2002). The principal difference between LiP and classic peroxidases is the ability of LiP to oxidize aromatic rings moderately activated by electron donating substitutes; whereas, common peroxidases act over aromatic substrates highly activated such ammine, hydroxyl, etc. How LiP participates in the redox reaction is not clear yet; however, a possible explanation for the ability of attack compounds with

highest redox potential is the production of veratryl alcohol radicals, compounds with higher redox potential than LiP's compounds I and II (Khindaria et al., 1996).

Manganese peroxidase (MnP)

Manganese peroxidases are qualified into the class 1, subclass peroxidase (E.C. 1.11.1.13). They were discovered by Kuwahara in 1984, in batch cultures of *Phanerochaete chrysosporium* (Dias et al., 2007). The active site of MnP shares similar properties with other peroxidases, but its redox potential is low if it is compared with the LiP (Sundaramoorthy et al., 1994). Similar to other heme peroxidases, MnP produces two reactive intermediaries of the enzyme (compounds I and II); however, this enzyme uses the Mn^{2+} from the soils like its favorite electron donor (Sundaramoorthy et al., 1994). The manganese peroxidase reaction oxidizes the Mn^{2+} to Mn^{3+}. The Mn^{3+} is a small compound with high redox power and diffusivity. These abilities allow it to start an inside attack over the plant cell wall, which facilitates the penetration and action of the other enzymes (Angel T., 2002; Hammel and Cullen, 2008). MnP is more specific over reduced substrates; however, it participates in the degradation of several compounds such as textile dyes, low-rank coals, lignin, PAH's, styrene, etc. (Martin, 2002; Mohorčič et al., 2006; Elisashvili et al., 2010; Huang et al., 2013a).

Ethanol production from cotton wastes

In general, the production of bio-ethanol from lignocellulosic material is based on three principal steps: 1) pretreatment, 2) saccharification, and 3) fermentation. In the first step, the aim is to reduce the lignin content in the biomass and make the cellulose and the hemicellulose more available for the saccharification process. The second step is to obtain the monosaccharaides present in cellulose (glucose) and hemicellulose (xylose, arabinose, galactose, and mannose). Finally, fermentation produces bio-ethanol production by microorganisms using the sugars produced during saccharification. Of these processes, pretreatment is the most challenging process because of the complex structure of both lignin and cellulose.

Traditional pretreatment technologies applied to cotton wastes

To produce bioethanol from cotton wastes (cotton gin trash), various pretreatment methods have been used: thermal (steam explosion), chemical, and biological pretreatments. Jeoh and Agblevor (2001) evaluated the use of steam explosion pretreatment for cotton gin waste. They achieved good production of sugars; however, they added a NaOH precipitation post-pretreatment to reduce the inhibitors produced by the steam explosion (Jeoh and Agblevor, 2001). The steam explosion with NaOH post-pretreatment was also used in the work of Agblevor et al., (2003). They found that ethanol production was affected by the feedstock origin, steam explosion severity,

sample heterogeneity, and feedstock composition (Agblevor et al., 2003). Shen et al., (2008, 2011) used a mixture of cotton gin trash and recycled paper sludge, they added paper sludge as an additional sugars source and an inhibitor remover because it contains calcium carbonate (Shen and Agblevor, 2011; Shen and Agblevor, 2008a). The addition of paper sludge allowed the removal of the overlimed post-pretreatment maintaining the same ethanol yields previously observed. The main concern with steam explosion pretreatment is the production of inhibitors; although, paper sludge maybe is a solution, its industrially the availability and transport of paper sludge are issues.

Chemical pretreatments were analyzed to produce ethanol from cotton wastes. Silverstein et al, (2007) evaluate the combination of chemicals (H_2SO_4, NaOH, H_2O_2, and O_3), residence time (30, 60, and 90 min), and reaction conditions (90°C and in an autoclave at 121°C) (Silverstein et al., 2007). Sulfuric acid pretreatment showed the best results under autoclave conditions; this produced high xylan solubilization, low lignin reduction, and higher glucan solubilization. The alkali hydrolysis produced higher lignin reduction (close to 60%), less xylan solubilization, and higher glucan solubilization versus the acid hydrolysis. Using hydrogen peroxide, the lignin reduction was less than the NaOH and slightly better than acid hydrolysis; whereas, opposite behavior was detected in the xylan solubilization. In addition, the ozone experiments produced low levels of lignin degradation and xylan solubilization (Silverstein et al., 2007). The best result was obtained using NaOH in combination with autoclave conditions (cellulose conversion 60%); it was followed by hydrogen peroxide (48% cellulose conversion) and sulfuric acid (23% cellulose conversion).

Another alternative is microbial pretreatment, Shi et al., (2008) evaluated *Phanerochaete chrysosporium* in a solid-state fermentation to reduce the lignin content of cotton wastes. This treatment achieved a lignin degradation of 27.6%, solids recovery of 71.1%, and availability of carbohydrates of 41.6%. These results are good for a cheap process like the solid-state fermentation; however, it has a long processing time that can take around 15 days (Shi et al., 2008). Additionally, Shi et al., (2009) evaluated the effect of microbial pretreatment over cotton stalks in submerged and solid-state fermentations. Both treatments produced high lignin degradation; however, that was not related with the cellulose conversion which was less than 20% (Shi et al., 2009).

Ligninolytic enzymes in bioethanol production

Delignification

One of the most important difficulties in the production of biofuels from lignocellulosic material is lignin removal. For that reason, ligninolytic fungi and their enzymes have been to pretreat different feedstocks with the intention of modifying the lignocellulose structure of those biomasses (Vivekanand et al., 2008; Wan and Li, 2011; Salvachúa et al., 2011). The use of ligninolytic enzymes in delignification process have been made in three different ways: 1) microbial delignification, 2) enzymatic delignification, and 3) laccase-mediator system delignification. Microbial delignification uses the entire microorganism for delignification. It can be performed with the target biomass in a submerged culture (Lu et al., 2010; Martín-Sampedro et al., 2011) or in

solid-state fermentation (Salvachúa et al., 2011; Wan and Li, 2010). Both cultivations have produced good delignification percentages; however, this is not always related to high glucose yields. The principal problem related with the microbial pretreatment is the long processing time needed compared with the other pretreatment technologies (Nigam et al., 2009). The period of time taken by the microorganisms to obtain high delignification percentages normally is not less than 15 days and can be up to 40 or 50 days (Wan and Li, 2011; Lu et al., 2010). However, this period will depends on the specific strain used.

Enzymatic delignification employs enzymatic extracts, purified or semi-purified enzymes, and commercial or native ligninolytic enzymes (Mattinen et al., 2011). Laccase is the principal enzyme used followed by MnP and LiP. However, some delignification pretreatments have been done by mixtures of two or three different ligninolytic enzymes (Costa et al., 2005; Archibald et al., 1997) Enzymatic processes has the same delignification percentages than microbial pretreatment; however, enzymatic processes need less time (between 24 and 96 h) than microbial pretreatment. Besides, the reduction in processing time, this methodology has two principal problems. First, the high costs, and second, the need to improve the process time to compete with the conventional pretreatments (Nigam et al., 2009). The use of fungal laccases in presence of redox mediators is known as *laccase-mediator system*. Redox mediators are chemical compounds, which act as electron carriers between the enzyme and the final substrate (Babot et al., 2011). The most used mediator compounds are 1-hydroxybenzotriazole (HBT), 2,2'-azino-bis(3-ethylbenzothiazoline-6-sulphonic acid) (ABTS), and some

natural mediators like syringaldehyde or vanillin. The principal application of laccase-mediator system is in paper industry for bleaching and delignification. However, this system has been used for delignification of some biofuels feedstocks as elephant grass, eucalypt wood, corn stover, wheat straw (Qiu and Chen, 2012; Chen et al., 2012; Gutiérrez et al., 2012).

Detoxification

Some of the conventional biomass pretreatment technologies have the disadvantage of producing toxic compounds from the plant cell wall components. These toxic compounds affect the efficiency of fermentative microorganisms and cellulolytic enzymes, which generates an overall ethanol yield reduction (Moreno et al., 2012). The detoxification process employs different strategies such as chemical, physical and biological. The biological detoxification process utilizes ligninolytic fungi or their enzymes with the intention of reduce the inhibition produced by the toxic compounds produced in the pretreatment (Chandel et al., 2007). The detoxification process is generically after pretreatment and can take normally between 1 to 12 h (Martín et al., 2002; Kolb et al., 2012; Jurado et al., 2009; Chandel et al., 2007). The detoxification process increase ethanol yields of 1–7 fold when phenolics are removed via laccases and 2–fold increase when phenolics, furans and acids were removed using ion exchange treatment (Chandel et al., 2007). The use of ligninolytic enzymes detoxification can reduce the cost of lignocellulosic ethanol production by using the complete slurry from

the pretreatment process, which will increase fermentation rates and ethanol yields (Moreno et al., 2012).

Enzymatic methodologies involve fastest reaction rates, higher specificity, and yield conversion compared with the same chemical reaction. In that way, ligninolytic enzymes offer a solution to biofuel industries because these enzymes have high redox potential, synergistic behavior, and can catalyze a wide number of substrates. However, this enzymatic option has been less studied than other methodologies employed in biofuels production and its cons and pros need to be considered. Delignification and detoxification processes have been done using microbial and enzymatic processes. In both methodologies the pros observed are: positive environmental impact, high delignification and detoxification, low sugar losses, and the possibility of develop a consolidate process. Nevertheless, these processes present different cons; one of these is the lack of modification in cellulose structure which is observed in both methodologies. Additionally, the cons of enzymatic process are high costs, low commercial availability, and mediator necessity. Unfortunately, in microbial methodology the principal limitation is the long time that this process takes. Besides the limitations and qualities, ligninolytic enzymes could be in a future a competitive option to conventional chemical and physical process used in biofuel production.

Cotton wastes thermal conversion

One of the most important technologies to produce energy from biomass is the thermal conversion. Thermal conversion is the biomass transformation in other chemical

compounds using high temperatures and pressures at different oxygen conditions. Gasification and pyrolysis processes are the two most important processes inside the thermal conversion. The first process is conducted at temperatures higher than 700 ºC and small oxygen quantities. On the other side, pyrolysis is conducted at lower temperatures (400–600ºC) and higher pressures, but with the complete absence of oxygen. In both processes, the final products are synthesis gas, bio-oil, and biochar; however, the proportions of these three products are completely related with the conditions used. The syngas can be used directly to produce energy (combustion) or liquid fuels using the Fischer-Tropsch process (Leibbrandt et al., 2013). The bio-oil can be upgraded to generate liquid biofuels as gasoline, diesel or JP8 (Butler et al., 2011). Whereas, the principal uses of biochar are soil amendment (Wu et al., 2012; Mukome et al., 2013; Deal et al., 2012) and activated carbons (Angın et al., 2013; Park et al., 2013).

The gasification of cotton wastes, as cotton gin trash and cotton plant trash, has been studied by different researches from laboratory scale to trailer-mounted gasification systems (Kantarelis and Zabaniotou, 2009; Capareda and Parnell, 2007; Karatas et al., 2013; Maglinao Jr. and Capareda, 2010; Maglinao and Capareda, 2008). All this studies showed the gasification as an alternative for power production from cotton wastes. The principal product from cotton wastes gasification is syngas (80–90%); nevertheless, 10 to 20% of the biomass is converted to biochar (Capareda and Parnell, 2007; Sadaka, 2013). Pyrolysis of cotton wastes is still in laboratory scale and the production of bio-oil, syngas, and biochar depends of the residence time of the biomass in the pyrolyzer (fast, intermediate, slow). Fast and slow pyrolysis helps the production of bio-oil and slow

pyrolysis increases the biochar production. Independent of the type of pyrolysis, biochar is going to be produced in quantities surrounded 12–35% of the original biomass (Kantarelis and Zabaniotou, 2009; Pütün et al., 2005; Zabaniotou et al., 2000). As described earlier, biochar is the final waste generated from the cotton wastes thermal conversion and there is not a process that can use effectively this byproduct besides the uses as soil amendment or activated carbon. This process is necessary to increase the competitiveness of any thermal conversion process.

Biochar depolymerization

A new option for biochar utilization is biochar depolymerization, biochar has a carbon content among 20 to 40%; however, it cannot be directly consumed by microbes or other organisms. To make this carbon available for consumption, it is necessary to depolymerize the biochar in less recalcitrant compounds that can be consumed by other organisms. The depolymerization of any type of biochar have not been evaluated before; nevertheless, the depolymerization of low-rank coal has been evaluated using physical, chemical, and biological treatments (Huang et al., 2013a; Huang et al., 2013b; Hofrichter et al., 1997). Low-rank coal can be related to biochar especially because presents similar structure and compositions. Huang et al., (2013a) depolymerized coal using potassium permanganate ($KMnO_4$), as chemical agent to increase the carbon bioavailability. After that treatment, the liquid phase was used in aerobic and anaerobic cultures producing biomass and biogas. Huang et al., (2013b) used a mixtures of chemical pretreatments (HNO_3, H_2O_2, $KMnO_4$, and NaOH) and enzymatic reactions (manganese peroxidase) to

depolymerize the coal with the objective to increase production of biogenic methane. The use of chemical and enzymatic combined treatments enhanced coal depolymerization, which generates different types of chemical products.

Microbial processing is other approach of coal depolymerization. In this case, microorganisms depolymerize coal using enzymatic and non-enzymatic mechanisms; the non-enzymatic mechanisms include production of alkaline substances and chelators. *Bacillus* sp. Y7 was capable of solubilize around 40% of lignite in 12 days; this process was performed by producing alkaline substances that facilitate coal transformation (Jiang et al., 2013). Quigley et al., (1988) evaluated several bacterial and fungal strains, and found that *Streptomyces setonii* could depolymerize coal by generating an alkali medium (Quigley et al., 1988). On the other hand, the enzymatic approach employs ligninolytic microorganisms or extracts from ligninolytic enzymes, these microorganisms are able to solubilize low-rank coal into different type of products such as humic and fulvic acids. Selvi et al., (2009) evaluated the depolymerization of three types of low-rank coal (lignite, sub-bituminous, bituminous) and different fungal strains. They found *Pleurotus djamor* as the most effective strain to depolymerize lignite and an inverse relation between the rank of coal and the depolymerization (Selvi et al., 2009). *Phanerochaete chrysosporium* transform 85% of the coal in smaller molecules, this transformation was mediated by the production of lignin and manganese peroxidases. Additionally, this study found a relation between the fungal depolymerization and the use of low-nitrogen media (Ralph and Catcheside, 1994). *Nematoloma frowardii* b19 and *Clitocybula duseni* b11 were utilized to degrade low-rank coal. Both degraded of coal humic substances.

The reaction showed an 80% of discoloration and the formation of yellowish products. Moreover, the research showed how the manganese peroxidase has an important role in degrading humic substances (Hofrichter et al., 1999). The coal solubilization has been evaluated in different reactor configurations (stirred tank, fluidized bed, and packed bed reactors). The best configuration was the stirred tank with a coal weight loss of 24.2%, followed by the fluidized bed and packed bed reactors. The study also found the packed bed as an inadequate reactor for fungal coal depolymerization because fungal accumulation creates pressure drops and clogs (Oboirien et al., 2013). *Trichoderma atroviride* was evaluated in a slurry bioreactor to depolymerize low-rank coal. In this study, the coal particle size and the initial load was evaluated. The highest depolymerization (28%) was achieved at particle size of 150–300 μm and 5% of coal initial load. In addition to fungal depolymerization of coal, some studies analyzed the fungal degradation of humic acids, fulvic acids, and some organic compounds. Claus and Filip (1998) evaluated the degradation of humic acids by *Cladosporium cladosporioides*, these fungi degraded around 60% of these substances, and this consumption was achieved by the production of ligninolytic enzymes. The crude extracts achieved low degradation, but when they were in presence of a redox mediator, the degradation achieved 50% (Claus and Filip, 1998). The use of extracts of manganese peroxidase from *Clitocybula dusenii* b11 were evaluated in the transformation of humic acids into low-molecular weight fulvic acids. The in-vitro depolymerization system achieved degradations from 50 to 71% in 168 h (Ziegenhagen and Hofrichter, 1998).

RESEARCH OBJECTIVES

This project wanted to increase the feasibility of produce biofuels from cotton wastes. Seeking that, this project proposed the evaluation of ligninolytic enzymes as an option to employ raw cotton wastes and cotton wastes thermal conversion byproducts as substrates to produce biofuels or other types of compounds. To do that, the objectives of the research follow:

- To determine the adequate pretreatments combination among ultrasonication, hot liquid water and ligninolytic enzymes that permit obtain the best ethanol production from cotton wastes.
- To evaluate the effect of alkaline-ultrasonication pretreatment in the ethanol production from CGT and the application of FTIR spectroscopy and principal component analysis as tools for fast analysis of CGT structure modifications.
- To select the best chemical treatment that can depolymerize the cotton wastes biochar and identify and characterize the modifications generated in the biochar liquid and solid phases after the chemical depolymerization.
- To select the best ligninolytic microorganism that can depolymerize the cotton wastes biochar and identify and characterize the modifications generated in the biochar liquid and solid phases after the biological depolymerization.

CHAPTER II

EVALUATION OF LIGNINOLYTIC ENZYMES, ULTRASONICATION AND LIQUID HOT WATER AS PRETREATMENTS FOR BIOETHANOL PRODUCTION FROM COTTON GIN TRASH*

INTRODUCTION

Cotton is the principal source of natural fibers for textile industries. It is one of the most abundant sources of agro-industrial biomass, with a production of 24 million tonnes in the world in 2006−2007 and an annual increase of 2%. In the USA, cotton production was nearly 4.1 million tonnes in 2007. The US crop 25%is in Texas, which represents over 6 million acres of cotton plants and a production of 4 million bales per year (USDA, 2008).

The high level of cotton production is directly related to the high production of wastes and residues. In the USA, nearly 2.5 million tonnes of waste is produced each year (White et al., 1996). The residues from cotton crop cultivation are of two types: cotton plant trash (CPT) and cotton gin trash (CGT). CPT is the residue that stays in the field after the harvest of cotton, whereas CGT is the residue that comes from the ginning process. Of these two types of wastes, CGT is very important to researchers and cotton producers because of the high production and the difficulties of disposing of it.

---

*Reprinted with permission from "Evaluation of ligninolytic enzymes, ultrasonication and liquid hot water as pretreatments for bioethanol production from cotton gin trash" by Plácido, J., Imam, T., Capareda, S., 2013. Bioresource Technology, 139, 203-208, Copyright 2013 by Elsevier

CGT is composed of pieces of sticks, leaves, bolls and soil cleaned from lint during the ginning operation. About 218 kg of cotton fiber generates 68−91 kg of CGT. Worldwide, the production of this waste is approximately 3.23 million tonnes per year (Jeoh and Agblevor, 2001). The USA produces about 1.8 million tonnes of CGT; Texas has an average of 800 tonnes of cotton gin trash in its 30 principal counties.

With this large quantity of wastes, final disposal is a major problem for the cotton industry, mainly during winter, when insects use these residues as survival sites (White et al., 1996). The conventional disposal method of CGT was incineration, which produced several health hazards and environmental pollution (Shen and Agblevor, 2008a). It was regulated by the federal law, making this disposal method economically unachievable. To solve this disposal problem, CGT has been used in different ways: in land filling, composting, microbial gum production, growth of edible fungus, activated carbon production, construction materials, and biofuel production (M. A. Macias-Corral et al., 2005).

The lignocellulosic material from CGT can be used for biofuel production. Lignocellulose is a polysaccharide combination of cellulose, hemicellulose, and lignin which are the dominant components of the plant cell wall. Lignocellulose is more than 60% of the organic matter of the plant species in the earth. Lignocellulosic material is considered the most abundant source of organic material from the wastes of agro-industrial activities. Use of this biomass to produce renewable energy has been investigated specifically in areas of pyrolysis, biogas, and bioethanol production.

Bioethanol is one of the most important bio-fuel products that can be produced from lignocellulosic material, such as CGT. By 2020,The United States regulation requires producing 36 billion gallons of biofuels, including 21 billion gallons from lignocellulosic material or other advanced fuel technologies. This regulation opens opportunities to develop new processes and to improve existing processes for biofuel production. In general the production of bio-ethanol from lignocellulosic material is based on three principal steps: 1) pretreatment, 2) saccharification, and 3) fermentation. In the first step, the aim is to reduce the quantity of lignin present in the biomass and make the cellulose and the hemicellulose readily available for the saccharification process. The second step is to extract the monosaccharides present in the cellulose (glucose) and the hemicellulose (xylose, arabinose, galactose and mannose). Finally, microbial fermentation of the sugars produced during saccharification yields bioethanol. The three step process can be modified to improve the yield of bioethanol from lignocellulosic biomass.

The objective of this chapter is to determine the best pretreatment combinations among ultrasonication, hot water, and ligninolytic enzymes to generate the highest increment in the cellulose conversion and ethanol yield in the saccharification and fermentation processes.

MATERIAL AND METHODS

Raw material

Samples of CGT were obtained from the Varisco Cotton Gin near College Station, Brazos County, Texas. The CGT samples were ground in a Wiley mill to obtain an average particle size of approximately 1 mm in diameter. This particle size reduction is important for successive pretreatment processes by ensuring uniform feedstock size.

Enzymes

The ligninolytic enzymes pretreatment used commercial laccase mediator systems PrimaGreen® EcoFade LT100 from Genencor International. This system is composed principally by a laccase from modified strains of *Cerrena unicolor* and the mediator 3,5-dimethoxy-4-hydroxybenzonitrile among other support components. The saccharification process was developed using the combination of 2 types of commercial enzymes from Genencor Inc. Accellerase 1500 is a cellulases complex and Accellerase XY is a hemicellulases enzyme complex. Both are produced with genetically modified strains of *Trichoderma reesei*. The first one has endoglucanase activity (2200–2800 carboxymethycellulose Units/g) and beta-glucosidase activity (525–775 pNPG Units/g) whereas the second one has xylanase activity with (20000–30000 acid birchwood xylanase units (ABXU)/g). The reported activities showed were given by Genencor Inc.

Pretreatments

In this research, three different pretreatments (ultrasonication, hot water and ligninolytic enzymes) and their combinations were evaluated to obtain the best ethanol production from CGT. The ultrasonication process was performed on a solution of 10% CGT biomass solids using an ultrasonicator (Hielscher Ultrasonic Processors, Ringwood, NJ, USA). The hot water pretreatment was performed in an autoclave using Erlenmeyer flasks with a solution of 10% solids at 121°C, 1.02 Atm for 1 h. The ligninolytic enzymes pretreatment used commercial laccase mediator systems PrimaGreen® EcoFade LT100 from Genencor International. These enzymatic reactions took place in 250mL Erlenmeyer flasks with 50 mL of phosphate buffer 25mM pH 6, an initial enzyme load of 3 g with a laccase activity of >5700 Genencor Laccase Units/g (enzymatic activity provided by Genencor), with 10% solids of CGT at 30°C, 150 rpm for 96 h in an incubator shaker (Innova, New Brunswick Scientific, NJ). The seven pretreatments evaluated follow; hot water (HW), ultrasonication (U), enzyme (E), ultrasonication+hot water (U+HW), ultrasonication+enzyme (U+E), hot water+enzyme (HW+E), ultrasonication+hot water +enzyme (U+HW+E). The experimental design was completely randomized with three replicates, using cellulose conversion and ethanol yield as response variables.

Saccharification process

The pretreated biomass samples were enzymatically hydrolyzed using the combination of two types of commercial cellulases from Genencor Inc.; Accellerase

1500, and Accellerase XY. The experiment had an initial enzyme loading of 10.45 mg protein/g of biomass of Accellerase 1500 + 1.29 mg protein/g of biomass of Accellerase XY. The process was performed in 250mL Erlenmeyer flasks with 50 mL of a solution of 50mM sodium acetate buffer at pH 4.8 for 96 h at 50°C and 125 rpm in an incubator-shaker (Innova, New Brunswick Scientific, NJ). After saccharification, the samples were centrifuged at 13,000 rpm for 20 minutes, and the supernatants were filtered through 0.5 μm hydrophilic PTFE syringe filters (Millipore, Billerica, MA). These samples were then analyzed for glucose, mannose, xylose, arabinose, galactose, and cellobiose, using high performance liquid chromatography (HPLC). The efficiency was calculated by comparing sugars yield (g) before and after enzymatic hydrolysis using the next equation:

$$\%\ \text{glucose conversion} = [c \times V/m] \times 100\%$$

Where *c* is the concentration (g/L) of sugars in the sample hydrolyzed as determined by HPLC, *V* is the total volume (L) hydrolyzed, *m* is the initial weight (g) of glucose or xylose determined through the NREL's protocols. The statistical analysis was made using three repetitions for a one way Anova and the Duncan´s multiple range test in the statistical software SAS system 9.0.

Fermentation process

The enzymatic hydrolyzate used for fermentation was inoculated with Ethanol Red (*Saccharomyces cerevisiae)* provided by Fermentis (Lesaffre Yeast Corp., Milwaukee, WI). The strain was activated using 0.5 g of dry yeast in 10 mL of the

inoculum broth. The composition of the inoculum broth was 0.2 g glucose, 0.05 g peptone, 0.03 g yeast extracts, 0.01 g KH_2PO_4, and 0.005 g $MgSO_4 \cdot 7H_2O$. The inoculums were shaken at 200 rpm in an incubator shaker at 38 °C for 25–30 min. The fermentation process was made in 125 mL Erlenmeyer flasks with 50 mL of the slurry supplemented with 0.3 g of yeast extract. The slurry was then incubated with 1 mL of freshly activated dry yeast (Ethanol Red) and run for a period of 72 h at 32 °C, pH 4 and 100 rpm. After the fermentation process, the treatment samples were centrifuged at 12,000 rpm for 15 min, and the supernatant was filtered through 0.5µm hydrophilic PTFE syringe filters (Millipore, Billerica, MA) and injected in the HPLC to perform the ethanol quantification. The ethanol yield was calculated from the ratio between the average produced ethanol and the theoretical ethanol production of 51.1 g of ethanol generated per 100 g of glucose in the biochemical conversion of the sugar. The response variable was the ethanol yield and was analyzed using the software SAS system 9.0 employing one way ANOVA and the Duncan´s multiple range test.

Analytical methods

To determine the structural composition of the CGT biomass before and after the pretreatments, the analytical protocols developed at the National Renewable Energy Laboratory (NREL) of the US Department of Energy were followed. This entailed determination of the following: (a) total solids in biomass and total dissolved solids in liquid process samples (b) extractives in biomass, and (c) structural carbohydrates and lignin in biomass (Sluiter et al., 2011). Fourier Transform InfraRed (FT-IR)

spectroscopy (Shimadzu, IR Affinity–1 with a MIRacle universal sampling accessory) was used to evaluate the structural properties of the CGT with and without pretreatments. The infrared spectra were collected in a range of 4000 to 700 cm^{-1} with resolution of 4 cm^{-1}. The analyzed compounds and their IR wave numbers are given in Table 1. To evaluate the cellulose conversion and the ethanol yield the samples were injected in a HPLC (Waters 2690, Separations Module, Waters Corporation, Milford, MA) equipped with auto sampler, a Shodex SP 810 packed column and a Refractive Index (RI) detector. Each sample was run for 25 min at a flow rate of 1 mL/min, 60°C using HPLC water as a mobile phase.

Table 1. Wave numbers of IR vibration frequencies used for CGT characterization.

Compound	Functional group	Wavenumber (cm^{-1})
Cellulose	β-D-cellulose	898
Cellulose	Intense polysaccharide	1030, 1050
Cellulose	C–O–C anti-symmetric stretch (β–1,4 glycosyl)	1170–1150
Lignin	Phenolic OH region and aliphatic CH stretch	1370
Lignin	Aromatic skeletal vibration and CH deformation	1514,1595
Hemicellulose	Ester carbonyls, C=O	1240, 1732

RESULTS AND DISCUSSION

Biomass characterization

Structural compositional analysis from the pretreated CGT and control (without pretreatment) from the Varisco Cotton Gin are shown in Table 2. The total extractives in the CGT samples were high (19.56%), where water extractives were 10−12% and such water extractive data has not been evaluated in other CGT studies. The ethanol extractives (8−10%) agreed with the values found in other CGT research studies which normally are between 7.9−14%. The biomass pretreated by HW, U+HW+E, HW+E, and U+HW showed 5 to 7% reduction in the extractives, and these reductions were principally related to the decrease in the water extractives. The ethanol extractives from these pretreatments were 3−5%. These results agreed with values reported by Bajwa et al., (2011), who analyzed the cotton linters, cotton burrs, and sticks separately.

In the control CGT sample, the acid insoluble material was 25.5%. The pretreated biomass presented a lignin decrease in almost all the pretreatments with the exception of HW whose lignin content was slightly increased. The two highest reductions in lignin content were by U+HW+E and HW+E pretreatments. In these cases, the enzymatic pretreatment benefited from the initial HW step, which facilitated the catalysis of the ligninolytic enzymes. However, not all the acid insoluble material corresponded to lignin, because the different compounds like cottonseed, small leaf, and the hulls present in the CGT, and can produce other acid insoluble compounds (Agblevor et al., 2006).

Table 2. Structural composition of untreated and pretreated cotton gin trash (CGT).

Compound	CGT	U+HW+E	HW	HW+E	U+HW	U	U+E	E
Water and ethanol extractives (%)	19.6	15.3	12.7	15.51	13.1	15.3	18.5	18.3
Acid insoluble material (%)	25.5	22.9	26.5	22.8	24.0	25.8	25.5	24.3
Arabinose (%)	1.5	1.2	1.7	1.4	1.9	1.5	1.7	1.6
Xylose (%)	5.7	5.7	6.4	5.6	6.4	5.5	5.7	5.9
Mannose (%)	1.1	1.4	1.2	1.3	1.4	1.3	1.4	1.2
Galactose (%)	1.7	1.6	1.9	1.4	2.6	1.7	1.6	2.1
Glucose (%)	24.9	29.6	32.1	26.5	30.5	25.7	25.6	26.3
Ash (%)	10.7	10.3	11.8	12.9	11.9	11.7	11.8	11.4

The value obtained for lignin (25%) is comparable to the values obtained from previous studies of cotton wastes. Agblevor et al., (2006) reported lignin content of 21 to 24% for CGT samples from four different gins; a higher lignin content was found in the studies with cotton stalks, where lignin contents were 30.1% and 27.8%, respectively (Silverstein et al., 2007; Akpinar et al., 2007). Lower lignin contents were found in the studies of Bajwa et al., (2011) in cotton linters (8.9%) and Philippoussis et al., (2001) in cotton wastes (10.15%); however, these two wastes were composed of less recalcitrant

parts of CGT, which explains their low lignin content (Philippoussis et al., 2001; Bajwa et al., 2011). The greatest decrease in the lignin content was in U+HW+E and HW+E pretreated biomass. It was similar to the values found using steam explosion in CGT (Jeoh and Agblevor, 2001), ozonation pretreatment (Silverstein et al., 2007), and lower than alkali (Silverstein et al., 2007), and microbial pretreatment (Shi et al., 2009) of cotton stalks.

The total carbohydrates content (35%, i.e., sum of all sugars) in the control CGT was similar to the study of Agblevor et al., (2006) for Suffolk and Emporia gins with 37% and 35% respectively. Additionally, xylose and glucose percentages corresponded to the values found in those gins. However, carbohydrates content (35%) is less than the ones obtained from Jeoh and Agblevor, (2001); 57% from Southside gin, Philippoussis et al. (2001); 52.52% from cotton wastes, and Bajwa et al., (2011); 86.9% from cotton linters. The HW pretreated biomasses presented a similar increment in the carbohydrates percentages, if they are compared against microbial (Shi et al., 2008), chemical (Silverstein et al., 2007), and steam explosion pretreatments (Agblevor et al., 2006). However, the total carbohydrates content, (35%) from this work were less than previous studies because the control biomass had lower quantities of carbohydrates (35%) compared to the control biomass from other studies. An explanation for the reduction in glucose content in the Varisco cotton gin´s CGT is related to the presence of more hulls, small leaf, high ash, and seeds, which are components richer in acid insoluble materials, and lower cellulose content than other CGT components (Agblevor et al., 2006). The xylan content was slightly increased by HW and U+HW pretreatments; also, in the other

pretreatments the xylan content was almost the same as the control CGT. The HW pretreatment was responsible for hemicellulose modification, which increased xylan availability (Laser et al., 2002). To increase the carbohydrates content in the original biomass, it is necessary to evaluate different seasons from the sampling area to avoid the variability that exists in CGT, which can be close to 30% (Agblevor et al., 2006). This difference is perhaps caused by the diversity between the feedstocks, the ginning method, and the sampling method (Agblevor et al., 2006).

FT-IR was used in this study to identify the structural changes presented in the CGT biomass after the different pretreatments (Figure 1). The analyzed peaks (Table 1) were seen in the control and pretreated samples of CGT, and any new strong peak appeared in the samples' spectra. The highest peaks in all the samples were the ones related to cellulose (1030, 1050, and 1170–1150 cm^{-1}), which also had the highest variation among the pretreatments. The principal variation in the cellulose peaks was presented in the 1030 and 1050 cm^{-1} peaks. These pretreatment peaks increased the strength of the signal compared with the control CGT; however, the enzymatic pretreatment obtained the same or lower values than the non-modified CGT. The HW pretreatments showed the highest differences in signals compared with the biomass without pretreatment. The pretreatment with the highest signals in the cellulose related peaks were the HW pretreatment, followed by U+HW, U+HW+E, and HW+E. Additionally, these pretreatments reduced the crystallinity index (A1430/A898) of the original CGT biomass by 22–26%, and these percentages were greater than those of

Goshadrou et al., (2011) for sweet sorghum bagasse (12−15%) using NaOH ultrasonication.

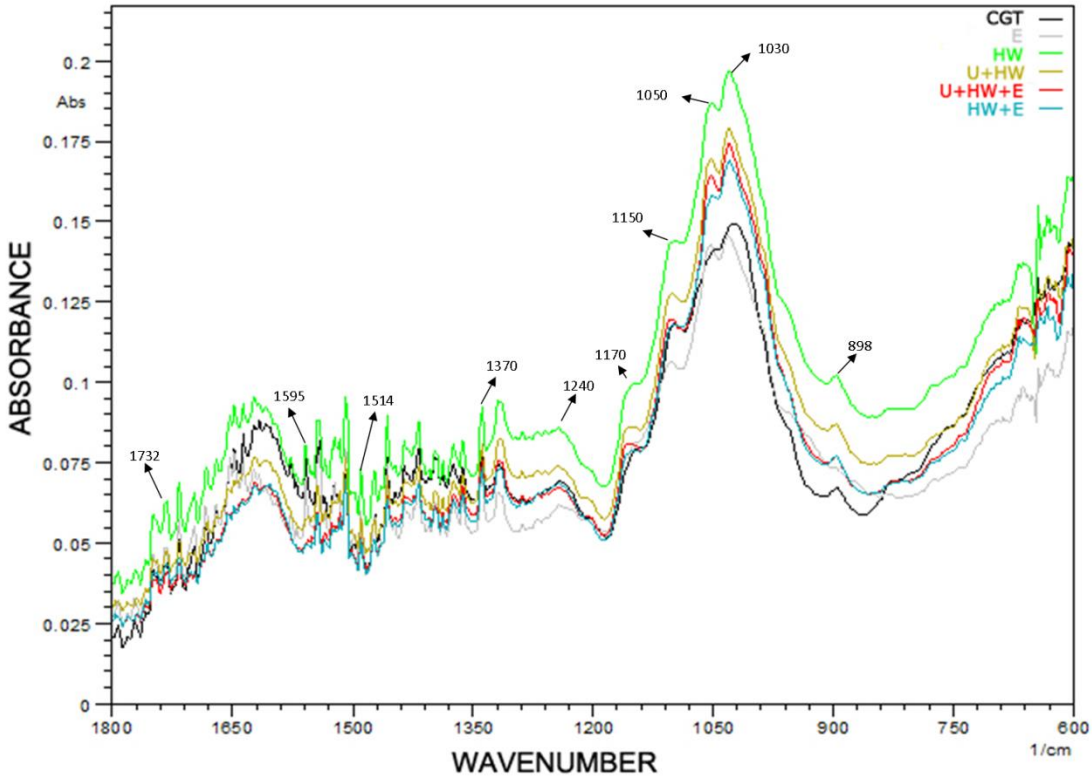

Figure 1. FT-IR spectra of pretreated and unpretreated CGT.

The absorption of the lignin informational peaks (1370, 1514, and 1595 cm^{-1}) was reduced in all the pretreated biomasses except for the biomass pretreated by HW, which increased the absorbance of these peaks. Similarly, absorbance increase after a pretreatment in the lignin signals has been observed in wheat straw after AFEX

pretreatment (Lee et al., 2010). The greatest reductions in lignin signals resulted from U+HW+E and HW+E pretreatments, which had a reduction in all the signals (1370, 1514, 1595 cm^{-1}) related to the lignin structure of CGT. The reduction in the lignin signals were principally observed in the 1595 cm^{-1}. This reduction is related to the modification in the lignin aromatic skeletal structure generated in the pretreatments mixture. Additionally, the enzymatic pretreatments made an important reduction in the bands of 1370 cm^{-1}, where the band was associated with the phenolic OH region of lignin. The reduction from the ligninolytic enzyme pretreatments can be explained by the laccases high affinity for phenolic compounds (Dias et al., 2007), which permit them to easily catalyze these phenols and modify this zone of the lignin structure. The 1514 cm^{-1} band was only reduced by the U+HW+E and HW+E pretreatments. This decrease shows positive interaction between the two pretreatments, and was not seen when HW or E was used alone. The decay of this signal has been connected with delignification in cellulose nanofibers production (Chen et al., 2011) in this research.

The hemicellulose signals showed the most variable behavior. In the 1240 and 1732 cm^{-1} signals, the U+HW and HW pretreatments presented an increment in the absorbance. The U+HW+E and HW+E pretreatments presented a signal reduction in the signal of 1732 cm^{-1}, and any effect over the 1240 cm^{-1}. The other pretreatments increased the 1732 cm^{-1} signal with a reduction at 1240 cm^{-1}. The variation in the signal intensity of 1732 cm^{-1} can be related to major exposure of the hemicellulose in the CGT biomass, which increased the absorption in the spectrum. This major exposure can be explained as the pretreatments resulted in modification of the hemicellulose structure or

disrupted some of the linkages between the hemicellulose and cellulose or lignin. Also, the reduction in this signal can be related to the releasing of sugars from the hemicellulose in the liquid medium and propitiate a reduction of this signal in the biomass. This kind of reduction in hemicellulose was also found in acid hydrolysis of cotton stalks (Silverstein et al., 2007).

Pretreatment evaluation

The evaluation of the pretreatment processes was made by the cellulose conversion to glucose and the ethanol yield from cellulose. The cellulose conversion was evaluated based on the effect of different pretreatments on the structures of the lignin, and the cellulose conversion to glucose after the saccharification process. In this response variable, the treatment averages for the cellulose conversions were statistically significant ($p < 0.05$), and the Duncan's test was used to evaluate the differences presented among the different pretreatments (Table 3). The highest cellulose conversion was achieved using the U+HW+E combination (Figure 2) with a 23.4% of cellulose conversion, followed by HW (16.6%), HW+E (16.0%), and U+HW (14%). The cellulose conversion and the increment in the intensity in the cellulose signals observed in their FT-IR spectrum, in comparison to the control CGT showed the importance of HW pretreatment to modify the cellulose structure, and increase the cellulose conversion. The ultrasonication pretreatment presented an intermediate action with an average cellulose conversion of 11.8%. The enzymatic pretreatment alone showed no significant difference in cellulose conversion compared to the untreated CGT biomass.

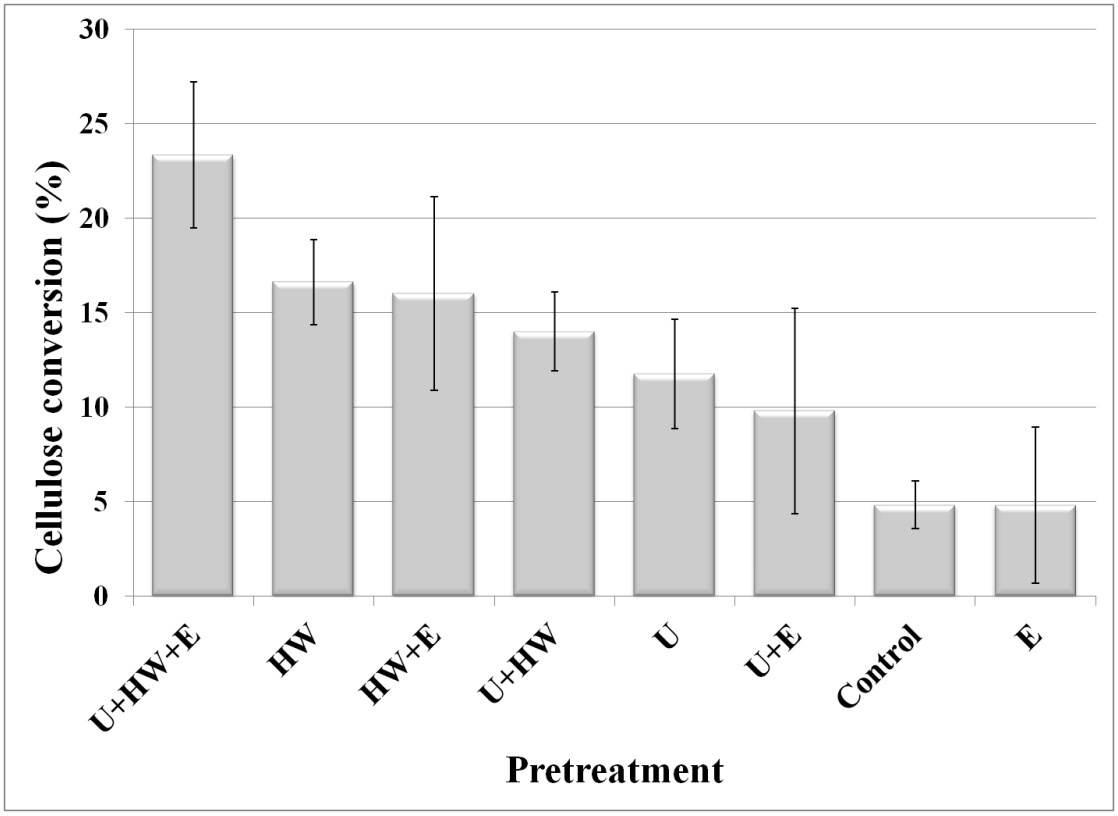

Figure 2. Bar plot for the cellulose conversion for each pretreatment process[1].

The cellulose conversion obtained by the U+HW+E combination (23.4%) on CGT presented better results than microbial pretreatment (18%) (Shi et al., 2009) and same results as sulfuric acid pretreatment (Silverstein et al., 2007), both over cotton stalks. However, these values are quite low compared to those reported in literature for CGT, where the conversion is between 40% and 80% when steam explosion pretreatment was used (Jeoh and Agblevor, 2001; Agblevor et al., 2003).

[1] In this dissertation, error bars correspond to each treatment standard deviation

Table 3. Duncan's multiple range test for the ethanol yield and cellulose conversion.

Pretreatment	Cellulose conversion (%)	Duncan´s Statistic[1]	Pretreatment*	Ethanol yield (%)	Duncan´s Statistic[1]
U+HW+E	23.4	A	U+HW+E	31.6	A
HW	16.6	B	HW	22.2	B
HW+E	16.0	BC	HW+E	21.6	B
U+HW	14.0	C	U+HW	18.5	C
U	11.8	C	U	15.7	C
U+E	9.80	C	U+E	13.3	C
Control	4.82	D	E	6.54	D
E	4.81	D	Control	6.45	D

1- Means with the same letter are not significantly different from each other

The difference between steam explosion and the U+HW+E combination is principally the severity of the physical pretreatment. Steam explosion presents higher severity because it has higher temperatures and higher pressures than hot water pretreatment. The importance of severity in cellulose conversion has been confirmed in different research studies, where severity was related to better structural transformation of lignin and cellulose in cotton residues (Jeoh and Agblevor, 2001; Silverstein et al., 2007). The need of a pretreatment before laccase-mediator systems to increase the cellulose conversion and delignification percentage has been studied using wheat straw, *Eucalyptus globulus* and *Hesperaloe funifera*, where all biomass needed a previous

steam explosion pretreatment (Qiu and Chen, 2012; Martín-Sampedro et al., 2011; Martín-Sampedro et al., 2012). Additionally, in wheat straw a previous silage step was necessary to increase the effectiveness of the laccase-mediator system (Chen et al., 2012). These studies found it impossible to accomplish significant lignin reduction and cellulose conversion with the laccase-mediator system alone, similar to the results obtained with CGT in this research. In contrast to these results of pretreatments, Gutierrez et al., (2012) found that the laccase-mediator system using hidroxybenzotriazole as mediator could obtain a lignin reduction without any additional pretreatment for elephant grass and eucalyptus wood besides a previous milling process. However, in that study, four steps of enzymatic pretreatment wecaused byre necessary to achieve significant lignin reduction (Gutiérrez et al., 2012). The increment in lignin degradation in laccase mediator system when a previous pretreatment was used is because these pretreatments helped to open channels inside the lignin structure, which generated an efficient and easy access to lignin by the enzymes. In nature, manganese peroxidase opens channels in lignin structure by using manganese cations which attack lignin and create enough space in lignin structure for access and catalysis of laccase and lignin peroxidase (Angel T., 2002). Similar to enzymatic pretreatment, ultrasonication by itself did not obtain great results in their research. Ultrasonication only obtained high results when used as an auxiliary or previous pretreatment to other pretreatments (Goshadrou et al., 2011), the necessity of other pretreatments combined with ultrasonication is important, because ultrasonication modifies the structure of the plant cell wall, but is not enough to improve the access and catalysis of cellulolytic enzymes.

However, ultrasonication is enough to improve the chemical attack in acid and alkali hydrolysis (Goshadrou et al., 2011).

This study is the first in literature that used a combination of ultrasonication, hot water and laccase-mediator system combined pretreatments. Additionally, the transformation of CGT to bioethanol that uses ultrasonication and laccase-mediator system as pretreatments have not been reported before steam explosion, chemical pretreatments and microbial pretreatments were studied on cotton residues (Silverstein et al., 2007; Agblevor et al., 2003; Agblevor et al., 2006; Jeoh and Agblevor, 2001; Shen and Agblevor, 2008a; Shi et al., 2009). The individual effect of the three pretreatments acted synergistically, producing significant improvement in cellulose conversion. This effect was not achieved by individual or with the other pretreatment combinations (Figure 2). An example of this synergistic process was U+HW+E and HW+E, which had similar reduction in the lignin peaks in their FT-IR spectrum; but the cellulose related peaks of U+HW+E had higher intensity than HW+E. This difference was caused by the use of ultrasonication in the selected pretreatment. The use of ultrasonication presents benefits for cellulose conversion; providing a larger surface area (Chen et al., 2011), improving mass transfer of the reaction reactants, changing the structure of cellulose and increasing *Vmax* of cellulases (Imai et al., 2004).

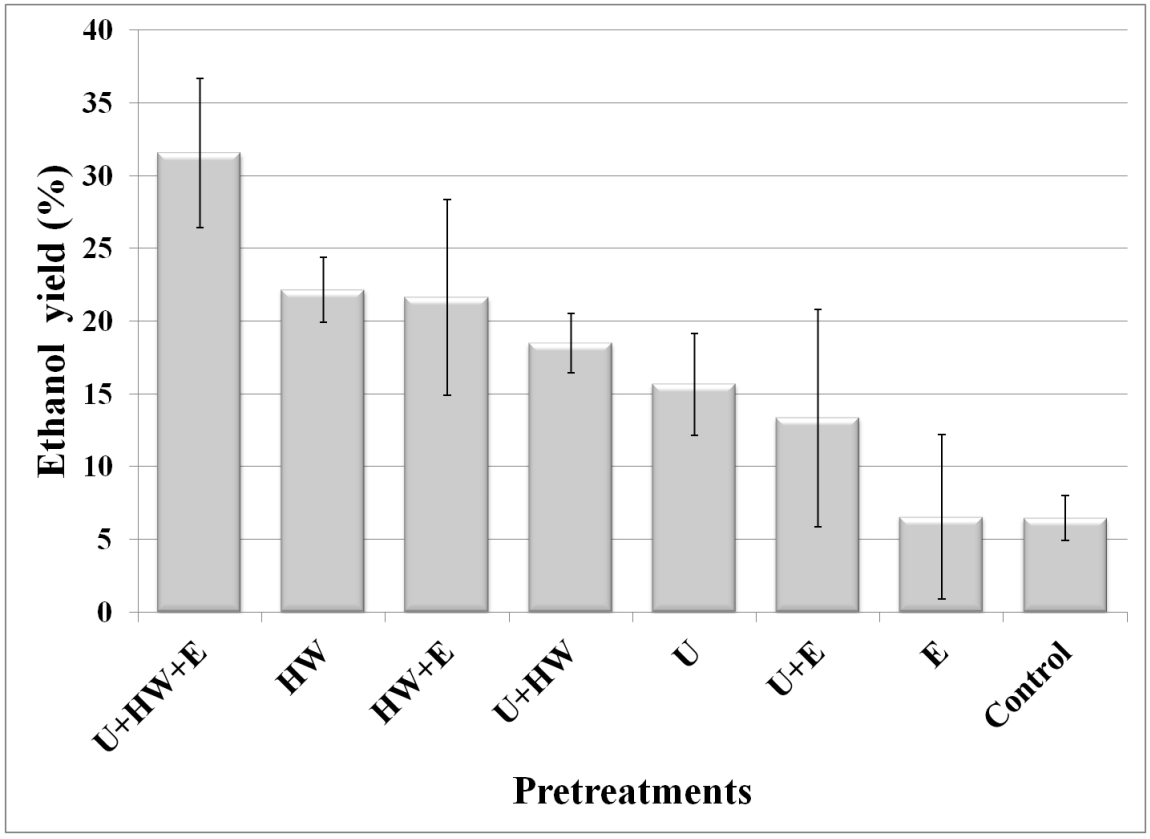

Figure 3. Bar plot for ethanol yield for each pretreatment.

Further effect of the three pretreatments was seen in the differences between the U+HW+E and U+HW. U+HW obtained higher intensity in the FT-IR cellulose peaks than U+HW+E, but U+HW did not have much modification in the lignin signals compared with U+HW+E. These differences are caused by the laccase-mediator systems, which affected the lignin structure by providing better access for cellulases to substrate by lignin structural changes (Chen et al., 2012), reducing the union of cellulases to lignin which reduces cellulose conversion (Qiu and Chen, 2012), and decreasing the concentration of inhibitory compounds (Moreno et al., 2012). The combination of the

two physical pretreatments with enzymatic process allows a considerable time reduction compared with the microbial enzymatic pretreatment alone and a significant toxicity reduction that makes unnecessary the mixture of CGT with other compounds (Shen and Agblevor, 2011) or toxic compounds precipitation (Agblevor et al., 2003). The next step for increasing the cellulose conversion will be use of higher temperatures and pressures in the hot water pretreatment without transforming the process in unviable economically and environmentally.

The ethanol yield presented significant statistical differences ($p<0.05$) among the evaluated pretreatments. In this step, the pretreatment that presented the highest ethanol yield was the U+HW+E combination with an ethanol yield of 31.6% and it resulted in a difference of 10% in comparison to the other pretreatment combinations (Table 3). The ultrasonication and the ligninolytic enzymes pretreatments presented low conversions of 10% and 4%, respectively, when performed alone, but when they were combined with the hot water, better results were obtained. The importance of the hot water pretreatment was also observed in the ethanol yield, where the four HW related pretreatments resulted in the highest ethanol production (see Figure 3). The ethanol yield obtained by the U+HW+E (31.6%) is comparable with the ethanol yield (27%) obtained using CGT from the Wakefield gin (Agblevor et al., 2003), and it is greater than the ethanol yield found using cotton stalks (13%) (Shi et al., 2009). However, these ethanol conversion values are low compared with those reported in literature using much higher temperature and pressure from steam explosion processes (Jeoh and Agblevor, 2001). Other studies with higher production of ethanol used transgenic microorganisms (Agblevor et al., 2006;

Jeoh and Agblevor, 2001; Agblevor et al., 2003), whereas in this study, the conventional fermentation yeast (*Saccharomyces cerevisiae)* was used for the final ethanol conversion process. Transgenic strains increased the total ethanol yield, because these microorganisms used both xylose and glucose to produce ethanol (Olofsson et al., 2008). However, in this study, the yeast converted only the glucose to ethanol; xylose was not converted.

CONCLUSIONS

In this study, bioethanol was produced from cotton gin trash using different pretreatments combinations; however, not all the combinations were competitive in terms of ethanol yield and cellulose conversion. The pretreatment combination that generated the highest cellulose conversion (23%) and ethanol yields (31.6%) were, sequentially the use of ultrasonication, hot water and ligninolytic enzymes. The use of U+HW+E pretreatment combination released high amounts of sugars increased delignification and modified the cellulose structure of the CGT confirmed by the FT-IR spectrum. The results obtained in this research showed an interesting mix of pretreatments for future cost-effective process to produce bioethanol from CGT.

CHAPTER III

ANALYSIS OF ALKALI-ULTRASONICATION PRETREATMENT IN BIOETHANOL PRODUCTION FROM COTTON GIN TRASH USING FT-IR SPECTROSCOPY AND PRINCIPAL COMPONENT ANALYSIS

INTRODUCTION

Cotton is one of the major crops grown in the world. In 2006–2007, the worldwide production was 24 million tons and it continues to increase by 2% each year (Sharma-Shivappa and Chen, 2008). The residues from cotton production are of two types: cotton plant trash (CPT), and cotton gin trash (CGT) (Rogers et al., 2002). CPT is the residue that stays in the field after the harvest of cotton; whereas, CGT is the residue coming from the ginning process. CGT is composed of pieces of sticks, leaves, bolls, and soil cleaned from lint during ginning. In fact, 218 kg of cotton generates 68–91kg of CGT (Sharma-Shivappa and Chen, 2008). Annually, the production of this waste in the U.S.A is around 2.26 million tonnes (Jeoh and Agblevor, 2001).

By 2020, The United States regulation requires the production of 36 billion gallons of biofuels, of which 21 billion should be produced from lignocellulosic materials or other new advanced fuels (Sissine, 2007). Agro-industrial waste (i.e., CGT) is one of the most significant sources of lignocellulosic materials, and bio-ethanol is one of the most essential bio-fuels produced from this kind of wastes. In general, bio-ethanol production from lignocellulosic material includes three principal steps: 1) pretreatment, 2) saccharification, and 3) fermentation. To produce bioethanol from agro-industrial

feedstocks, different kinds of pretreatments have been investigated. These are generally divided into physical, physicochemical, chemical, and biological (Sarkar et al., 2012). In CGT, the pretreatment principally used is physicochemical (steam explosion) followed by chemical (acid or basic hydrolysis) and biological (fungal or enzymatic) pretreatment (Silverstein et al., 2007; Shen and Agblevor, 2008b). Current biomass pretreatment process utilizes energy intense methodologies (high pressures and temperatures) and harsh chemical compounds.

To overcome the issues related with the traditional pretreatment process; new pretreatment strategies have been evaluated and developed. One of these strategies is the combination of ultrasonication, hot liquid water, and ligninolytic enzymes (Plácido et al., 2013). The ultrasonication and hot liquid water modified the lignin and cellulose structure; whereas, the ligninolytic enzymes treatment realized a detoxification and delignification process. This combination generated an ethanol yield of 30% and cellulose conversion of 23% (Plácido et al., 2013); however, both results need to be increased. Cellulose conversion and ethanol yield can be improved by modifying the pretreatment conditions. Several works proved the efficiency of basic hydrolysis to decrease the lignin content in biomass (Chaudhary et al., 2012). Additionally, in sweet sorghum bagasse, the combination of alkaline hydrolysis simultaneously with ultrasonication augmented the final ethanol yield and cellulose conversion (Goshadrou et al., 2011).

The use of ultrasonication and alkali-hydrolysis has not been tested in CGT; thus, the synergic effect of these technologies may raise delignification, cellulose conversion,

and ethanol yield from CGT. The effect of these pretreatments over the CGT structure can be determined using structural component analysis (Sluiter et al., 2011) or/and the biomass Fourier transform infrared (FT-IR) spectrum. In this moment, FT-IR is principally applied to study qualitatively the modifications in the structure and is not utilized for quantitative analysis. However, FT-IR is a fastest technique compared with the traditional structural examination and can be used as a tool to identify qualitatively modification in biomass structure after different pretreatments. As a complementary tool to FT-IR spectroscopy, multivariate statistical techniques have been employed to identify the modifications in the FT-IR spectra and evaluate the difference between the different treatments. One of these multivariate methods is the principal component analysis (PCA), this technique reduces the dimensionality of the data by explaining the variance-covariance structure of a set of variables using few linear combinations of these variables. The use of PCA facilitates the visualization of the spectra changes, and the identification of the most important features of the FT-IR spectra as the peak shifts and non-symmetries (Popescu and Simionescu, 2012). The use of FT-IR coupled with PCA in pretreated and un-pretreated CGT has not been evaluated in any other research. In the future, this type of methodology can be applied in quality or process control, and if it is coupled with regression techniques, it can be useful to make quantitative evaluations of the biomass composition.

This research evaluated the application of alkaline-ultrasonication pretreatment as a methodology to increase the ethanol yield produced from CGT using the combination of ultrasonication, hot liquid water, and ligninolytic enzyme. Additionally, the FT-IR and

PCA were utilized as a tool to analyze the modifications in the biomass structure after pretreatment methodologies.

MATERIALS AND METHODS

Substrate

The samples of CGT were obtained from the Varisco Cotton Gin near College Station, Brazos Valley County, Texas. The CGT samples were ground in a Wiley mill to achieve an average particle size of approximately 1 mm in diameter.

Pretreatments

The experiment followed the selected sequence of pretreatments such as ultrasonication, hot liquid water, and ligninolytic enzymes (Plácido et al., 2013). However, the ultrasonication step was modified to simultaneously perform a basic hydrolysis using different concentrations of NaOH. Table 4 list the experiments utilized in this paper. The experimental design was completely randomized with the NaOH concentration as factor with four levels (0, 5. 10, and 15% w/v) and a control of unpretreated CGT. All the experiments were developed in three replicates using cellulose conversion and ethanol yield as response variables. The ultrasonication process employed a solution of 10% solids of CGT biomass and the corresponding NaOH concentration for 1 hour. The ultrasonicator (Hielscher Ultrasonic Processors, Ringwood, NJ, USA) was set at the highest value of amplitude (100%) and cycle (1). The biomass

was not washed before the hot water treatment, thus remaining particles of NaOH can be present for the hot water treatment. The hot liquid water pretreatment used Erlenmeyer flasks with 10% solution solids at 121°C, 1.02 Atm for 1 h in an autoclave. The ligninolytic enzymes pretreatment consist of the commercial laccase mediator system PrimaGreen® EcoFade LT100 from GENENCOR, International. The enzymatic reactions were performed in 250 mL Erlenmeyer flasks with 50 mL of phosphate buffer 25 mM pH 6, an initial enzyme load of 3 g with a laccase activity of >5700 Genencor Laccase Units/g (enzymatic activity provided by Genencor), with 10% solids of CGT at 30°C, 150 rpm for 96 h (Innova, New Brunswick Scientific, NJ).

Table 4. Pretreatments evaluated in the experiment

Ultrasonication + hot liquid water + Ligninolytic enzymes (U+HW+E),
Ultrasonication/NaOH5% + hot liquid water + enzymes (U-NaOH5%+HW+E)
Ultrasonication/NaOH10% + hot liquid water + enzymes (U-NaOH10%+HW+E)
Ultrasonication/NaOH15% + hot water + enzymes (U-NaOH15%+HW+E)

Saccharification process

The saccharification process employed the combination of two types of commercial cellulases: Accellerase 1500 and Accellerase XY (GENENCOR, Palo Alto, California). The experiment had an initial enzyme loading of 10.45 mg protein/g of biomass of Accellerase 1500 + 1.29 mg protein/g of biomass of Accellerase XY. The

process utilized three replicates in 250 mL Erlenmeyer flasks with 50 mL of a solution of 50 mM sodium acetate buffer at pH 4.8 for 96 h at 50^0C and 125 rpm in an incubator/shaker (Innova, New Brunswick Scientific, NJ). Cellulose conversion was calculated by using the following:

$$\%\ \text{glucose conversion} = [c \times V/m] \times 100\%$$

Where, *c* is the concentration (g/L) of sugars in the sample hydrolyzed as determined by HPLC, *V* is the total volume (L) hydrolyzed, *m* is the initial weight (g) of glucose or xylose determined through NREL protocols. The statistical tests were performed in the software SAS system 9.3.

Fermentation process

Ethanol Red (*Saccharomyces cerevisiae)* provided by Fermentis (Lesaffre Yeast Corp., Milwaukee, WI) was employed for the fermentation process. The activation of the strain was in 0.5 g of dry yeast in 10 mL of the inoculum broth. The composition of the inoculum broth had 0.2 g glucose, 0.05 g peptone, 0.03 g yeast extracts, 0.01 g KH_2PO_4, and 0.005 g $MgSO_4.7H_2O$. The inoculums were shaken at 200 rpm in an incubator shaker at 38 °C for 25–30 min. The fermentation process was performed in 125mL Erlenmeyer flasks with 50 mL of the slurry supplemented with 0.3 g of yeast extract. The slurry was then incubated with 1 mL of freshly activated dry yeast (Ethanol Red) and run for a period of 72 h at 32 °C, pH 4, and 100 rpm. The ethanol yield was calculated from the ratio between the average produced ethanol and the theoretical ethanol production of 51.1 g of ethanol generated per 100 g of glucose in the biochemical conversion of the

sugar. The response variable was the ethanol yield, and it was analyzed using the software SAS system 9.3 employing one way ANOVA and the LSD test.

High performance liquid chromatography

After each of the processes (saccharification and fermentation), the samples were centrifuged at 10,000 rpm for 10 min, and the supernatants were filtered through 0.45 μm hydrophilic PTFE syringe filters (Millipore, Billerica, MA). These samples were then analyzed for glucose, mannose, xylose, arabinose, galactose, and cellobiose concentration using high performance liquid chromatography (HPLC) (Waters 2690, Separations Module, Waters Corporation, Milford, MA) equipped with auto sampler, Shodex SP 810 packed column and a Refractive Index (RI) detector. Each sample ran for 25 min at a flow rate of 1 mL/min, 60°C using HPLC water as mobile phase.

Structural composition analysis

To determine the structural composition of the CGT biomass before and after the pretreatments, the analytical protocols developed at the National Renewable Energy Laboratory (NREL) of the US Department of Energy were followed. This entailed determination of the following: (a) total solids in biomass and total dissolved solids in liquid process samples (b) extractives in biomass, and (c) structural carbohydrates and lignin in biomass (Sluiter et al., 2011), the past protocols were developed using dried biomass. Fourier Transform InfraRed (FT-IR) spectroscopy (Shimadzu, IR Affinity–1 with a MIRacle universal sampling accessory) was used to evaluate the structural

properties of the CGT with and without pretreatments. The infrared spectra collected range was 4000 to 700 cm^{-1} with a resolution of 4 cm^{-1}. The compounds analyzed and their wavenumbers are given in Table 1. The spectra examination was developed using principal component analysis (PCA) in the range between 800 and 1800 cm^{-1}. The proc princomp of the SAS system 9.3 was employed for the PCA calculations using the correlation matrix of the data.

RESULTS AND DISCUSSION

Cellulose conversion

The effect of alkali-ultrasonication employed two response variables, cellulose conversion and ethanol yield. Figure 4 shows the bar plot of the cellulose conversion for each pretreatment. The experiments with pretreatments evidence an increment between 16–35% in the cellulose conversion over the unpretreated biomass. Additionally, the treatments with alkali-ultrasonication revealed a conversion larger than the treatment with only ultrasonication; this increment fluctuated between 11–18%. The statistical analysis (Table 5) indicates that the alkali hydrolysis pretreatments are not different each other. However, the treatment U-NaOH15%+HW+E and U-NaOH10%+HW+E were statistically different compared with the U+HW+E. The 5% treatment did not get significant differences against the U+HW+E. It indicates that 5% treatment increased the cellulose conversion similar to U-NaOH15%+HW+E, but the increment is not enough to be different than the pretreatment without alkali hydrolysis.

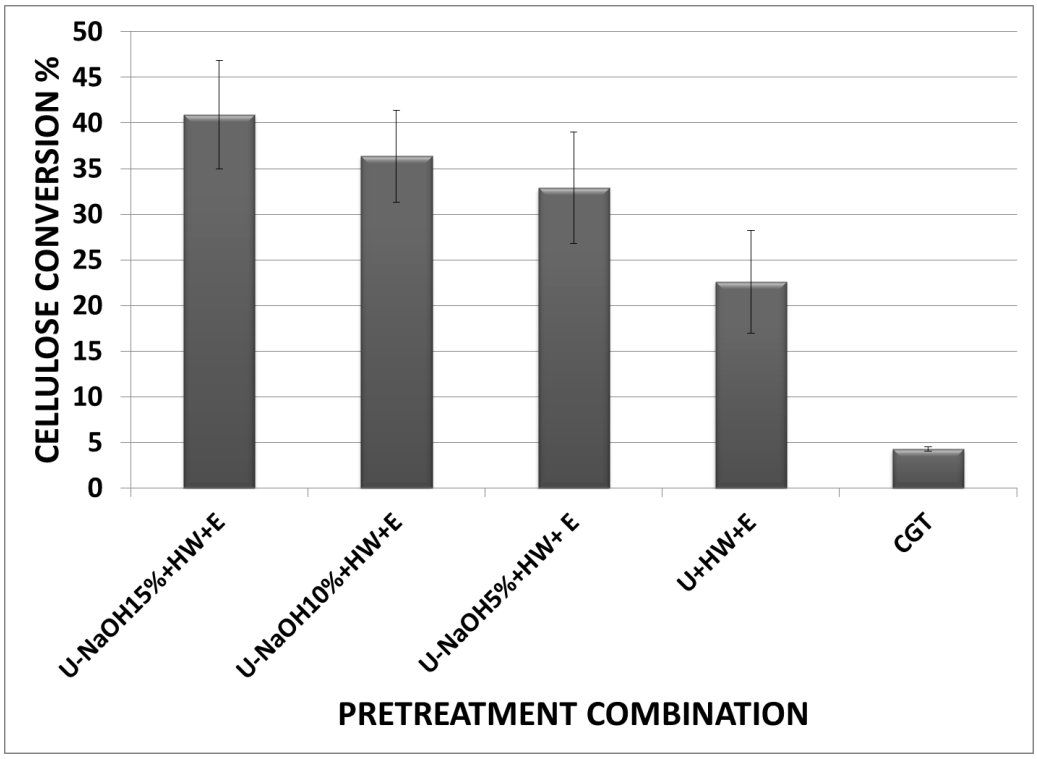

Figure 4. Bar plot of pretreatment combination versus cellulose conversion. Error bars are each treatment standard deviation

The U-NaOH15%+HW+E's cellulose conversion (40%) of CGT was larger than microbial pretreatment (18%) (Shi et al., 2008) and sulfuric acid pretreatment (Silverstein et al., 2007) both over cotton stalks. Additionally, the cellulose conversion in this research is comparable with the achieved by steam explosion with a severity factor of 2 (42%) in CGT (Jeoh and Agblevor, 2001). Nevertheless, the U-NaOH15%+HW+E conversion is lower than the results accomplished in CGT with a

severity factor of 4.68 (66.88%) (Jeoh and Agblevor, 2001), and the steam explosion of CGT and recycled paper sludge (73.8%) (Shen and Agblevor, 2008b).

Table 5. LSD's test for the cellulose conversion and ethanol yield

Pretreatment	LSD's Statistic[1]	Cellulose Conversion (%)	Pretreatment	LSD's Statistic[1]	Ethanol Yield (%)
U-NaOH15%+HW+E	A	0.40±0.05	U-NaOH15%+HW+E	A	0.64±0.13
U-NaOH10%+HW+E	A	0.38±0.05	U-NaOH10%+HW+E	AB	0.58±0.05
U-NaOH5%+HW+E	AB	0.31±0.06	U-NaOH5%+HW+ E	B	0.51±0.07
U+HW+E	B	0.22±0.05	U+HW+E	C	0.28±0.08
CGT	C	0.04±0.01	CGT	D	0.08±0.10

1- Means with the same letter are not significantly different from each other

The NaOH hydrolysis has been evaluated in other cotton wastes as textile wastes (Jeihanipour and Taherzadeh, 2009) and cotton stalks (Silverstein et al., 2007). In both wastes, the use of NaOH improved the cellulose conversion, similar to the results displayed in this study. The cellulose conversion using alkali-ultrasonication on CGT (40%) was larger than the conversion found by Silverstein et al., (2007) in cotton stalks

(21%), but it was lower than Kaur et al., (2012) over cotton stalks (63%) and Jeihanipour and Taherzadeh (2009) in textiles wastes (99%). The difference between CGT and textile wastes is associated with their structures because textile wastes comprise lower content of lignin, composition that allows an easy access to the cellulose. Alkali hydrolysis has been utilized in several types of biomass (sugarcane bagasse, sweet sorghum bagasse, corn stover, etc.) to reduce the lignin content (Chen et al., 2009). This pretreatment is normally related with high lignin removal because the NaOH breaks the ester bonds cross-linkage present in lignin and xylan (Chaudhary et al., 2012). This reaction augments the biomass porosity allowing an easier access of the enzymes to the cellulose. The lignin reduction is necessary to enhance the cellulose conversion or ethanol yield. However, it should be associated with modifications in the cellulose structure. In that way, alkali hydrolysis normally does not produce large modifications in the cellulose structure, and this type of modification is necessary to increase the cellulose conversion (Silverstein et al., 2007). The combination of alkaline pretreatment and ultrasonication have been evaluated in sugarcane bagasse and rice straw. In sugarcane, alkaline-ultrasonication boosted the cellulose conversion approximately 50% against the unpretreated biomass and 40% versus the pretreatment without ultrasonication (Velmurugan and Muthukumar, 2012). The difference between the pretreated and unpretreated biomass coincide with the results of this research (Figure 4). In rice straw, the alkaline-ultrasonication had greater cellulose conversion than the unpretreated biomass and the alkali pretreatment; nevertheless, the difference between the alkali pretreatment and the alkaline-ultrasonication was small (Kim and Han, 2012). The

cellulose conversion can be enhanced by different strategies such optimizing the severity of the liquid hot water pretreatment or improving the conditions of the ligninolytic enzymes and ultrasonication pretreatment (reaction time, temperatures etc.).

Ethanol yield

The second variable analyzed for the pretreatments was the ethanol yield (Figure 5). This variable evidenced a clear difference (55–20%) between the pretreated biomass and the unpretreated biomass. The ethanol yield produced by the alkali-ultrasonication treatments increased compared with the U+HW+E treatment. It indicates a beneficial effect in the use of alkali hydrolysis with the ultrasonication pretreatment for the ethanol production. The highest ethanol yield was obtained in the U-NaOH15%+HW+E and U-NaOH10%+HW+E pretreatments with 63 and 58% correspondingly. The statistical analysis of the experiment (Table 5) describes that U-NaOH15%+HW+E and U-NaOH10%+HW+E were not statistically different. In contrast, U+HW+E and U-NaOH5%+HW+E were statistically similar.

The U-NaOH15%+HW+E's ethanol yield was greater than the reported by Shen and Agblevor (2011) on a mix of CGT and recycled paper sludge (40%). Additionally, our results are comparable with that described for CGT using steam explosion and a severity of 3.47 (58.1%) (Jeoh and Agblevor, 2001). However, the ethanol yield of this research is lower than that described by Jeoh and Agblevor (2001) using steam explosion pretreated CGT with a severity factor of 3.56, and lower than the detailed by Agblevor, et al., (2003) in CGT with conversions around 78–95% (Agblevor et al., 2003).

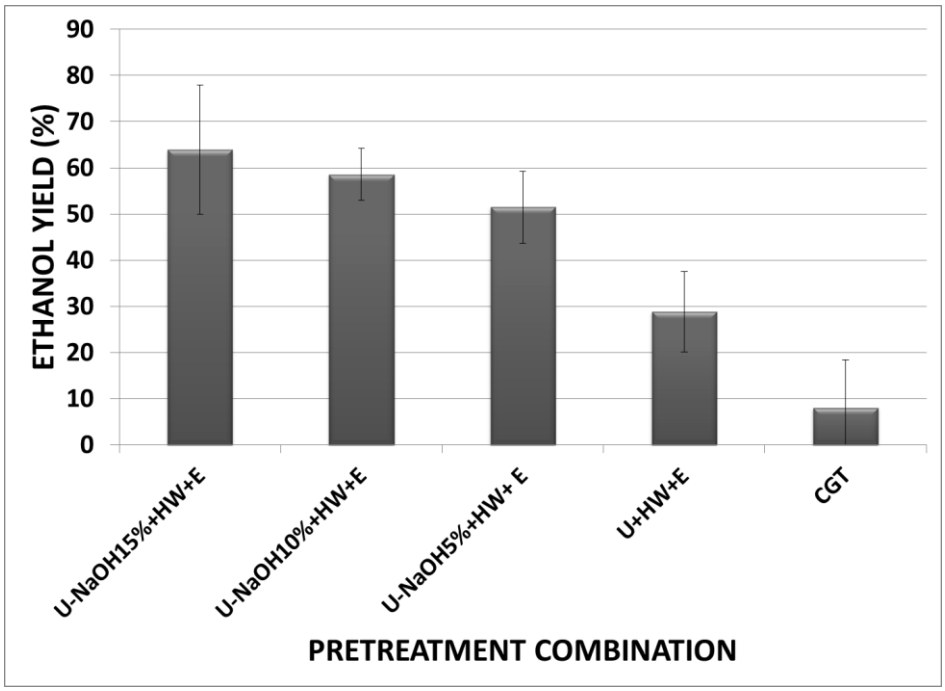

Figure 5. Bar plot for ethanol yield for each pretreatment. Error bars are each treatment standard deviation.

The increment in the ethanol yield using NaOH and ultrasonication have been found in other feedstock such as hazelnut husks (Goshadrou et al., 2011), cotton stalk (Kaur et al., 2012), and sugarcane bagasse (Goshadrou et al., 2011). The ethanol yield produced in sugar cane bagasse (81%) and hazelnut husks (76.7%) were greater than the U-NaOH15%+HW+E pretreatment (63%); whereas, the alkali-ultrasonicated cotton stalk had a lower ethanol yield (41%) (Kaur et al., 2012) than the pretreatment combination selected in this research.

Structural analysis

Table 6 illustrates the composition of the biomass at the end of the pretreatments. The principal differences were in the glucose and acid insoluble material.

Table 6. Structural composition of untreated and pretreated cotton gin trash (CGT)

Compound	CGT	U+HW+E	U-NaOH5% +HW+E	U-NaOH10% +HW+E	U-NaOH15% +HW+E
Water and ethanol extractives(%)	19.6	15.3	14.9	14.3	14.5
Acid insoluble material(%)	25.5	22.9	20.5	19.5	18.7
Arabinose(%)	1.5	1.2	1.3	1.4	1.9
Xylose(%)	5.7	5.4	5.3	5.1	5.2
Mannose(%)	1.1	1.3	1.1	1.3	1.3
Galactose(%)	1.7	1.6	1.3	1.4	1.2
Glucose(%)	24.9	29.8	31.3	33.1	35.5
Ash(%)	10.7	10.3	11.7	12.1	12.5

The use of alkaline ultrasonication produced a decrease in the lignin content, and this was related with the concentration of NaOH. The highest reduction occurred in the

treatment with 15% of NaOH; whereas, the 10 and 5% treatments exhibited similar values. In studies with sweet sorghum, the alkali-ultrasonication reduced the lignin content 6–10% (Goshadrou et al., 2011), which a similar level as the found in CGT. The glucose percentage in alkali-ultrasonication treatments increased in comparison with the untreated CGT and the U+HW+E treatment. Similar to the lignin percentage, the greatest change was in the U-NaOH15%+HW+E treatment. In this case, the increment was around 10% compared with the original biomass and 6% versus the U+HW+E treatment. In this variable, the treatment with 10% presented glucan content greater than the 5% treatment. The other sugars exhibited slightly diminutions compared with the untreated CGT and U+HW+E treatment.

FT-IR was performed in this study to monitor the structural changes in the CGT biomass according with the pretreatments employed. The analyzed peaks (Table 1) and new strong signals were followed in all the samples. Figure 6 shows the FT-IR spectra of the pretreatment sequence of U-NaOH15%+HW+E. The addition of NaOH produced an increment in the signals at 800–900 cm^{-1} and 1300–1500 cm^{-1}, the outstanding peak was the signal at 1431 cm^{-1} followed by the 1402 and 1327 cm^{-1}. These peaks are related with the presence of NaOH because they augmented depending of the NaOH concentration and were only observed in the pretreatments with alkali hydrolysis. These signals reduced through the pretreatments; in fact, after the laccase pretreatment and the enzymatic hydrolysis these peaks were not seen. The reduction in the NaOH peaks indicate that this compound did not have considerable concentrations that could affect the saccharification and fermentation processes.

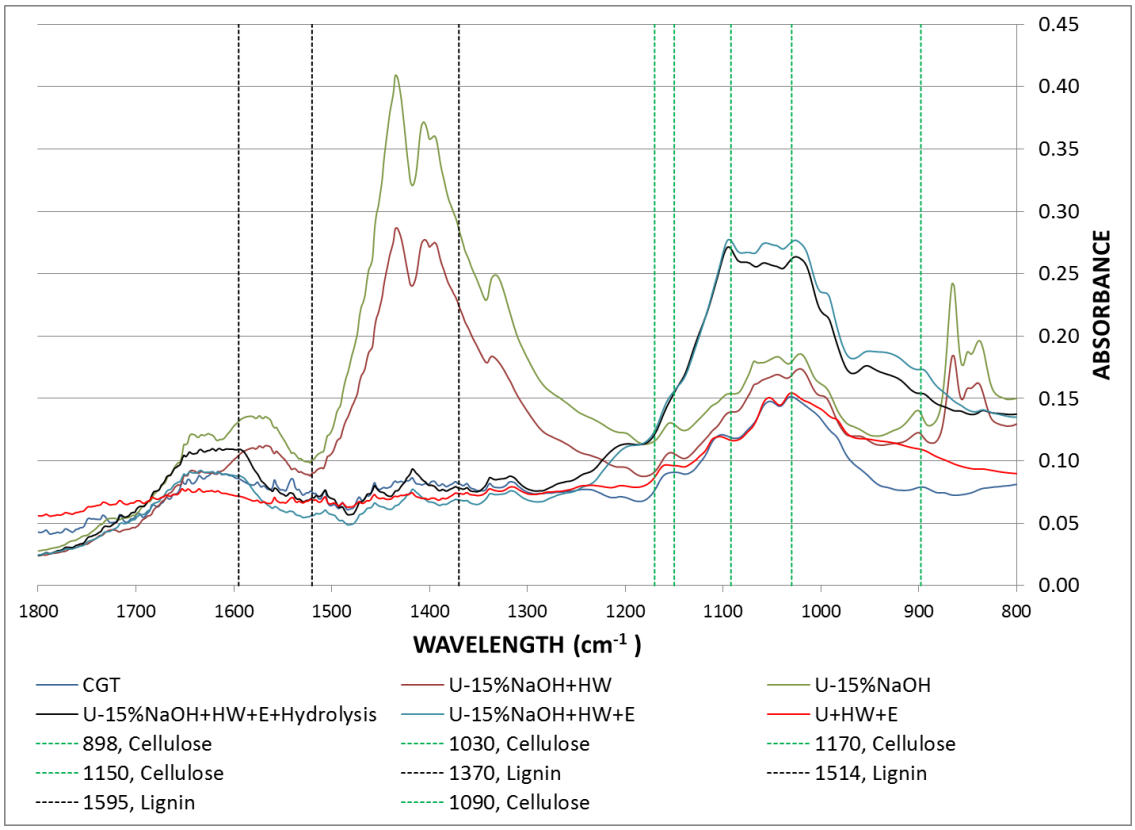

Figure 6. FT-IR spectra for the different steps in the U-NaOH15%+HW+E pretreatment

The absorbance in the cellulose's peaks (898, 1030, 1050, 1090, and 1170–1150 cm^{-1}) increased at the end of the four experiments. The highest increment in all the pretreatments was the 1090 cm^{-1} peak followed by the signals at 898, 1030, and 1050 cm^{-1}. U-NaOH15%+HW+E (Figure 3) obtained the highest increment among the treatments in all the cellulose picks followed by U-NaOH10%+HW+E pretreatment. The absorbance in the cellulose signal increased according to the pretreatments that were added, showing a synergic effect of the pretreatments over the cellulose structure. In addition to the cellulose peaks analysis, the cellulose total crystallinity index (TCI) was

utilized to evaluate deeper the cellulose structure. The TCI has been used to express the relative amount of crystalline material in cellulose, and it can be defined using the FT-IR using the absorbance at A1430/A898 (Goshadrou et al., 2011). At the end of the four trials, the TCI decreased in 46, 63, 66, and 67% for the pretreatments U+HW+E, U-NaOH5%+HW+E, U-NaOH10%+HW+E, and U-NaOH15%+HW+E, respectively. The reduction in the TCI coincides with the final results observed in the ethanol yield (Figure 5). The decrease in the TCI after alkaline-ultrasonication pretreatment was also noticed in the work of Goshadrou et al., (2011) over sweet sorghum bagasse, but in this case the shrinkage was lower (13%).

In the fully pretreated biomass, the absorbance in the lignin signals (1370, 1514, and 1595 cm^{-1}) reduced compared with the unpretreated biomass. The hemicellulose signals (1240, 1732 cm^{-1}) obtained the most variation among the four experiments evaluated. In these peaks, U+HW+E and U-NaOH15%+HW incremented the values and U-NaOH10%+HW+E and U-NaOH5%+HW reduced the absorbances. These differences can be attributed to the CGT composition and the pretreatment interactions. The increment in the cellulose peak, the diminution in the crystallinity index and lignin content are some of the reasons why this pretreatment combination produced a cellulose yield and ethanol conversion higher than the others. The peaks of 898 and 1030 cm^{-1} displayed a considerable drop compared with the pretreated biomass; whereas, the other peaks did not show any significant change. These differences can be used to follow the hydrolysis reaction of CGT biomass using the FT-IR.

Principal Component Analysis of the FT-IR spectrum

This is the first study that use FT-IR spectrum and principal components to analyze the changes produced in the CGT biomass after different pretreatments for ethanol production. The principal component analysis (PCA) correlated the changes in the absorbance in the FT-IR spectrum and discriminated or grouped the variations in the biomass structure after the different pretreatments. The PCA variables were the spectrum wavenumbers in the range 800–1800 cm^{-1}. The pretreatments (U, HW, and E), and the saccharification process were the variables applied for the grouping. The PCA used 626 observations, 525 variables, and the covariance matrix. The variance explained by the PCA using the two initial principal components (PRIN 1, PRIN2) was 91%, 76% from PRIN1 and 15% from PRIN2. PRIN1 and PRIN2 loading's plots (Figure 7) identified which wavenumbers were the most important in the variability explained for each principal component (Popescu and Simionescu, 2012; Monti et al., 2013). PRIN1 did not display negative loadings for any of the wavenumbers; however, PRIN2 has negative and positive loadings.

In both cases, different minimum and maximum points were possible to identify; the most notable point was at 1090 cm^{-1} signal. This signal exhibited high peaks in both principal components, in PRIN1 the signal was the lowest point between 800 and 1200 cm^{-1}; in contrast, in PRIN2, it was the highest point in the complete plot. This wavenumber has been connected with different types of cellulose; this is an indication of the effects of the treatments over the CGT cellulose.

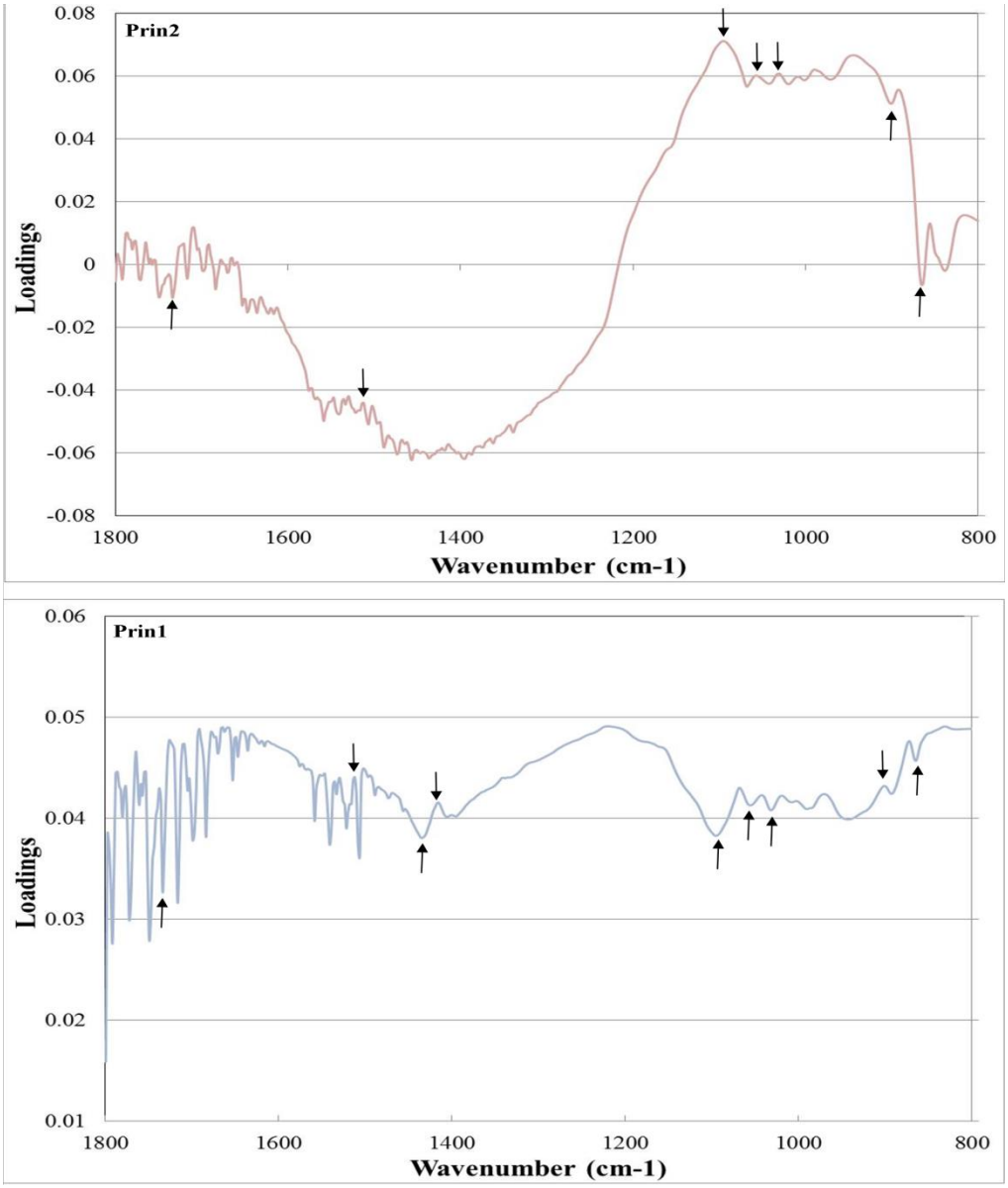

Figure 7. Loading plots of PC1 and PC2 for the CGT FT-IR spectra.

Other significant signal was the 864 cm^{-1}; this signal was a minimum in both principal components and corresponds with one of the NaOH signals found in the FT-IR spectrum (Figure 6). Another signals linked with the NaOH were detected in the PRIN1

loading plot; these signals correspond to 1431 and 1416cm^{-1}. The first one is a minimum peak and the second one is a maximum point. These peaks are clearly observed in the FT-IR spectra of the pretreated biomass with alkali-ultrasonication and hot liquid water (Figure 6). The cellulose signals found in the loading plots were the signals at 898 (B-D-cellulose), 1030 and 1050 cm^{-1} (Intense polysaccharide), and 1090 cm^{-1} (Cellulose II and amorphous cellulose) (Goshadrou et al., 2011; Krasznai et al., 2012). These points were perceived in PRIN1 and PRIN2 loading plots; in PRIN1, 898 and 1090 cm^{-1} were minimums and 1030 and 1050 cm^{-1} were a maximum, which is an opposite behavior compared with PRIN2. These signals showed values in the PRIN2 larger than PRIN1, which represents the importance of PRIN2 for the cellulose signals explanation. The most significant lignin signal in the loading plots was the signal at 1514 cm^{-1} which is related with the aromatic skeletal vibration and CH deformation. In the same way, the most influential hemicellulose signal in the loading plot was the 1732 cm^{-1}, this signal was a minimum in both cases and relates the modifications in the esters found in the hemicellulose.

Using the scores plot of the pretreatments (Figure 8) the PCA could group the pretreatments in four clusters, each one associated with the three pretreatments and the saccharified biomass. The groups that displayed the highest separation were the complete pretreated biomass and the saccharified biomass. The clusters were clearer in the treatments U-NaOH15%+HW+E and U-NaOH10%+HW+E. In these cases, the pretreatments were located sequentially through the PRIN2 axis, this sequence was the same as the experimental order (ultrasonication, hot water, and enzyme). The

saccharified biomass spectrum was placed between the HW pretreatment and the enzyme pretreatment. This behavior was also observed in the full FT-IR spectrum where the line of the saccharified biomass descends compare with the U-NaOH15%+HW+E. This reduction is detected in the wavenumbers that correspond to the cellulose signals (Figure 6). The scores plot for the 10% concentration has the saccharification and the full pretreatment clusters closer than the 15% concentration plot. In the pretreatment U-NaOH5%+HW+E, the ultrasonication and hot-liquid-water pretreatment groups had similar scores, and the separation between them was not clear (Figure 8). In contrast, the separation between the other two clusters improved versus the 10% plot. The scores plot of the U+HW+E discriminates clearly the sonication pretreatment; nevertheless, the other three groups were not evidently distinguished. In the future, the use of PCA in the CGT FT-IR spectra can be implemented in the quality control of the biomass for bioethanol production and to predict the behavior of the CGT after different kind of pretreatments (Ferreira et al., 2001).

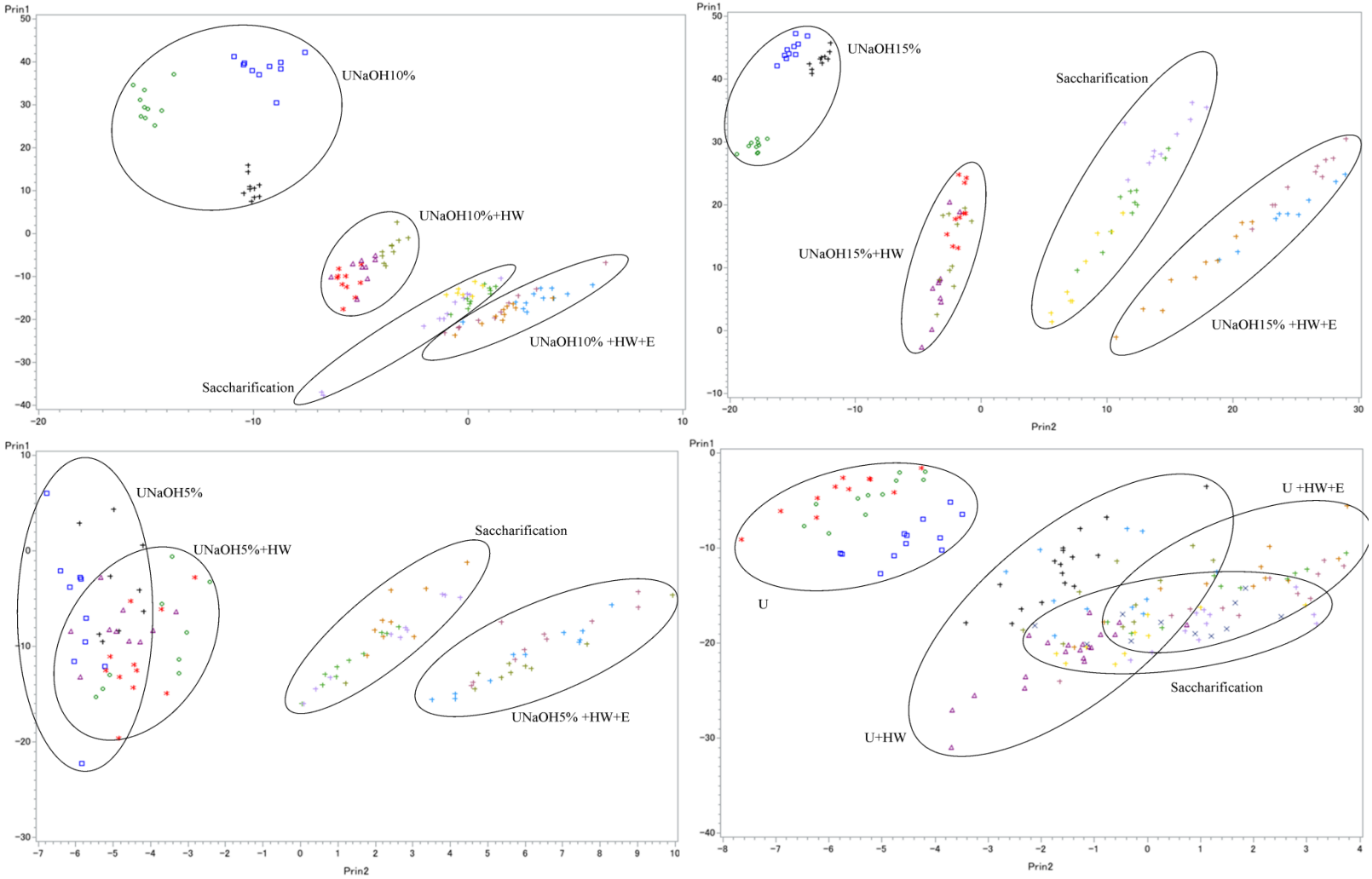

Figure 8. Scores scatter plot of PC1 and PC2 for the CGT FT-IR spectra.

CONCLUSIONS

In this research, the addition of alkali-ultrasonication pretreatment to hot liquid water and ligninolytic enzyme pretreatments increased the cellulose conversion in 9–18% and the ethanol yield in 16-35% versus the treatment without alkali-ultrasonication. From these pretreatments, the U-NaOH15%+HW+E pretreatment exhibited the highest cellulose conversion (41%) and ethanol yield (64%). The use of FT-IR and principal components was effective as a tool to identify the variations in the signal of the cellulose, hemicellulose, and lignin from CGT after the different pretreatments. Additionally, the PCA could separate and identify the CGT biomass from different types of pretreatments and identify the signals with the most variation inside the spectra. In the future, this type of discrimination technique can be used in the bioethanol industry for quality control and prediction analysis.

CHAPTER IV

DEPOLYMERIZATION OF BIOCHAR FROM COTTON WASTES USING CHEMICAL TREATMENTS

INTRODUCTION

One of the most important technologies to produce energy from biomass is the thermal conversion. Thermal conversion is the biomass transformation in other chemical compounds using high temperatures and pressures at different oxygen conditions. Gasification and pyrolysis processes are the two most important processes inside the thermal conversion. The first process is conducted at temperatures greater than 700 ºC and low oxygen concentrations. The second process, pyrolysis is conducted at lower temperatures (400–600ºC) and higher pressures, but with the complete absence of oxygen. In both processes, the final products are synthesis gas, bio-oil, and biochar; however, the proportions of these three products are completely related with the temperatures and pressures used. The syngas can be employed directly to produce energy (combustion) or liquid fuels using the Fischer-Tropsch process (Leibbrandt et al., 2013). The bio-oil can be upgraded to generate liquid biofuels as gasoline, diesel or JP8 (Butler et al., 2011). The principal uses of biochar are soil amendment (Wu et al., 2012; Mukome et al., 2013; Deal et al., 2012) and activated carbons (Angın et al., 2013; Park et al., 2013).

The gasification of cotton wastes, as cotton gin trash and cotton plant trash, has been researched by different studies from laboratory scale to trailer mounted gasification systems (Kantarelis and Zabaniotou, 2009; Capareda and Parnell, 2007; Karatas et al., 2013; Maglinao Jr. and Capareda, 2010; Maglinao and Capareda, 2008). All these studies showed the gasification as an alternative for power production from cotton wastes. The principal product from cotton wastes gasification is syngas (80–90%); nevertheless, 10 to 20% of the biomass is converted to biochar (Capareda and Parnell, 2007; Sadaka, 2013). Unlike gasification, pyrolysis of cotton wastes is still in laboratory scale. The production of bio-oil, syngas and biochar depends on the residence time of the biomass in the pyrolyzer (fast, intermediate, slow). Fast and slow pyrolysis helps the production of bio-oil; in contrast, slow pyrolysis increases the biochar production. Independent of the type of pyrolysis, biochar will be produced in quantities between 12–35% of the original biomass (Kantarelis and Zabaniotou, 2009; Pütün et al., 2005; Zabaniotou et al., 2000). As described earlier, biochar is the final waste generated from the cotton wastes thermal conversion, and there is not a process that can effectively use this byproduct besides soil amendment or activated carbon. This process is necessary to increase the competitiveness of any thermal conversion process.

Biochar carbon content is between 20 to 40%; however, it cannot be directly consumed by microbes or other organisms or applied in other chemical process. To make this carbon available for consumption, it is necessary to depolymerize the biochar in less recalcitrant compounds that can be utilized in other process. A new option for the biochar utilization is the biochar depolymerization. At this moment, the

depolymerization of any type of biochar has not been evaluated before; nevertheless, the depolymerization of low-rank coal has been evaluated using physical, chemical, and biological treatments (Huang et al., 2013b; Hofrichter et al., 1997). Low-rank coal can be related to biochar especially because they share some attributes as structural similitude, low energy content and low carbon content. Huang et al., (2013a) depolymerized coal using potassium permanganate ($KMnO_4$) to increase the carbon bioavailability; after that treatment, the liquid phase was analyzed in aerobic and anaerobic cultures, producing biomass and biogas. Huang et al., (2013b) employed a mixture of chemical pretreatments (HNO_3, H_2O_2, $KMnO_4$, and NaOH) and enzymatic reactions (manganese peroxidase) to depolymerize the coal with the objective of raising the production of biogenic methane. The use of chemical and enzymatic combined treatments enhanced the coal depolymerization, generating different types of chemical products.

The microbial process is other approach to coal depolymerization. In this case, different types of microorganisms principally producers of ligninolytic enzymes were used. This approach uses the structural similarities between low-rank coal and lignin. The most common fungi belonged to the white root fungi group which includes such species as *Trametes versicolor, Phanerochaete chrysosporium, and Nematoloma frowardii* etc. In this approach, microorganisms can transform the complex structures in low-rank coals into smaller organic compounds that can be consumed for biosynthesis of specific organic molecules (Huang et al., 2013b).

The methodologies applied in the low-rank coal depolymerization can be mimicked in the biochar depolymerization. In this paper, the depolymerization

methodology selected was the use of chemical compounds, which can transform or liberate the compounds in the biochar in less recalcitrant compounds that can be utilized in other processes as substrate or as final product. Examples of these products are the humic and fulvic acids, some of the principal compounds obtained from the low-rank coal depolymerization. Because of the biochar composition and extreme conditions in which it is generated, some other components can be generated in addition to the fulvic and humic substances.

This research aim was to select the best chemical treatment as a methodology to depolymerize the cotton wastes gasification biochar, and identify and describe the modifications occurred to the biochar liquid and solid phase after the chemical treatments.

MATERIALS AND METHODS

Substrate

The biochar was obtained after the gasification process of cotton stalks from J.G Boswell, San Joaquin valley, California. The gasification process was done at 500–600 °C using the TAMU Fluidized Bed Gasifier. It is a 305 mm diameter skid-mounted fluidized bed gasifier with a rating of 70 kg/hr. The biochar obtained from the gasifier was filtered using a mesh of 255µm.

Chemical depolymerization of biochar

Biochar depolymerization was evaluated using three variables (chemical compound, concentration and treatment conditions) in a factorial design of 3×3×2. The levels in the chemical compound variable were three: sulfuric acid (H_2SO_4), sodium hydroxide (NaOH), and potassium permanganate ($KMnO_4$). The chemical concentrations evaluated were 2.5, 5 and 10%, and the treatment conditions evaluated were 50°C for 24 h at 150 rpm and 120°C 1h, 1.02 Atm in an autoclave. The experiment was performed using a solution of 10%. The water controls were employed in the two thermal conditions. The experimental statistical analysis was performed using the software SAS system 9.3.

Repetitive biochar depolymerization

The autoclaved treatments of H_2SO_4, NaOH, and $KMnO_4$ at [10%] were used to evaluate the repetitive depolymerization of biochar. At the end of the reaction, the biochar solution was centrifuged at 5000 rpm (SIGMA Laborzentrifugen GmbH) for 5 min at room temperature, the liquid part was removed, and the biochar was added into a fresh solution of chemicals. The biochar recycling was evaluated three times.

Depolymerized biochar characterization

After the chemical depolymerization, the biochar solution was centrifuged at 5000 rpm (SIGMA Laborzentrifugen GmbH) for 5 min at room temperature to separate the liquid and the solid phases. The liquid phase was refrigerated at −20 °C until use. The

biochar was put it to dry in a convection oven at 120 °C until the water was removed from the sample.

Solid phase analysis

The treated and untreated solid samples were analyzed using the Fourier Transform InfraRed (FT-IR) spectroscopy, the ultimate and the proximate analysis. The FT-IR (Shimadzu, IR Affinity–1 with a MIRacle universal sampling accessory) was employed to evaluate the structural properties of the biochar with and without treatments. The infrared spectrum was collected from 4000 to 700 cm^{-1} with a resolution of 4 cm^{-1}. The ultimate analysis or elemental composition of the biochar samples was determined using Vario MICRO Elemental Analyzer (Elementar Analysemsysteme GmbH, Germany) following the ASTM standard D3176. The biochar proximate analysis was accomplished in accordance with the ASTM standards D 3175 and E1755.

Liquid phase analysis

The liquid phase was analyzed using the FT-IR spectroscopy and the UV-Vis. The FT-IR (Shimadzu, IR Affinity–1 with a MIRacle universal sampling accessory) was used to evaluate the biochar depolymerization by following the production of new signals in the liquid phase's spectrum compared with the controls. The UV-Vis (Cole Palmer UNICO 2800) analyses were measurements at specific wavelengths for the evaluation of the degree of depolymerization of the biochar and some chemical properties of the compounds in the liquid. The degree of biochar depolymerization was

measured by the increment in the absorbance at 450 nm (Selvi et al., 2009; Jiang et al., 2013). The $E_{270/400}$, $E_{465/665}$, $E_{250/365}$, $E_{280/472}$, $E_{280/664}$, $E_{472/664}$, coefficients were calculated to identify some characteristics of the compounds found in the liquid phase (Timofeevna Shirshova et al., 2006; Albrecht et al., 2011; Peuravuori and Pihlaja, 1997).

Analysis of the depolymerization products

The liquid samples from ATC-$KMnO_4$ [10%] treatment were used to partially separate and characterize the compounds produced. The liquid samples were rotovaporated to reduce the water content and increase the concentration of the depolymerization products. After rotovaporation, the polarity of the products was evaluated adding 100 µL of the sample into 1 mL of solvents with different polarities (hexane, ethyl acetate, acetonitrile, and methanol). A methanol precipitation performed the evaluation of the silicon compounds in the samples. The precipitation was carried in falcon tubes using 20mL of the original sample in a relation 1:1 of methanol/sample. After the methanol addition, the sample was agitated for 30 min and later centrifuged at 5000 rpm for 5 min. After that, the supernatant and precipitate were separated. The supernatant was rotovaporated to remove the methanol and the solid was dried at 60 ºC for 24 h. After the rotovaporation the supernatant was dried at 105 ºC for 4 h. The dried supernatant was resuspended in 2 mL of a 1:1 methanol/water solution. The solid and liquid phases were separated and dried at 105 ºC for 4 h. All the solids and liquids obtained in the purification process were evaluated using FT-IR spectroscopy.

RESULTS AND DISCUSSION

Chemical depolymerization of biochar

Proximate and ultimate analysis

To identify the variations in the biochar composition, ultimate analysis, proximate analysis, and FT-IR spectroscopy were employed. The proximate and ultimate analysis results are shown in Table 7. The volatile combustible matter (VCM) increased in almost all the treatments compared with the untreated biochar. The only treatments that presented a reduction in this variable were the two water controls. This reduction can be explained by the removal of water solubles compounds from the biochar to the liquid phase (Lin et al., 2012). The treatments with H_2SO_4 [10%] with and without autoclave exhibited the largest increments in the VCM percentage. In these treatments, the VCM augmented 22% and 24% versus the untreated biochar. The H_2SO_4 [5%] with and without autoclave conditions increased the VCM 14% and 12%, respectively.

Table 7. Proximate and Ultimate analysis of treated and untreated biochar

Treatment	VCM (%)	Fixed Carbon (%)	Ash (%)	N (%)	C (%)	H (%)	S (%)	O (%)
Untreated Biochar	28.29±1.28	2.53±4.59	69.19±4.67	1.50±0.15	20.11±0.94	1.84±2.37	1.06±0.33	6.31±0.95
H_2O	27.22±1.95	8.46±0.38	64.33±1.83	1.60±0.13	25.58±3.22	1.16±0.16	0.42±0.05	6.91±0.89
NaOH [2.5%]	31.24±4.41	7.52±2.40	61.24±3.44	1.50±0.12	21.93±2.45	1.13±0.16	0.31±0.05	13.89±1.69
NaOH [5%]	32.02±3.46	3.57±4.02	64.41±3.31	1.50±0.15	23.01±2.65	1.21±0.26	0.32±0.04	9.56±0.77
NaOH [10%]	34.38±1.67	3.84±2.78	61.78±3.74	1.37±0.12	18.30±1.54	1.24±0.08	0.22±0.04	17.09±1.45
H_2SO_4 [2.5%]	34.04±2.03	0.71±1.26	65.26±1.61	1.73±0.28	23.36±3.32	1.07±0.23	4.05±0.53	4.53±1.09
H_2SO_4 [5%]	40.70±1.94	–4.60±2.10	63.90±1.09	1.55±0.29	17.94±7.04	1.86±0.23	7.15±1.33	7.60±2.63
H_2SO_4 [10%]	52.32±3.00	–4.61±1.03	52.29±2.32	1.62±0.23	16.82±4.26	1.25±0.23	7.72±2.58	20.29±4.83
$KMnO_4$ [2.5%]	32.24±2.37	0.82±2.25	66.95±0.94	1.52±0.22	18.15±4.04	0.97±0.22	0.31±0.08	12.10±2.14
$KMnO_4$ [5%]	35.01±0.43	–1.92±1.39	66.92±1.06	1.55±0.14	18.51±2.70	1.07±0.18	0.28±0.07	11.68±1.77
$KMnO_4$ [10%]	35.02±1.54	–4.59±1.2	69.57±1.11	2.11±0.17	17.20±3.61	1.08±0.24	0.14±0.04	9.88±2.01
ATC-H_2O	26.11±0.90	10.52±0.97	61.31±0.65	1.71±0.26	23.64±6.15	1.01±0.15	0.63±0.18	11.70±1.69
ATC-NaOH [2.5%]	30.24±3.33	8.16±2.99	61.60±1.52	1.71±0.32	23.40±5.72	0.95±0.24	0.56±0.15	11.78±1.79
ATC-NaOH [5%]	28.02±1.31	5.41±0.89	66.57±0.42	1.49±0.29	17.26±5.70	0.88±0.32	0.46±0.13	13.34±1.61

Table 7. Continued

Treatment	VCM (%)	Fixed Carbon (%)	Ash (%)	N (%)	C (%)	H (%)	S (%)	O (%)
ATC-NaOH [10%]	28.34±1.07	2.54±1.38	69.12±1.70	1.35±0.19	15.66±2.05	0.93±0.15	0.47±0.04	12.47±2.61
ATC-H_2SO_4 [2.5%]	32.13±1.31	0.85±2.68	67.02±1.46	1.90±0.35	24.60±8.80	1.13±0.32	4.24±1.70	1.11±0.59
ATC-H_2SO_4 [5%]	42.30±1.79	–4.21±0.53	61.91±2.17	1.67±0.33	20.51±5.35	1.05±0.26	8.25±3.37	6.62±2.33
ATC-H_2SO_4 [10%]	50.15±8.23	–5.33±2.06	55.18±8.09	1.50±0.23	17.09±4.65	1.63±0.69	11.73±3.67	12.88±2.31
ATC-$KMnO_4$ [2.5%]	32.15±4.01	–1.05±3.77	68.90±0.39	1.53±0.16	20.77±3.50	1.19±0.18	0.25±0.10	7.36±1.99
ATC-$KMnO_4$ [5%]	35.45±4.78	–6.03±2.55	70.59±3.25	1.55±0.10	12.94±1.99	1.03±0.19	0.39±0.07	13.51±2.59
ATC-$KMnO_4$ [10%]	34.08±2.70	–7.96±1.41	73.88±3.17	1.50±0.23	13.38±4.18	1.24±0.28	0.40±0.12	9.60±1.2

The other treatments' VCM increased between 1% and 7% compared with the original biochar. The ash content decreased in almost all the treatments. The treatments with an increment in the ash content were the ATC- $KMnO_4$ [10%] and [5%]. The lowest ash percentage was obtained by the ATC- H_2SO_4 [10%] and H_2SO_4 [10%]; in these two treatments the ash content decreased 14% and 17% respectively. The other treatments reduced the ash content between 1% and 8%. The fixed carbon increased in all the NaOH treatments and controls. These increments varied from 1% to 8%, and the greatest increments were observed in the two water controls. The other chemical treatments reduced the fixed carbon; however, many of them presented negative values for the fixed carbon. The presence of negative values in the fixed carbon was associated with a mass increment in the sample after the ash measurement. This increment can be explained by reactions between the compounds formed in the biochar depolymerization reaction, the remaining sulfuric acid or potassium permanganate, the metal crucible, and the air. The velocity of these reactions was probably increased by the high temperature (450 ºC) in which the ash analysis was developed

Each variable was independently analyzed using the SAS software. In this analysis, the treatments presented significant differences in the variables evaluated; additionally, in all the variables, the factors (chemical, concentration, conditions) did not have triple interactions. The VCM Anova showed how the chemical type and the concentrations were the principal responsible for the differences in the treatments. The un-autoclaved interaction plots served to analyze the effect of these factors over the VCM. The autoclave factor only affected the treatments with NaOH at [5%] and [10%].

In these treatments, the VCM of the autoclaved treatment decreased between 4–6% versus the un-autoclaved treatment. The other NaOH treatments did not present significant changes between the autoclaved and un-autoclaved treatment (<2%). In contrast, the H_2SO_4 was the chemical that generated the highest increment in the VCM; this difference is most notorious in the [5%] and [10%] concentrations where these treatments are 7–15% greater than the following treatment. In the same way, the $KMnO_4$ treatments presented the next high VCM percentages; however, the differences between them and the NaOH are only significant in the autoclaved treatments with concentrations of [5%] and [10%]. The concentration's effect is different among the three chemicals. In the sulfuric acid, the VCM percentage increased with the rise of H_2SO_4 concentration; this increment had a similar slope in both autoclaved and un-autoclaved treatments. Different than H_2SO_4, $KMnO_4$ and NaOH did not have the same relation between VCM and concentration. $KMnO_4$ presented a slightly increment between [2.5%] and [5%], but in the [10%] treatment, the VCM did not varied significantly versus the [5%] experiment. In the NaOH, the VCM changed slightly among treatments. It decreased in the autoclave treatments when the concentration increased. However, it augmented in the un-autoclaved treatments when the NaOH concentration was higher.

Similar to VCM, The ash percentage was analyzed using the interaction plots. The autoclave conditions have an ash percentage larger than the un-autoclaved treatments. This difference was most significant in the $KMnO_4$ treatments, where all the concentrations showed greater ash values in the autoclaved treatment. This modification is less considerable in the H_2SO_4 and NaOH treatment; however, the NaOH [10%]

concentration exhibited the highest differences between the autoclaved an un-autoclaved treatments. The $KMnO_4$ treatment had the highest ash percentage of all the chemicals. In contrast, the H_2SO_4 treatments produced the lowest ash concentration in the treatments with [5%] and [10%]; however, at [2.5%] the lowest ash percentage belonged to the NaOH treatments. The effect of the concentration on the ash content showed two types of behaviors. First, the sulfuric acid reduced the ash percentage when its concentration increased. Second, the NaOH and $KMnO_4$ augmented the ash percentage when their concentration increased.

The compositional analysis (Table 7) was done to know the content of carbon, nitrogen, hydrogen, sulfur, and oxygen. Nitrogen and oxygen increased in almost all the treatments and hydrogen decreased in all the treatments. Among these elements, the highest variation was observed in oxygen concentration. As expected, the sulfur percentage augmented in the treatments with sulfuric acid; however, the other treatments exhibited a reduction in the sulfur content compared with the original biochar. The carbon content exhibited the largest variations. In this case, reductions and increments were perceived in values around 1% to 7%. The treatments ATC- $KMnO_4$ [10%] and ATC- $KMnO_4$ [5%] generated the highest reduction in the carbon content with a drop of 7% in both treatments. Additionally, the majority of treatments with increments in the carbon content were related with the [2.5%] concentration.

FT-IR analysis

The biochar's FT-IR analysis followed the chemical modifications happened in the biochar's structure. The FT-IR spectrums of the treated and untreated biochar are shown in Figures 9, 10, and 11.

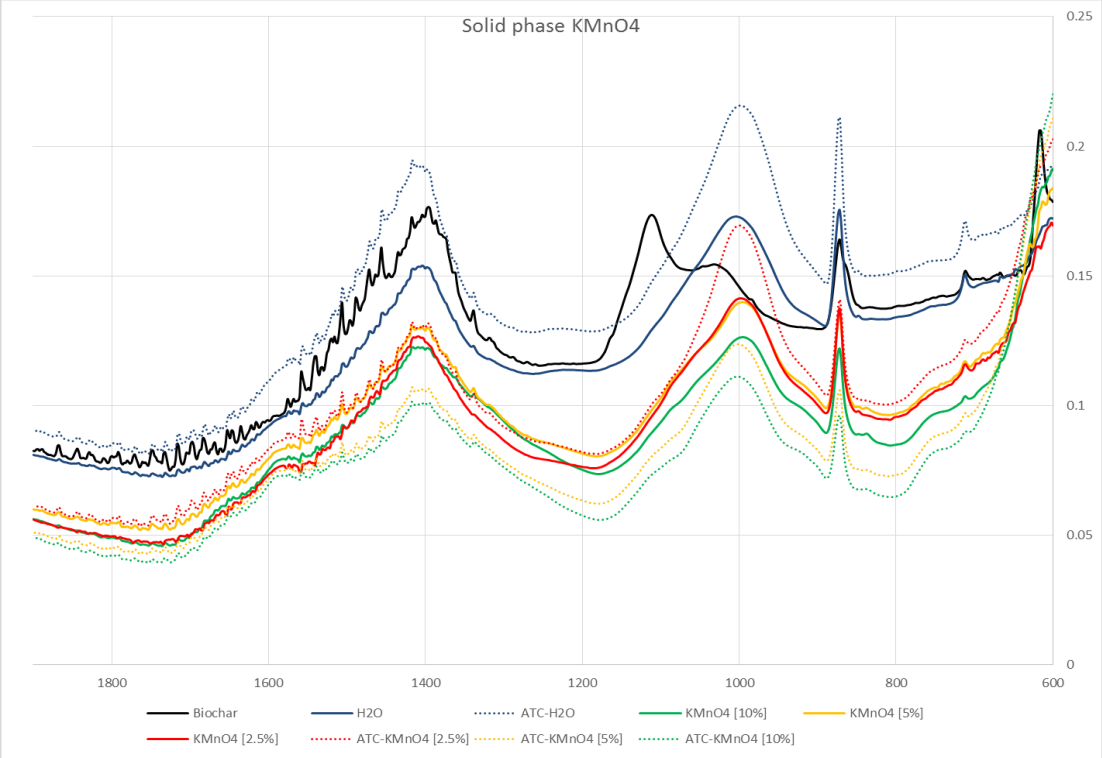

Figure 9. FT-IR spectra of the $KMnO_4$ treatments solid phase.

The most significant peaks in the original biochar were observed at 617, 712, 1110, 1030, 872, 1396, 1980, 2160, 2345, and 2884 cm^{-1}. However, the highest peaks

were 712, 872, 1030, 1110, and 1396 cm^{-1}. The 712 cm^{-1} peak is related with calcium carbonate ($CaCO_3$) (Reig et al., 2002), an inorganic compound found in biochars from different types of feedstocks (Yuan et al., 2011). The 872 cm^{-1} is related with lone aromatic C–H wag which indicates the existence of adjacent aromatic hydrogens (Kaal et al., 2012). The 1030 cm^{-1} peak is correlated with the Si–O stretching and an indication of SiO_2. This compound is in the biochar because it makes part of the bed material of the gasification system, and small particles of it can be included in the final biochar. The signal at 1110 cm^{-1} is related with the C–O stretch and principally the C–O–C interaction (Dong et al., 2013). Finally, the 1396 cm^{-1} signal is assigned to $–COO^-$ symmetric stretching (Xu et al., 2011).

The two water controls produced modifications in the FT-IR spectrum versus the untreated biochar. The most significant modification was the transformation of the peaks at 1110 and 1030 cm^{-1} in a wider peak around 1000 cm^{-1}; this signal is associated with Si–O vibrations. The complete reduction of the 1110 cm^{-1} peak can be related with the hydrolysis of the esters present in the biochar. All the $KMnO_4$ treatments increased the signal in the band between 3100 and 3600 cm^{-1} which is related with the O–H stretch (Figure 9). The width and asymmetry of this band indicates strong hydrogen bonds associated with alcohols and phenols (Maiti et al., 2007). The largest increment in this signal was observed in the treatments with autoclave conditions. Additionally, to the hydrogenation band, the $KMnO_4$ treatments modified the intensity of the other peaks. The peaks observed in the water controls reduced their absorbance after the $KMnO_4$ treatment. The reduction in the signal intensity for the potassium permanganate

treatments is related with the concentration increment. The reductions in the 1000 and 1396 cm^{-1} kept the proportions with the water controls; however, the 872 cm^{-1} signal reduced its proportions compared versus the other peaks. The treatments that produced the biggest reductions in the 872 cm^{-1} signal are the same that generated the biggest reduction in the carbon content; ATC- $KMnO_4$ [10%] and ATC- $KMnO_4$ [5%].

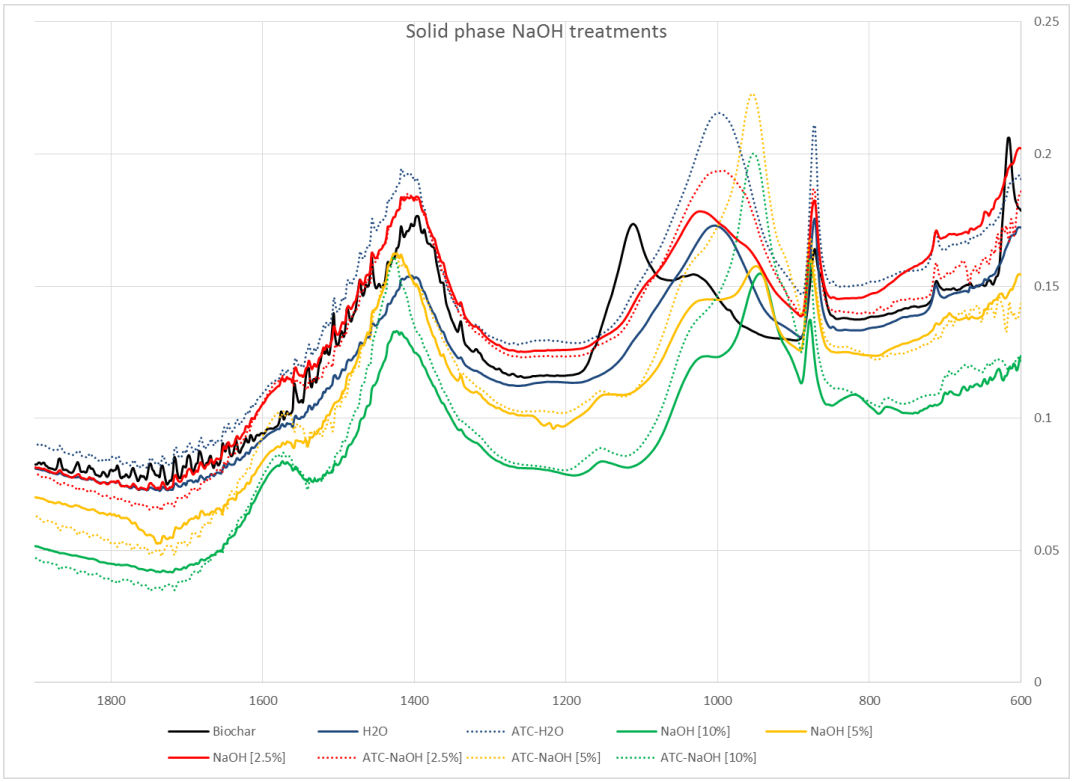

Figure 10. FT-IR spectra of the NaOH treatments solid phase.

The NaOH treatments presented two types of spectrums (Figure 10). First, the NaOH [2.5%] treatments had a spectra similar to the water control spectra. Second, the

NaOH [5%] and NaOH [10%] experiments which generated different signals compared with the original biochar and the controls. On one hand, the [2.5%] concentration showed a reduction in the peaks' intensity compared with the water controls; nevertheless, the peak profile was almost the same. On the other hand, the NaOH [5%] and NaOH [10%] experiments have the same peaks than the [2.5%] treatment, and the addition of new peaks. The largest peak was the 950 cm^{-1} signal, this is related with the C–H stretching vibration observed in methyl and methylene groups. The 1153 and 1570 cm^{-1} signals were found in these treatments too. They are related to the Asymmetric C–O–C stretching vibration and COO– groups, respectively (Maiti et al., 2007). Similar to the $KMnO_4$ treatments, the 872 cm^{-1} signal was reduced in the NaOH treatments that generated the greatest carbon reduction.

The greatest modifications in the biochar structure were observed in the sulfuric acid treatments (Figure 11). The H_2SO_4 [2.5%] and H_2SO_4 [5%] presented a similar type of spectrum; nevertheless, it was different than the [10%] concentration, the untreated biochar, and the water controls. These treatments have new peaks and the removal of other ones when they are compared with the controls. The spectra of these H_2SO_4 treatments did not have the peaks at 872 and 715 cm^{-1} and the signals between 1300 and 1600 cm^{-1}. Nevertheless, these treatments generated new peaks at 1614, 1140, 1110, 1084, 1000 and 650 cm^{-1}. The signal at 650 cm^{-1} is related with remaining particles of sulfuric acid (Kuwata et al., 2009). The 1084 and 1140 cm^{-1} signals represent the C–O bonds, which indicate a more quantity of oxygen bonds in the biochar (Hina et al., 2010). Furthermore, the 1614 signal is related with the $–COO^-$ anti-symmetric

stretching. In contrast with the H_2SO_4 [2.5%] and H_2SO_4 [5%], the H_2SO_4 [10%] treatments generated other type of spectrum. The H_2SO_4 [10%] treatments produced the largest modifications of all the spectrums; these treatments increased the intensity in all the signals, and generated new signals that were not observed in the other treatments.

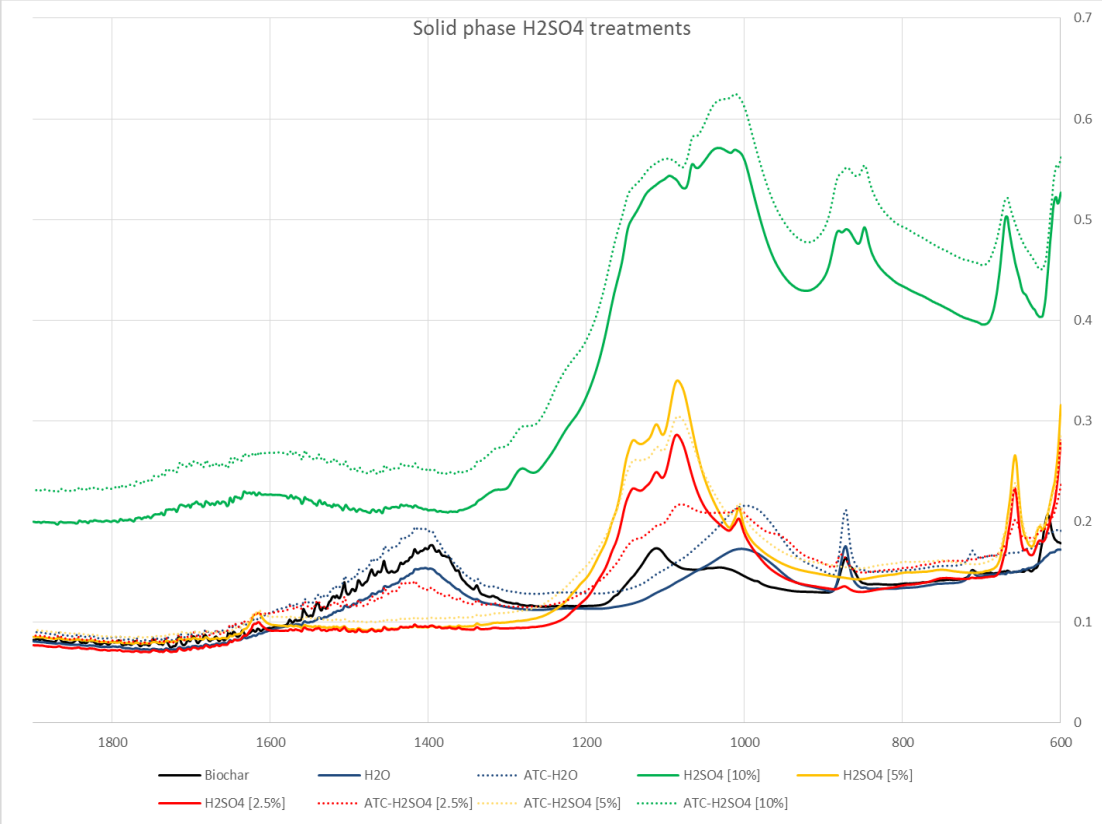

Figure 11. FT-IR spectra of the H_2SO_4 treatments solid phase.

The most important signals were 1285, 1100, 1063, 1032, 1000, 872, 866, 845 and 650 cm^{-1}. The presence of these new signals reveals the production of new type of

compounds in the biochar. These new compounds can be created by modifying the original compounds or by breaking down them. The signals around 650 and 1105 cm^{-1} are related with the sulfuric acid (Kuwata et al., 2009). The signal around 1032 cm^{-1} is related with the symmetric S=O stretching (Yu et al., 2011). All these structural modifications are related with the increment in the volatile compounds and the reduction in the carbon content of the biochar treated with sulfuric acid at [10%] concentration. The highest concentration of sulfuric acid allowed a most significant effect over the biochar in the production of new linkages and compounds versus the low sulfuric acid concentrations.

Liquid phase characterization

UV-Vis spectrophotometry

After the chemical treatments, the liquid phase properties' changed. In some cases the original solution turned to a yellowish/brownish liquid. This color modification happened in all the NaOH treatments, and the autoclaved $KMnO_4$ treatments. The $KMnO_4$ un-autoclaved treatments kept the purple color characteristic of the $KMnO_4$ solutions, and the absorbance at 450 nm was blocked by the $KMnO_4$ signals. On the other hand, the H_2SO_4 treatments did not produce a change in the solution's color; they kept the colorless characteristic of the original solution. The degree of biochar depolymerization measured by the increment in the absorbance at 450 nm of the liquid phase is shown in Figure 12. All the NaOH and $KMnO_4$ treatments generated higher

signals than the water controls; in contrast, the H_2SO_4 treatments did not produced any increment in this wavelength.

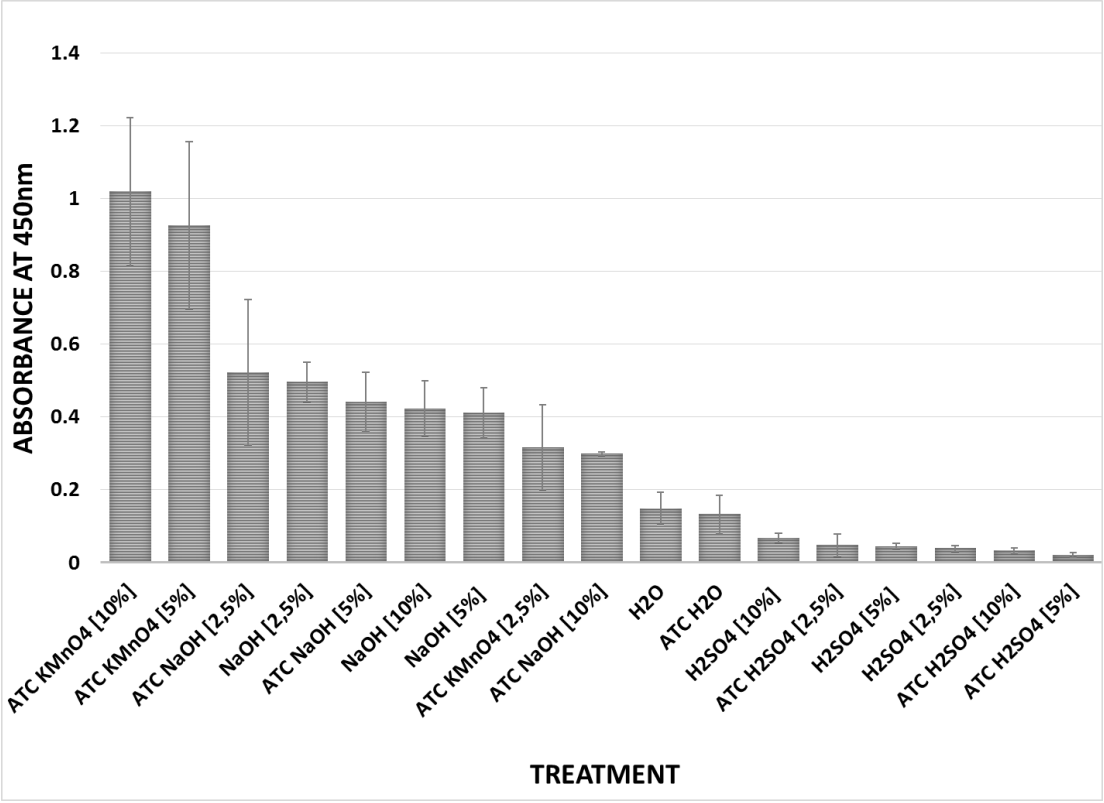

Figure 12. Biochar depolymerization at 450 nm using chemical treatments

The highest depolymerization was performed by the treatments ATC- $KMnO_4$ [10%] and ATC- $KMnO_4$ [5%]. They obtained the highest absorbance at 450 nm and with a considerable difference between them and the next treatments. The next treatments were the NaOH treatments. The 450 nm signal has been correlated with fulvic

and humic acids (Selvi et al., 2009), and these compounds have been produced by the depolymerization of low-rank coal using $KMnO_4$ and NaOH (Huang et al., 2013a). The depolymerization of biochar by the $KMnO_4$ treatment is possible because this is a chemical with high oxidative power and is well known in the oxidation of aromatic compounds with benzilic hydrogens. Additionally, the $KMnO_4$ can realize an overoxidation of the phenolic rings and polynuclear aromatic compounds, a reaction that will generate the opening of the aromatic rings and the production of different compounds (Huang et al., 2013a).

The UV-Vis is an informative method to describe some of the structural characteristics of the humic substances. The absorbances obtained at the analyzed wavelengths are shown in Table 8. The 280 nm signal is related with the total aromaticity and the presence of aromatic compounds, such as phenols, benzoic acids, polycyclic aromatics etc. At 280 nm all the treatments had absorbances greater than the water controls except the H_2SO_4 [2.5%] treatments. This result shows that all the treatments liberated aromatic compounds to the liquid phase. Additionally, the highest absorbance was observed in the treatments ATC-$KMnO_4$ [10%], H_2SO_4 [10%], ATC-$KMnO_4$ [5%], and ATC-H_2SO_4 [10%]. The sulfuric acid treatments did not show high absorbance at 450 nm but they showed high absorbance at 280 nm. This difference is related with the depolymerization of biochar and the formation of aromatic compounds that can be observed at a 280 nm.

Table 8. UV-Vis absorbances at the analyzed wavelengths

Treatments	280nm	340nm	365nm	400nm	436nm	465nm	665nm
ATC-$KMnO_4$[10%]	47.4	8.06	4.77	2.65	1.28	0.73	0.02
ATC-$KMnO_4$[5%]	40.38	8.17	2.78	2.43	1.15	0.68	0.01
ATC-$KMnO_4$[2.5%]	10.05	2.62	1.25	0.69	0.39	0.24	0.01
ATC-H_2SO_4[10%]	28.67	11.68	4.26	0.29	0.04	0.02	0.01
ATC-H_2SO_4[5%]	18.96	2.85	0.98	0.09	0.03	0.013	0.01
ATC-H_2SO_4[2.5%]	1.69	0.47	0.29	0.10	0.06	0.038	0.01
ATC-NaOH[10%]	8.24	4.05	2.15	0.76	0.36	0.23	0.01
ATC-NaOH[5%]	9.61	4.72	2.64	1.07	0.53	0.34	0.01
ATC-NaOH[2.5%]	9.01	4.49	2.64	1.14	0.62	0.41	0.02
ATC-H_2O	3.45	1.65	0.58	0.31	0.16	0.09	0.01
NaOH[10%]	7.39	3.44	2.23	0.97	0.52	0.34	0.03
NaOH[5%]	6.95	3.31	2.17	0.95	0.51	0.33	0.03
NaOH[2.5%]	7.47	3.55	2.36	1.08	0.61	0.40	0.04
H_2SO_4[10%]	41.25	14.62	6.70	0.06	0.10	0.05	0.03
H_2SO_4[5%]	16.95	1.98	0.95	0.07	0.02	0.01	0.02
H_2SO_4[2.5%]	1.01	0.37	0.23	0.08	0.05	0.03	0.01
H_2O	2.59	1.32	0.83	0.35	0.18	0.12	0.01

Different than the H_2SO_4 treatments, the $KMnO_4$ treatments had high absorbances at 450 and 280 nm; this indicates aromatic compounds in the fulvic and humic acids generated by the $KMnO_4$ treatments. The signals at 340 and 365 nm are associated with aromatic compounds and correlate with the size of the molecules. In these wavelength, ATC-$KMnO_4$ [10%], H_2SO_4 [10%], ATC-$KMnO_4$ [5%], and ATC-H_2SO_4 [10%] exhibited the largest absorbances, However, at 340 and 365 nm the highest signals were observed in the H_2SO_4 treatments. The intensity of 436 nm signal helps to differentiate between humic substances rich in carboxylic and phenolic groups and humic substances rich in aliphatics, carbohydrates, aromatics or amides. At 436 nm, the treatments with signals above the controls were the NaOH and $KMnO_4$ treatments. In this case, the highest absorbances are related with humic substances with a high content of carboxylic and phenolic groups. The greatest absorbance was detected in the ATC-$KMnO_4$ [10%] and ATC-$KMnO_4$ [5%]. The intensity of these absorbances is related with carboxylic and acid groups in the acids produced by the $KMnO_4$ treatments. The correlation between the absorbances at 465 nm and 665 nm is related with the condensation degree of the humic substances and the aromaticity. The 465/665 nm relation of the chemical treatments had a high value in the treatments with KMnO4 and NaOH. This high ratio is related with large quantities of large amounts of aliphatic structures and low condensed aromatics. The highest ratio was achieved by the autoclaved $KMnO_4$ treatments followed by the autoclaved NaOH treatments.

FT-IR analysis

In addition to the UV-Vis analysis, FT-IR helps to identify the variation in the samples' spectrum after the chemical treatments. The chemical compounds and their respective concentrations were used as controls to know the characteristic signals of each compound. After the chemical treatments, the liquid phase obtained from the reaction between the chemicals and the biochar showed different peaks and bands than the controls.

The $KMnO_4$ (Figure 13) treatments share the same principal bands; however, the intensity and narrowness of these bands depends on the concentration and conditions employed. The un-autoclaved treatments have a distinctive signal at 910 cm^{-1}; this signal is a characteristic peak of the $KMnO_4$ in solution and correlates with the purple color in the un-autoclaved treatments. The three bands found in the $KMnO_4$ treatments are broad and were generated at 1000–1200, 1200–1500, and 1500–1700 cm^{-1}. The 1000–1200 cm^{-1} band is related with C–O and Si–O linkages. These two bonds can be in the liquid phase compounds because carbon and silicon are present in the biochar and could react with the $KMnO_4$. The highest absorbance in this band was the 1100 cm^{-1} signal which correlates with both types of linkages.

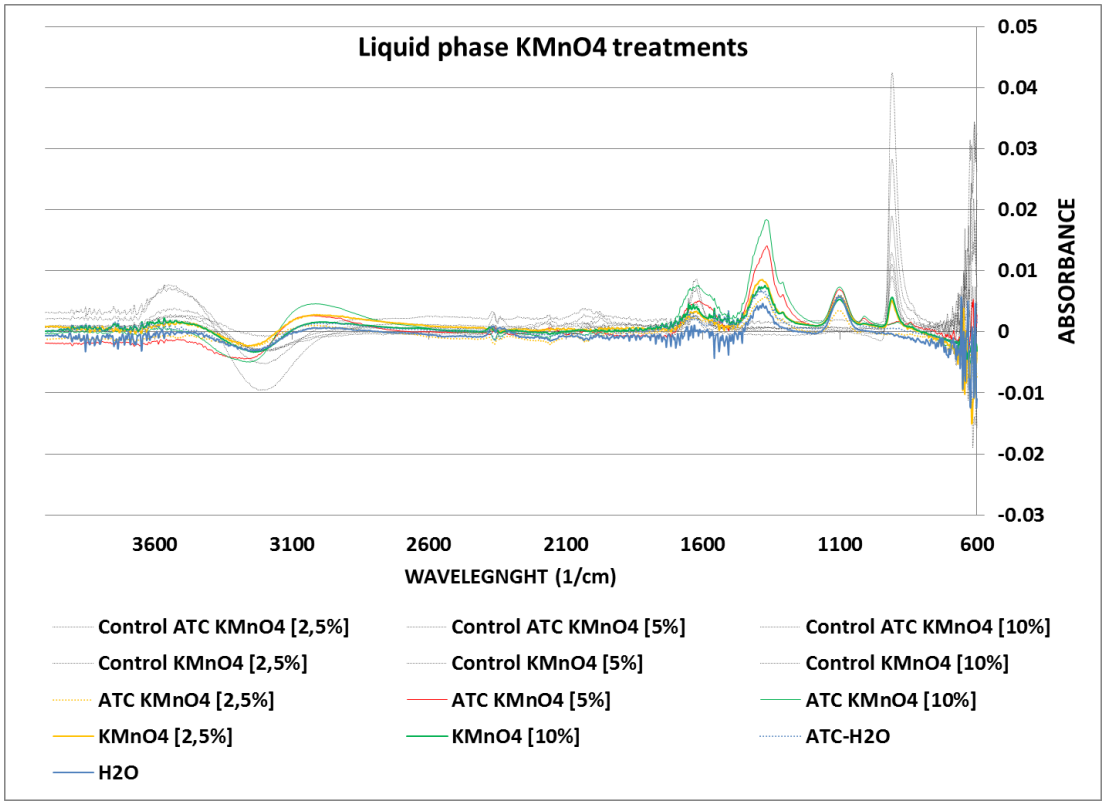

Figure 13. FT-IR spectra of the $KMnO_4$ treatments liquid phase.

The strongest band was the 1200–1500 cm^{-1} band, and is associated with C–O–C and C–OH bending. This band has two intense signals, a large one at 1365 cm^{-1}, which reveals C–H bonds, and a small one at 1305 cm^{-1}, which shows methylene groups. The 1500–1700 cm^{-1} band is related with aromatic rings and double bonds, in this zone the significant peaks were the 1683 cm^{-1} related with C=O linkages, 1615 cm^{-1} associated with C=C bonds and aromatic structures, and 1560 cm^{-1} connected with amides groups. In Addition to these peaks, the ATC-$KMnO_4$ [10%] and ATC-$KMnO_4$ [5%] treatments have a broad peak from 970 to 1030 cm^{-1}, with the highest absorbance at 1010 cm^{-1}.

This signal can be related with silicon-containing compounds (Si–O bond) or with C–O chemical bonds such alcohol, phenols, esters, amides and carboxylic acids (Semenova et al., 2007). In terms of intensity, the treatment that showed the highest intensity in all the peaks was the ATC-$KMnO_4$ [10%] followed by the ATC-$KMnO_4$ [5%]; however, in these treatments, the signals at 1200–1500 and 1500–1700 cm^{-1} were greater than any other $KMnO_4$ treatment. In these treatments, the peaks at 1365 cm^{-1} and 1305 cm^{-1} showed a sharper definition compared with the other treatments.

The NaOH treatments spectra (Figure 14) exhibited a large number of bands; however, these bands are related with the NaOH. Compared with the controls, the treatments displayed two new bands. These bands are found at 1000–1200 cm^{-1} (C–O, and Si–O) and 1200–1500 cm^{-1} (C–O–C and C–OH bending) in all the NaOH treatments. The 1000–1200 cm^{-1} band has a similar behavior compared with the $KMnO_4$ one; nevertheless, the 1200–1500 cm^{-1} showed a different behavior. In this band, the NaOH treatments exhibited a narrow peak with the highest absorbance at 1390 cm^{-1} and any type of shoulder. This signal has been associated with C–H bonds. The principal difference among the NaOH treatments spectrum is the intensity of their bands; the treatments with high concentration achieved high absorbance, and the treatments with autoclaved conditions presented higher signals than the un-autoclaved treatments. However, the difference between the autoclaved and un-autoclaved treatments is more significant in the band of 1200–1500 cm^{-1}, where the signals of the autoclaved treatments are higher and sharper.

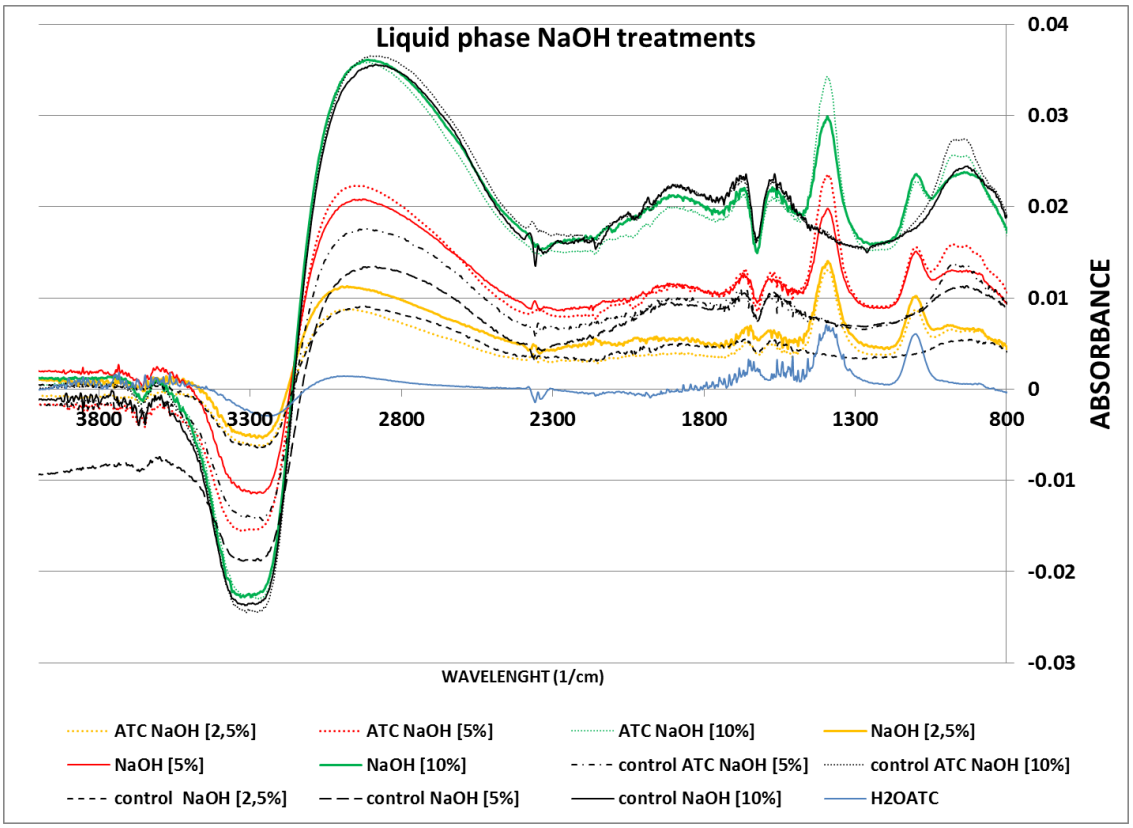

Figure 14. FT-IR spectra of the $KMnO_4$ treatments liquid phase.

The spectra of the H_2SO_4 treatments (Figure 15) varied among the three concentrations. The spectra of the [2.5%] concentration treatments showed a unique band at 1000–1200 cm^{-1} (C–O, and Si–O); this band has a similar high between the un-autoclaved and the autoclaved treatment. The H_2SO_4 [2.5%] controls without biochar had different peaks that were not exhibited in the experiments, these results shows that almost all the H_2SO_4 reacted with the biochar. The H_2SO_4 [5%] treatments showed three signals from 1000–1300 cm^{-1}, the highest signal coincide with the 1000–1200 cm^{-1} band; meanwhile, two shoulders appeared one at 1200 cm^{-1} and other at 1050 cm^{-1}.

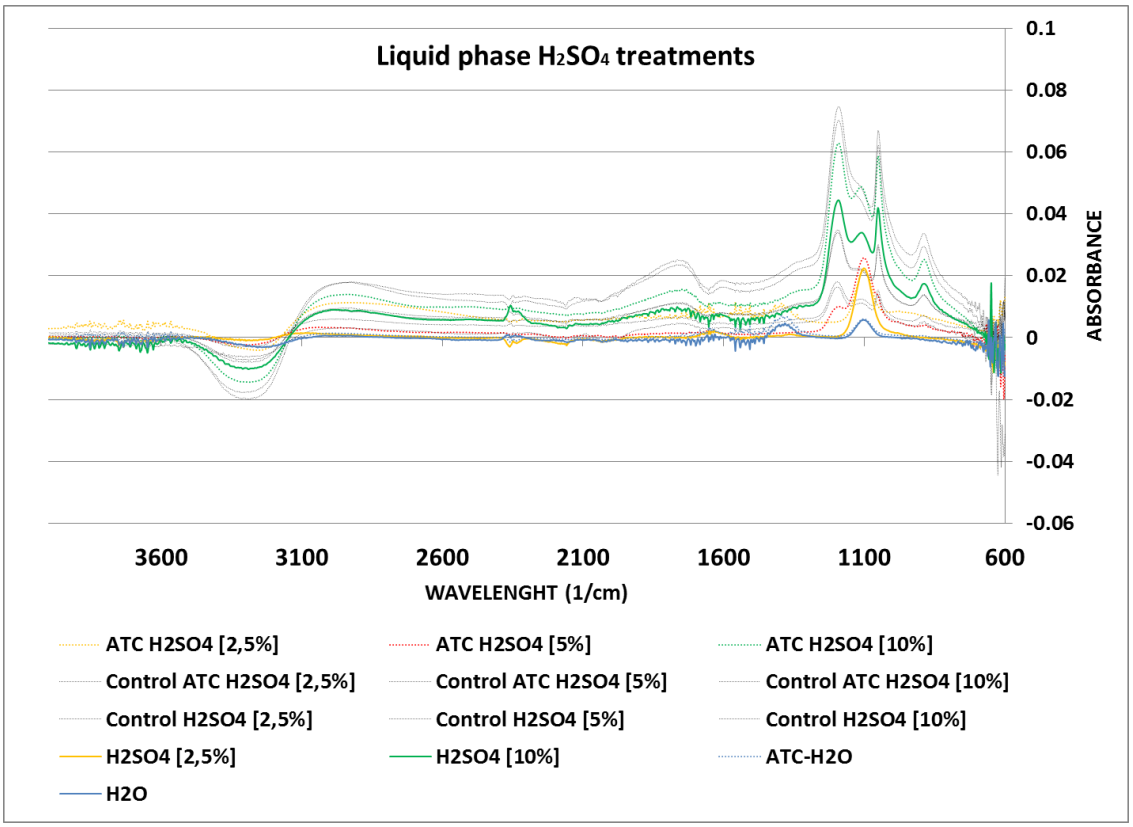

Figure 15. FT-IR spectra of the H_2SO_4 treatments liquid phase.

These final two peaks were also found in the H_2SO_4 controls; however, in the experiments they have absorbances lower than the controls. These reductions reveal the reaction of H_2SO_4 with biochar, but they also reveal remaining sulfuric acid in the solution. The H_2SO_4 [10%] treatments had the spectrum with large absorbances; however, they were the most similar to the H_2SO_4 controls. Besides the similitude with the controls, the treatments have the same band as the other H_2SO_4 treatments at 1000–1200 cm^{-1}.

Repetitive biochar depolymerization

The repetitive biochar depolymerization was done with the ATC- $KMnO_4$ [10%], ATC- H_2SO_4 [10%], and ATC-NaOH [10%] treatments. Those treatments were selected because they presented the largest modifications in biochar liquid and solid phases. The NaOH and $KMnO_4$ treatments had the greatest depolymerization in the liquid phase and the H_2SO_4 exhibited the greatest modifications to the biochar solid phase. The repetitive experiments evaluated how the selected chemical treatments interact with the remaining components in the biochar, and if it is possible to keep depolymerizing the biochar. After each cycle, the solid and liquid phase was analyzed.

Solid phase analysis

The solid phase was analyzed using the ultimate and proximate analyses and the FT-IR spectroscopy. The ultimate and proximate analyses are shown in Table 9. After three cycles, the ATC-NaOH [10%] treatment exhibited an increment in the ash content and a reduction in the VCM percentage. In the same treatment, the nitrogen, sulfur, and carbon percentage decreased; while the oxygen increased. The largest decrease was in the carbon content, which reduced in 10% from the original biochar compared with the final cycle. The ATC- H_2SO_4 [10%] showed increments of 5% after each cycle in the VCM%; this increment produced the biochar with the highest VCM percentage (64%) of all treatments. In addition, the ash content decreased in 40% from the original biomass to the third cycle; this reduction was done in a rate of 10% per cycle. The biochar's elemental composition showed a constant increment in the hydrogen and oxygen content

through the cycles, and a carbon augmentation after the first cycle. The increment in the carbon content is explained by the reduction of the ash content. The ATC- $KMnO_4$ [10%] treatment exhibited a different behavior in the ash and VCM content versus the other treatments. In this treatment, the ash content increased after each treatment 5 to 9%; the increment in the ash is probably related with the production of potassium or manganese compounds. The VCM % augmented in the first cycle; however, it decreased in cycle 2 and 3 in a rate of 10% each. The compositional analysis of the ATC- $KMnO_4$ [10%] showed a carbon decrement in all the cycles. In fact, after the final cycle, the carbon content was 1.42%, which is a reduction of 94% compared with the original biochar. This decrease was achieved principally after the first and second cycle where the carbon content was 4.86%; this drop corresponds to 88% of the total carbon present in the original biochar. The carbon abatement in the solid phase indicates the carbon transformation in compounds in the vapor or liquid phases. The other elements did not exhibit strong variations in their percentages.

The FT-IR spectra of all treatments are shown in Figure 16. The ATC-NaOH [10%] spectrum showed almost the same peaks through the three cycles; however, a new signal was generated after the third cycle at 905 cm^{-1}; this signal is related with epoxy groups.

Table 9. Proximate and ultimate analysis of the repetitive biochar depolymerization treatments.

Treatment	VCM (%)	Fixed Carbon (%)	Ash (%)	N (%)	C (%)	H (%)	S (%)	O (%)
Untreated Biochar	*28.2±1.2*	*2.53±0.5*	*69.1±4.6*	*0.95±0.2*	*22.4±2.9*	*1.06±0.3*	*0.98±0.24*	*8.36±1.6*
Cycle 1-H_2O	29.2±4.9	13.9±3.6	56.7±8.2	0.80±0.2	24.1±8.9	1.27±0.1	0.42±0.23	16.5±3.5
Cycle 2-H_2O	31.5±3.9	11.5±4.1	56.9±7.4	1.09±0.2	34.2±1.8	1.63±0.2	0.37±0.02	7.29±1.5
Cycle 3-H_2O	23.5±0.1	9.63±0.5	66.7±0.4	0.77±0.3	20.5±4.2	2.35±1.1	0.44±0.15	9.08±3.8
Cycle 1 ATC-NaOH [10%]	33.2±4.7	-2.46±4.3	69.2±0.7	0.44±0.0	18.3±4.9	1.84±0.2	0.40±0.08	9.72±4.6
Cycle 2 ATC-NaOH [10%]	33.5±1.6	-2.11±1.1	68.5±0.5	0.33±0.1	17.4±2.2	1.66±0.2	0.27±0.04	11.8±2.8
Cycle 3 ATC-NaOH [10%]	26.6±0.8	0.57±1.1	72.7±0.3	0.30±0.1	13.2±5.2	1.18±0.9	0.24±0.05	12.5±1.2
Cycle 1 ATC-H_2SO_4 [10%]	54.5±2.2	-4.57±2.5	50.0±3.5	0.49±0.1	12.1±2.5	1.42±0.2	10.7±1.2	26.8±1.3
Cycle 2 ATC-H_2SO_4 [10%]	59.1±2.5	0.72±2.1	40.1±4.6	0.64±0.2	18.7±8.5	1.56±0.9	8.52±3.6	28.4±8.9
Cycle 3 ATC-H_2SO_4 [10%]	64.4±0.9	6.20±5.5	29.3±5.1	0.50±0.1	16.4±7.0	2.85±0.5	8.16±0.5	45.1±3.8
Cycle 1 ATC-$KMnO_4$ [10%]	33.5±2.7	-6.82±2.3	73.2±0.7	0.42±0.1	13.0±4.9	1.42±0.3	0.38±0.09	11.1±5.7
Cycle 2 ATC-$KMnO_4$ [10%]	22.0±0.3	-6.83±1.2	84.7±1.6	0.16±0.0	4.8±1.3	1.41±0.2	0.16±0.02	8.07±0.1
Cycle 3 ATC-$KMnO_4$ [10%]	15.2±1.3	-3.50±0.7	88.2±1.0	0.08±0.0	1.4±1.3	0.89±0.7	0.18±0.01	9.22±3.0

After the final cycle, the ATC-NaOH [10%] treatment exhibited reductions in the signals at 1570 and 1153 cm^{-1}, the last one was removed completely from the spectrum. These signals are associated with esters and acids, and their reduction is probably associated with the reaction between compounds with this groups and the NaOH. On the other hand, the signals at 872 and 950 cm^{-1} increased after cycles 2 and 3; these signals are linked with aromatic groups and methyl and methylene groups.

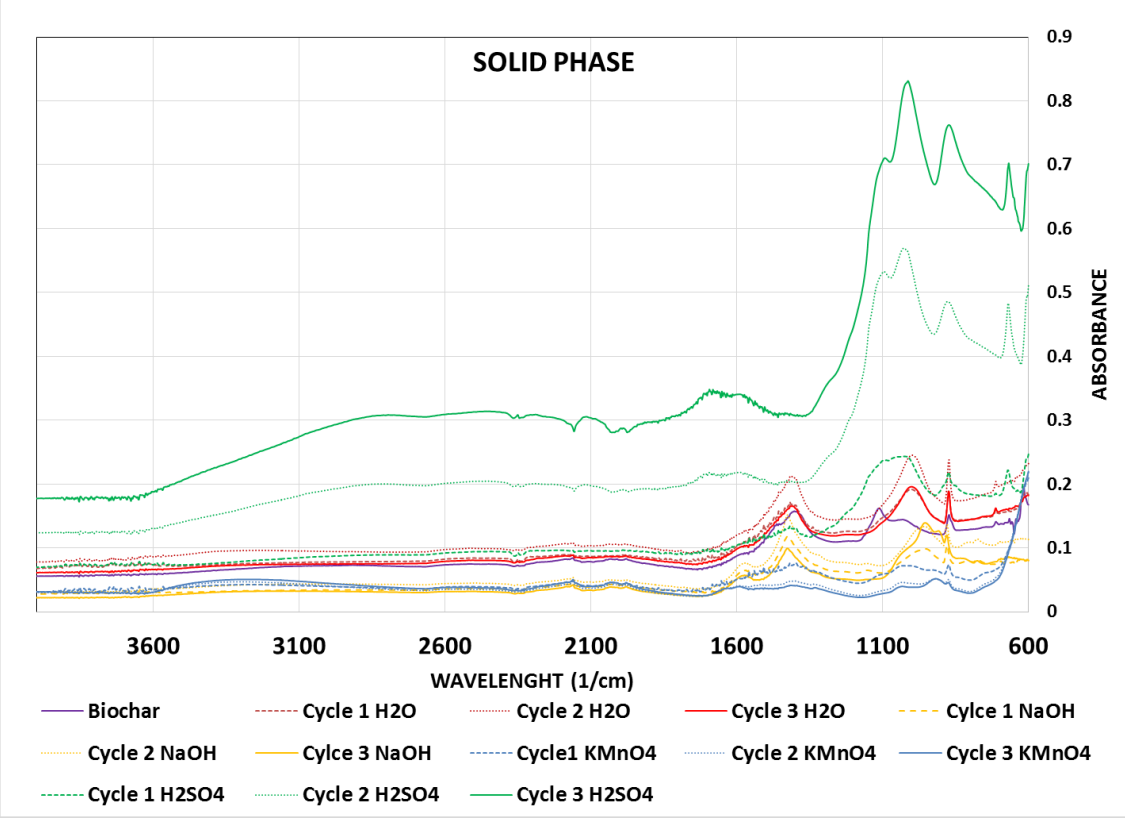

Figure 16. FT-IR spectra of the repetitive experiments solid phase

The ATC- H_2SO_4 [10%] treatment FT-IR analysis showed an increment in the high and definition of the peaks after each cycle. After cycle two and three, the FT-IR showed four clear peaks at 670, 872, 1015, and 1025 cm^{-1}; the signals at 670 and 1025 cm^{-1} are associated with sulfur compounds. The first one indicates remaining sulfuric acid; similarly, the second one describes S=O linkages. Furthermore, the signal of 875 cm^{-1} correlates with aromatic compounds. The increment in this signal is associated with the reduction in the ash content, which allows the aromatic compounds to generate higher peaks.

The ATC- $KMnO_4$ [10%] spectrum exhibited four bands at 800–1200, 1200–1700, 1700-2300, 3100-3600 cm^{-1} in the three cycles. The ATC- $KMnO_4$ [10%] treatment generated an increment in the band at 3100-3600 cm^{-1} after each treatment; this zone is associated with the O–H stretch. The additional three zones showed a reduction in the absorbances and modifications in the peaks in there. In the 800–1200 cm^{-1} zone, three peaks were observed at 872, 920, and 1030 cm^{-1}. These signals are detected in the three cycles; however, the intensity in these signals varied in each cycle. The signal at 1030 cm^{-1} presented the biggest modification; it changed from the largest signal in the first cycle to the smallest one in the third one. The 872 cm^{-1} signal (aromatic groups) decreased after each cycle; although, in the third cycle the reduction in this peak was lower. The 920 cm^{-1} signal did not change after the third cycle. The band at 1200–1700 cm^{-1} changed from a broad band in the first cycle to three peaks in that band in the last two cycles, the peaks were observed at 1330, 1396, and 1590 cm^{-1}. These signals are related with the OH bending, $–COO^-$ symmetric stretching and C=C

double bond vibration of the aromatic ring. The reduction observed in different peaks of the ATC- $KMnO_4$ [10%] cycles correlates with the reduction in the carbon content showed in the compositional analysis of the cycles.

Liquid phase

After each cycle, the liquid phase was evaluated using the FT-IR and the UV-Vis spectrometry. The UV-Vis was used to determine the depolymerization through the cycles at A_{450}. Figure 17 exhibits the absorbances obtained in each treatment and their cycles. The ATC- $KMnO_4$ [10%] treatment showed the highest depolymerization of all treatments in the first and second cycles. However, the absorbance reduced between cycle 1 and cycle 2. In the third cycle, the depolymerization could not be detected because part of the $KMnO_4$ did not react, and the $KMnO_4$ coloration interfered with the depolymerization measurement. The lack of reaction in the third cycle correlates with the low carbon percentage observed in the biochar after the second cycle (Table 9), indicating that the carbon in the biochar was not enough to react with all the $KMnO_4$ in the solution. These results evidence that is possible to reuse the biochar in order to augment the depolymerization.

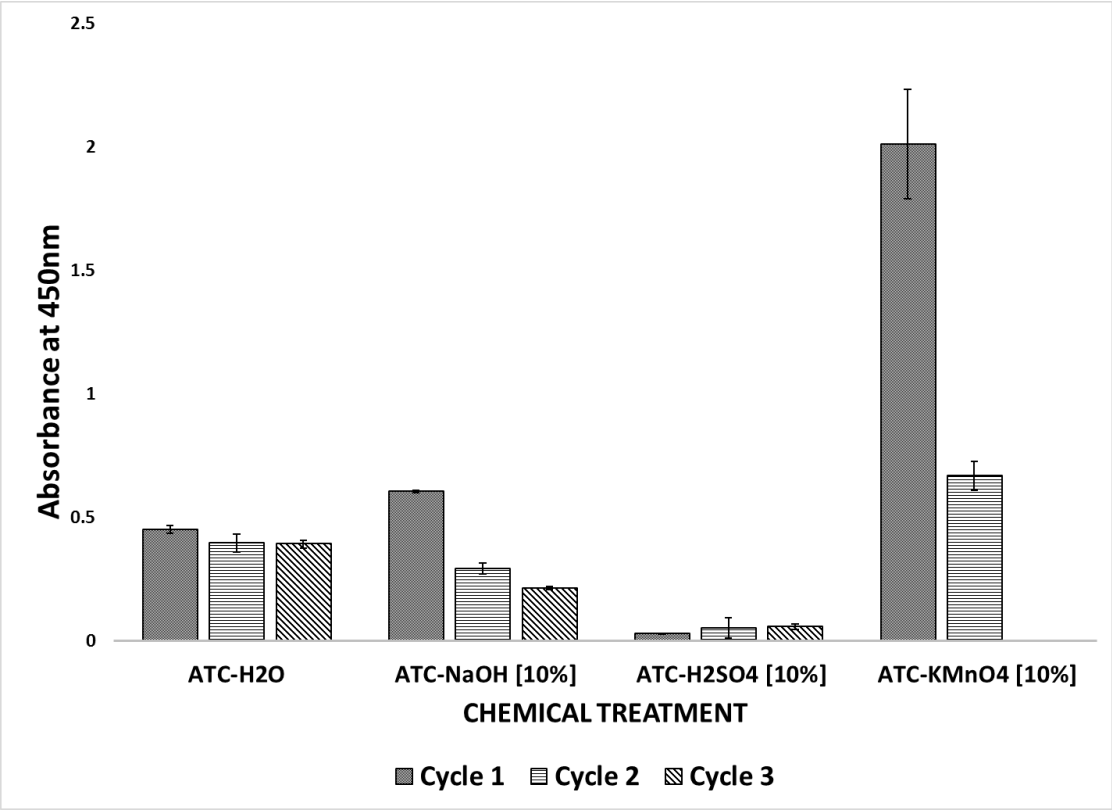

Figure 17. Repetitive biochar depolymerization at 450 nm

The ATC-NaOH [10%] treatment generated depolymerization in the three cycles reducing the absorbances after each treatment. Even though, all the NaOH cycles presented depolymerization; however, the absorbances associated with these cycles were lower than the observed in the $KMnO_4$ treatment. Similar to the initial results, the ATC-H_2SO_4 [10%] treatment did not produced molecules that can be detected at 450 nm and after each cycle the absorbance at this wavelength was almost the same.

Table 10. UV-Vis absorbances at the analyzed wavelengths in the cycles experiment.

Treatments	280	340	365	400	436	465	665
Cycle1-H_2O	7.01	3.81	2.25	0.94	0.54	0.36	0.03
Cycle2-H_2O	2.52	1.53	1.09	0.61	0.44	0.35	0.14
Cycle3-H_2O	1.50	1.17	0.82	0.58	0.44	0.36	0.24
Cycle1 ATC-NaOH[10%]	10.20	5.71	3.37	1.37	0.73	0.49	0.03
Cycle2 ATC-NaOH[10%]	3.99	2.25	1.25	0.60	0.34	0.25	0.05
Cycle3 ATC-NaOH[10%]	1.77	0.99	0.66	0.37	0.24	0.19	0.06
Cycle1 ATC-H_2SO_4[10%]	8.40	3.28	1.18	0.09	0.03	0.02	0.01
Cycle2 ATC-H_2SO_4[10%]	1.63	0.78	0.33	0.07	0.05	0.05	0.04
Cycle3 ATC-H_2SO_4[10%]	0.69	0.26	0.13	0.06	0.05	0.05	0.04
Cycle1 ATC-$KMnO_4$[10%]	67.4	10.3	10.2	4.6	2.49	1.58	0.09
Cycle2 ATC-$KMnO_4$[10%]	54.8	10.1	7.0	2.5	0.94	0.47	0.15
Cycle3 ATC-$KMnO_4$[10%]	69.2	74.1	58.2	8.0	4.4	21.7	5.5

Table 10 describes the other wavelengths evaluated. In these signals, the highest absorbances were found in all the first cycles of each treatment. The first cycle of the H_2SO_4 treatment presented significant absorbances at the A_{280}, A_{340}, and $A_{365\ nm}$; however, these signals were reduced notably in the second and third cycle, this indicates that the reaction with the H_2SO_4 did not generated as much aromatic compound in the second and third cycle compared with the first one. The ATC-NaOH [10%] cycles

showed a reduction in the absorbance at all the signals after each cycle. In the ATC-$KMnO_4$ [10%], the signals at A_{280}, A_{365} A_{400}, A_{436}, and A_{465} decreased between the first and second cycle. These modifications indicate that the liquid phase of the second cycle contains small quantities of aromatic groups, high degree of condensation, and compounds containing less carboxylic and phenolic groups.

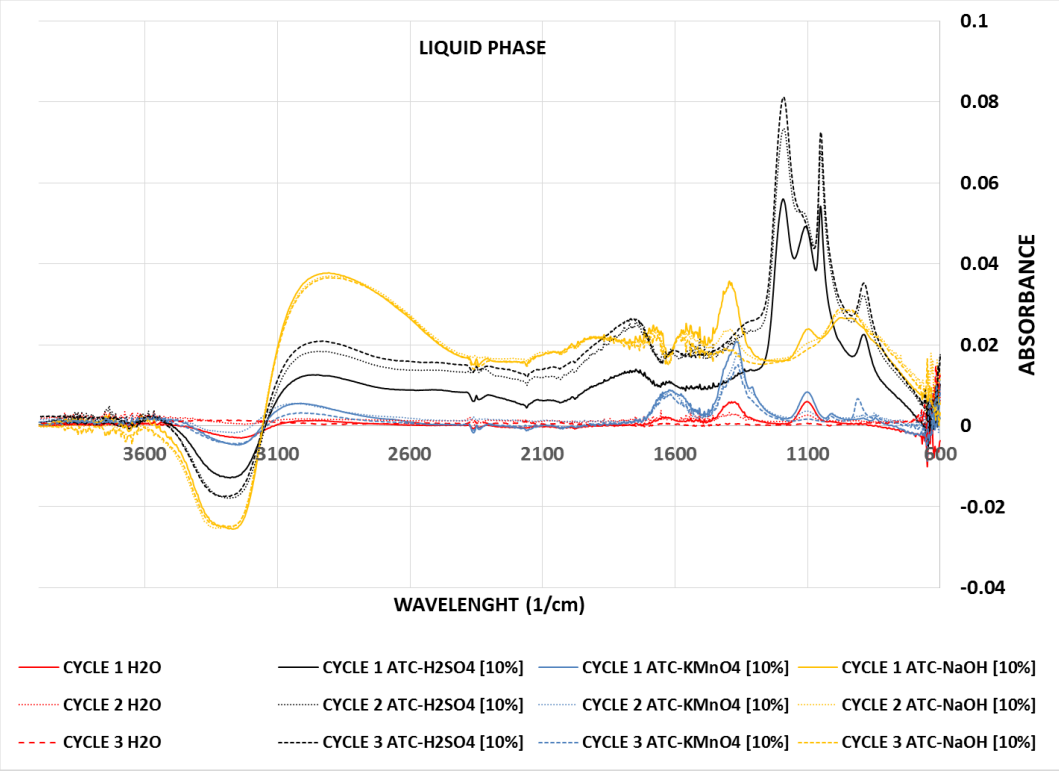

Figure 18. FT-IR spectra of the repetitive experiments solid phase

The liquid phase's FT-IR spectra are shown in Figure 18. The ATC- H_2SO_4 [10%] FT-IR spectrum exhibited in the three cycles all the signals related with the

H_2SO_4 controls; however, in the first cycle, the spectrum showed a band at 1000–1200 cm–1 that is different from the controls. After that cycle, the spectrum looks more like the controls and the signal at 1000–1200 cm^{-1} is not observed. The FT-IR analysis of the $KMnO_4$ displayed the same signals previously observed at 970–1030, 1000–1200, 1200–1500, and 1500–1700 cm^{-1}; however, these signals exhibited reductions in their intensity through the cycles. The signal that had the most significant reduction was the 1000–1200 cm^{-1} band; the signal is large at the first cycle, reduced in more than 50% in the second cycle and did not appear in the third cycle. This reduction indicates low quantity of compounds with C–O and/or Si–O linkages in the liquid samples. The band at 1200–1500 cm^{-1} shrank after each cycle; however, this band is the highest peak in each spectrum. This band is associated with different types of carbon bonds such as C–O–C, C–OH, C–H and C=H. The band at 1500–1700 cm^{-1} had similar intensity in the three cycles. As mentioned before, the third cycle displayed a purple color associated with the remaining $KMnO_4$; this color is correlated with the signal at 910 cm^{-1}, which was only identified in the third cycle. The ATC-NaOH [10%] had a reduction in its two principal signals 1000–1200 and 1200–1500 cm^{-1}. Between the first and the second cycle the reduction was larger than between the second and third cycle. Similar to the $KMnO_4$ treatment, the most intense signal was the 1200–1500 cm^{-1}. In the ATC-NaOH [10%] and ATC- $KMnO_4$ [10%] treatments, the reduction in the signals at 1000–1200 and 1200–1500 cm^{-1} can be associated with the drop in the absorbance in the UV-Vis analysis of the liquid and the reduction in the carbon content observed in the compositional analysis of the biochar. These results evidence the biochar

depolymerization and the consequent production of new components in the liquid phase after each cycle.

Analysis of the depolymerization products

The depolymerization products after the ATC-KMnO4 [10%] treatment were evaluated to identify and characterize the compounds generated. The first step was the rotovaporation. After the rotovaporation of 50 mL of sample approximately 5mL of a brownish liquid was obtained. Samples from this brownish liquid were mixed with solvents with different polarity. The liquid formed two phases with all the nonpolar solvents (hexane, ethyl acetate, acetonitrile) evidencing a polar nature. The samples could mix with methanol; however, when the liquid was mixed with large quantities of methanol a white precipitate was produced. After the production of this white precipitate, a methanol precipitation was performed using the depolymerized liquid without rotovaporation. In this experiment, the liquid solution with methanol exhibited a considerable precipitation. The compound produced had a beige color, was soluble in polar liquids as water or methanol, highly hygroscopic and its consistency varied depending on how long it is exposed to the environment.

The FT-IR spectroscopy (Figure 19) was used to analyze the pellet produced. The spectrum has two large signals at 611 and 1100 cm^{-1} and 5 other small signals (900, 984, 1335, 1425, and 1585). On one hand, the signal at 611 cm^{-1} is related with the pure Si–O stretching or the Si–Si linkage and the 1100 cm^{-1} signal is associated with C–O and Si–O bonds. On the other hand, The 1585 cm^{-1} peak is related with C=C bonds, the

1425 cm^{-1} is associated with C–N stretching, and 1335 cm^{-1} is associated with Si–O bonds. The results obtained from the FT-IR suggest that the pellet is a compound rich in Si–O bonds. When the spectrum of the precipitate was compared with the spectrometer's library, the search did not generate any compound with the same spectra. Nevertheless, the largest signals observed in the precipitate were found in the spectra of compounds with silicon such silica, silicates and siloxanes.

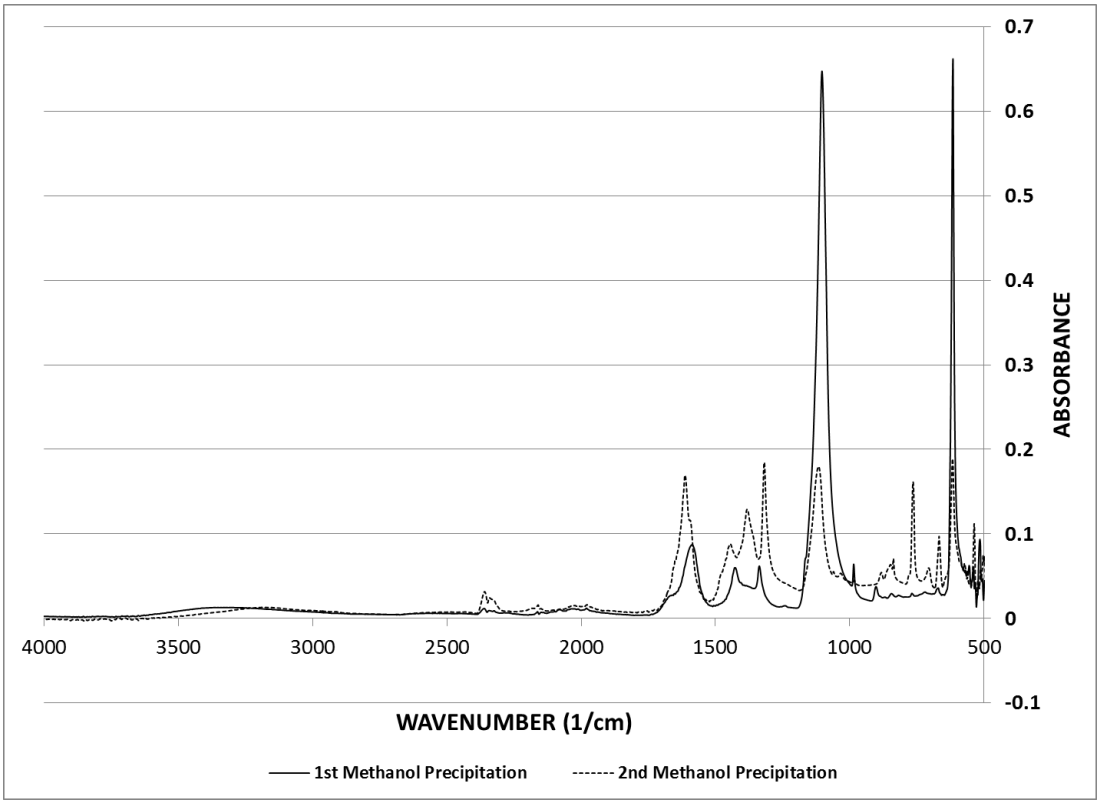

Figure 19. FT-IR spectra of the solids produced by methanol precipitation

The production yield of the silicon compounds was 400mg/5g biochar. In fact, keeping the same yield, it will be possible to produce 80kg of these compounds from each ton of cotton wastes gasification biochar. Depending of the compound quality, the selling price of each kilogram can oscillate between 10 and 200 dollars. The quality and properties of the silicon compounds produced from the biochar is part of the future work related with this investigation.

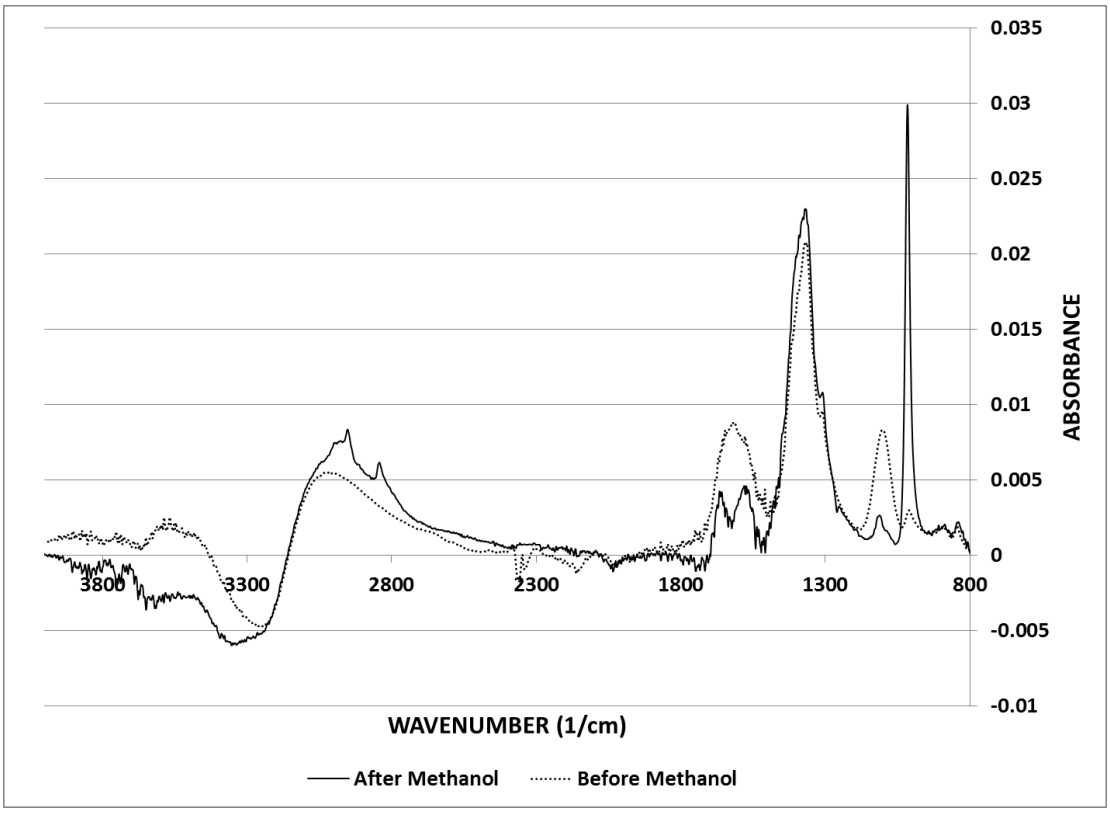

Figure 20. FT-IR spectra of the liquid phase after and before methanol precipitation

After the pellet removal, the supernatant was rotovaporated to take out the methanol and evaluate the changes in the liquid phase spectrum (Figure 20). The most significant modifications in the spectra were the large reduction in the 1100 cm^{-1} signal (Si–O), the considerable increment in the 1010 cm^{-1} (Si–O bond or C–O chemical bonds), and the split of the 1500–1800 cm^{-1} band in two peaks at 1680 and at 1580 cm^{-1}. The effect of the methanol precipitation in the liquid phase was evidenced principally in the 1100 cm^{-1} signal, this signal reduced in the supernatant and increased in the precipitated solid. This is an evidence of the production of silicon related compounds from biochar. Using the ATC-H_2O treatment was possible to produce a methanol precipitate; however, this compound exhibited a different FT-IR spectrum compared with the ATC-$KMnO_4$ [10%] precipitate. Additionally, the water control produced low quantity of precipitate (50mg) compared with the ATC-$KMnO_4$ [10%] (400mg).

After the FT-IR analysis, the rotovaporated sample was dried at 105 ºC, the solid obtained had a dark brown color and some small crystals inside. To remove the crystals a second methanol extraction was performed. In this case three components where produced, first a solid phase, second a brownish color liquid and third an uncolored liquid. The brownish and uncolored liquids were immiscible which allowed their separation. The brownish liquid and the solid obtained were evaluated using the FT-IR spectra. The solid precipitated has a beige color and a strong polar nature and less hygroscopic than the first precipitate. The FT-IR spectrum of the solid part is showed in Figure 19. This spectrum exhibited 5 strong signals 611 cm^{-1} (Si–O or Si–Si linkages), 763 cm^{-1} (C–H benzene ring), 1110 cm^{-1} (C–O–C interaction or Si–O bonds), 1319 cm^{-1}

(C–OH bending vibration), and 1614 cm^{-1} ($–COO^-$ anti-symmetric stretching); 4 medium size signals 665 cm^{-1} (COO^-), 1381 cm^{-1} (C–OH), and 1445 cm^{-1}(OH), and 3 small ones (705 cm^{-1}, 848 cm^{-1}, and 880 cm^{-1}). Different than the first solid, the second precipitate has lower signals in the Si–O signals, which indicates lower levels of silicon. One on hand, this compound can be the mixture of different substances which explain the significant intensity in the carbon related signals. On the other hand, this precipitate can be a carbon silicon mixture that can be synthetized after the $KMnO_4$ treatment in the biochar. Further tests need to be done for the identification of the compounds produced after the reaction between $KMnO_4$ and the cotton wastes biochar.

The production of silicon related compounds from pyrolysis and gasification biochar has been studied principally in rice husk; however, in that biomass, the silica is produced directly from the pyrolysis of the rice husks and can be later transformed in other compounds (Shen et al., 2014; Li et al., 2012). In cotton wastes biochar, the production of silicon related compounds were a result of the treatment ATC-KMnO4 [10%]. The production of silicon related compounds from biochar using KMnO4 has not been reported in other biochar or biomass. However, the $KMnO_4$ has been used as pretreatment for the production of crystal and amorphous silica from rice husk (Javed et al., 2010). In this case, the rice husk silica was produced by a combustion process after the $KMnO_4$ treatment. In rice husk, the $KMnO_4$ acted reduced the organic compounds in the rice husk and act as an oxidizing agent during thermal degradation. In cotton stalks, the $KMnO_4$ can transform the biochar's organic compounds and lead to the releasing of biochar's silicon compounds. Additionally, $KMnO_4$ can catalyze the reaction between

the existing silicon compounds and the organic compounds in the biochar. Based in the FT-IR spectra information is possible to assume that silica or silane related compounds were produced from the reaction of biochar and $KMnO_4$ under autoclave conditions. Further investigations in the production of silicon related compounds from cotton wastes biochar will need to optimize the production of silicon related compounds, standardize the extraction and purification methodology and complete the identification of the silicon compounds produced by using more specific techniques.

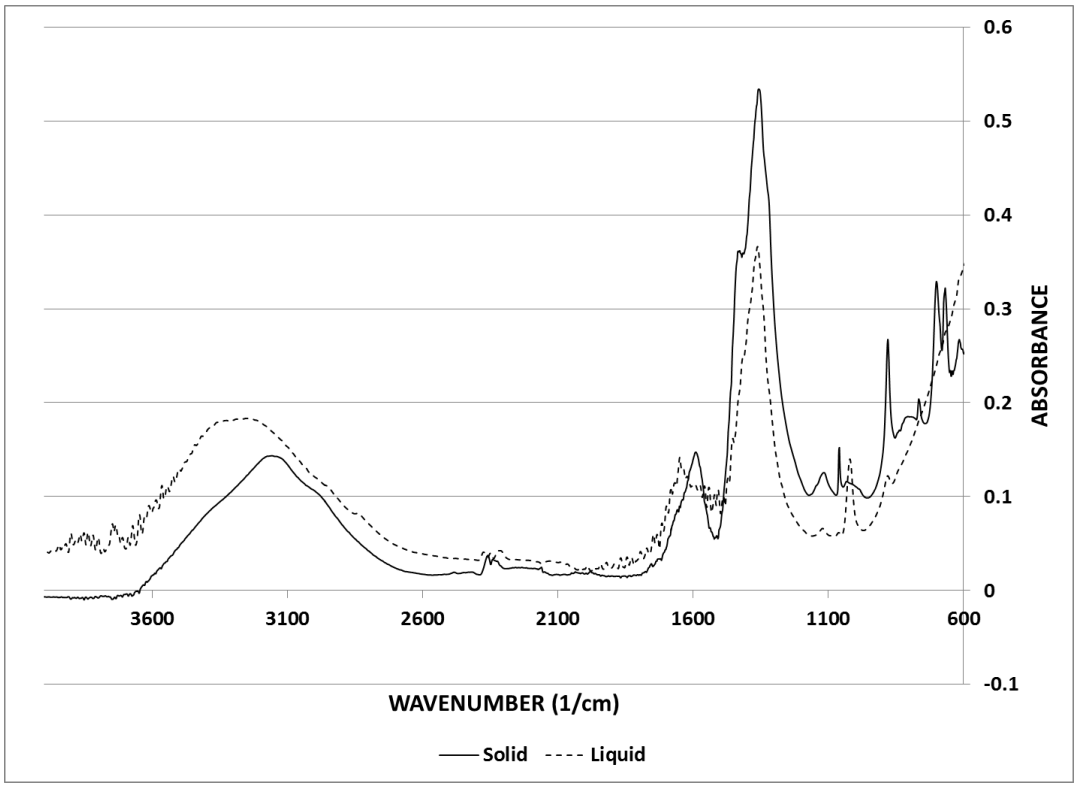

Figure 21. FT-IR spectra of the brown compound produced after the second methanol addition

The brownish liquid produced from the second precipitation was analyzed in its solid form and liquid form using the FT-IR spectra (Figure 21). On one hand, the liquid sample has 4 strong signals a peak at 1010 cm^{-1}, and three wide bands 1200–1500 cm^{-1}, 1500–1800 cm^{-1}, and 2500-3800 cm^{-1}. The strongest signal is obtained in the band of 1200–1500; the largest absorbance was identified at 1365 cm^{-1}. These specific signal and band corresponds with the largest signal observed in the liquid phase after the biochar depolymerization. The strongest band was the 1200–1500 cm^{-1} band and is related with C–O–C and C–OH bending. The largest peak at 1365 cm^{-1} represents C–H bonds. The 1500–1700 cm^{-1} band reveals aromatic rings double bonds. The 2500-3800 cm^{-1} band was only observed in this liquid and it is associated with the O-H and N-H stretching. On the other hand, the solid sample presented bands at 1200–1500 cm^{-1}, 1500–1800 cm^{-1}, and 2500-3800 cm^{-1}, 3 medium intensity signals 665 cm^{-1} (COO^{-}), 705 cm^{-1} (C–H), 880 cm^{-1}(Si–O and Si–H), and 4 low intensity signals 611 cm^{-1} (Si–Si and Si–O), 1110 cm^{-1} (Si–O), 1050 cm^{-1} (primary alcohols). The new peaks observed in the brown solid compared with the brown liquid, indicates similar silicon particles than the second solid. This association can be made because the brownish solid (Figure 21) and the second precipitate (Figure 19) share some of the medium and small size signals.

The brown liquid can be associated with humic substances and principally with fulvic acids. The reasons of that association are: first, the sample did not have precipitates after a pH reduction below 2. The only humic substance soluble at pH below 2 is the fulvic acids. Second, the FT-IR spectra of the brown liquid is similar to the FT-IR spectra obtained in fulvic acids obtained from composting (Ait Baddi et al., 2004),

laurentian fulvic acid (Wang et al., 1990), fulvic fractions obtained by acetone extraction(Gessa et al., 1983), swannee river fulvic acid (Elkins and Nelson, 2001). In all these cases, their spectra exhibited similar strong peaks or bands than the brownish liquid produced by the depolymerization of cotton wastes gasification. The production of fulvic acids from biochar has not been reported in any other paper. However, the effect of $KMnO_4$ on organic matter has been evaluated in different subjects as removal agent of organic matter in waters, chlorination activity, and coagulation and sedimentation methodologies. Further studies in the production of fulvic acids from cotton wastes gasification biochar need to confirm the production of fulvic acid by the use of affinity chromatography, characterize the fulvic acids produced, and evaluate the effect of the fulvic acids produced in agricultural crops.

The option of produce fulvic acids and silicon related compounds from cotton wastes gasification biochar opens the door for a new path of research in the biomass thermal conversion, this line of research can increase the income generated from the cotton wastes transformation and can make more competitive the biofuels production compared with the fossil fuels.

CONCLUSIONS

The chemical treatments depolymerized the biochar in other components. The ATC- H_2SO_4 [10%] treatment produced the largest modifications in biochar solid phase, and the ATC-$KMnO_4$ [10%] generated the largest depolymerization. This treatment reduced the carbon content (7%) in the solid phase versus the original biochar, and had

the greatest absorbance at 450 nm in the liquid phase. the ATC-$KMnO_4$ [10%] were partially separated using methanol precipitation. With this methodology, two types of silicon related compounds and a brown liquid associated with fulvic acids were obtained. This research is the first steps in the development of a process to transform cotton wastes biochar into valuable products using chemical treatments.

CHAPTER V

BIODEPOLYMERIZATION OF COTTON WASTES BIOCHAR BY LIGNINOLYTIC MICROORGANISMS

INTRODUCTION

The biomass conversion to biofuels is done principally by biochemical and thermal conversions. In one hand, the Biological conversion is the use of microorganisms or enzymes for the transformation of biomass in biofuels; in there, biogas and bioethanol are the two principal members. On the other hand, thermal conversion is defined as the biomass transformation in chemical compounds using high temperatures at different oxygen conditions. Gasification and pyrolysis are the two most important processes inside the thermal conversion. Gasification is performed at temperatures higher than 500 ºC and small oxygen quantities. In contrast, pyrolysis is conducted at lower temperatures (400-600ºC) and with complete absence of oxygen. In both processes, the final products are synthesis gas, bio-oil and biochar. The syngas can be used directly to produce energy (combustion) or to generate liquid fuels using the Fischer-Tropsch process. The bio-oil can be upgraded to generate liquid biofuels as gasoline, diesel or JP8. The biochar uses are soil amendment (Mukome et al., 2013) and activated carbons (Angın et al., 2013).

The gasification of cotton gin trash and cotton plant trash has been studied at different scales and has been shown as a viable alternative for energy production (Karatas et al., 2013; Maglinao Jr. and Capareda, 2010). The principal product from cotton wastes gasification is syngas (80-90%); nevertheless, 10 to 20% of the biomass is converted to biochar. As described earlier, biochar is the final waste generated from thermal conversion, and there is not a process that can use this byproduct besides soil amendment or activated carbon. To increase the use of thermal conversion as a competitive energy production strategy; it is necessary to develop a process that allows the transformation of biochar in a valuable product.

A new option for biochar utilization is the depolymerization. Depolymerization is the transformation of biochar's complex structures in less recalcitrant compounds. The Biochar's carbon content is around 20 to 40%; however, in that form, it cannot be employed in other process or be consumed by microbes or other organisms. To make this carbon available for consumption, it is necessary to depolymerize the biochar in less recalcitrant compounds. At this moment, the depolymerization of any type of biochar has not been evaluated; nevertheless, the depolymerization of low-rank coal has been performed using physical, chemical and biological treatments (Huang et al., 2013a; Huang et al., 2013b; Hofrichter et al., 1997). Low-rank coal can be related to biochar because both present similar chemical structure and composition (Sadaka et al., 2014).

The biological depolymerization use microorganisms or their enzymes to depolymerize coal using enzymatic and non- enzymatic mechanisms. On one hand, the non-enzymatic mechanisms include production of alkaline substances and chelators.

Bacillus sp. Y7 was capable of solubilize around 40% of lignite in 12 days, this process was carried by the production of an alkaline substance that facilitate the coal transformation (Jiang et al., 2013). Quigley et al., (1988) evaluated several bacterial and fungal strains, and found that *Streptomyces setonii* could depolymerize coal by generating an alkali medium (Quigley et al., 1988). On the other hand, the enzymatic approach employs ligninolytic microorganisms or ligninolytic enzymes. These microorganisms are able to solubilize low-rank coal into different types of products such as humic and fulvic acids using laccase, manganese peroxidase (MnP), and lignin peroxidase (LiP). Selvi et al., (2009) evaluated the depolymerization of three types of low-rank coal (Lignite, Sub bituminous, Bituminous) and different fungal strains. They found *Pleurotus djamor* as the most effective strain to depolymerize lignite, and an inverse relation between the rank of coal and the depolymerization (Selvi et al., 2009). *Phanerochaete chrysosporium* transformed 85% of the coal in smaller molecules, this transformation was mediated by the production of LiP and MnP. Additionally, this study found a relation between the fungal depolymerization and the use of low nitrogen media (Ralph and Catcheside, 1994). *Nematoloma frowardii* b19 and *Clitocybula duseni* b11 transformed coal humic substances, the reaction showed an 80% of discoloration and the formation of yellowish products (Hofrichter et al., 1999). The coal solubilization has been evaluated in different reactor configurations (stirred tank, fluidized bed and packed bed reactors). The best configuration was the stirred tank with a coal weight loss of 24.2% (Oboirien et al., 2013).

The research aim was to select the best ligninolytic microorganism among *Phanerochaete chrysosporium* ATCC 24725, *Ceriporiopsis subvermispora* ATCC 90466, *Postia placenta* ATCC 44394, and *Bjerkandera adusta* ATCC 62023 that can depolymerize cotton wastes biochar and to know the depolymerization kinetic of the selected microorganism.

MATERIALS AND METHODS

Substrate

The biochar was obtained after the gasification process of cotton stalks from J.G Boswell, San Joaquin valley, California. The gasification process was done at 500–600 °C using the TAMU Fluidized Bed Gasifier. It is a 305 mm diameter skid-mounted fluidized bed gasifier with a rating of 70 kg/hr. The Biochar obtained from the gasifier was filtered using a mesh of 255 μm.

Microorganisms

The biological material involved in this research were *Phanerochaete chrysosporium* ATCC 24725, *Ceriporiopsis subvermispora* ATCC 90466, *Postia placenta* ATCC 44394, and *Bjerkandera adusta* ATCC 62023, all of them donated by Dr. Daniel Cullen from the USDA Forest Products Laboratory. The strains were kept in PDA agar at 4ºC until use.

Biological depolymerization experiments

The experiments used the Kirk's culture medium: KH_2PO_4 (0.20 g/L), $MgSO_4.7H_2O$ (0.05 g/L), $CaCl_2$ (0.01g/L), ammonium tartrate (0.22 g/L), glucose (10 g/L), thiamine (0.10 g/L), 10 mL/L of trace elements solutions. Trace elements solution composition: $CuSO_4$ $7H_2O$ (80 mg/L), H_2MoO_4 (50 mg/L), $MnSO_4$ (33 mg/L), $ZnSO_4.7H_2O$ (43 mg/L) and $Fe(SO_4)_3$ (50 mg/L) (Hofrichter et al., 1999). The experiment employed 250 mL Erlenmeyer and 50mL of Kirk's medium. The solution was inoculated with four 10 mm plugs of active mycelium and put it at 150 rpm and 30 °C. The biochar was added to the culture at day 10^{th} to produce a biochar solution of 0.5%. The biochar and the fungus were kept at the previous conditions for other 10 days. The experiment utilized a completely randomized design with four replicates for each fungus. At the end of the experiment, the results were analyzed using the software SAS system 9.3. The depolymerization kinetic was performed to the fungi with the highest biochar depolymerization. The kinetic was executed during 35 days using the same conditions used in the past experiment. The variables evaluated in the depolymerization kinetic were the glucose content, depolymerization, and enzymatic activity.

Enzymatic activities determination

The laccase activity was calculated using the enzymatic oxidation of ABTS (2,2'-azino-bis(3-ethylbenzothiazoline-6-sulphonic acid)). The reaction was followed spectrophotometrically using the change in the absorbance at 420 nm and a molar extinction coefficient of ε_{420}= 36000 $M^{-1}cm^{-1}$. The LiP activity measured the formation

of veratryl aldehyde from veratrly alcohol using the absorbance changes at 310 nm and a molar extinction coefficient of ε_{310}= 9300 $M^{-1}cm^{-1}$. The measurement of the MnP used the absorbance change at 469nm produced by the oxidation of 2,6-dimethoxypenol (DMF) (ε_{469}= 27500 $M^{-1}cm^{-1}$). All the enzymatic activities were reported in units (U), which are defined as the quantity of enzyme that catalyze 1μmol of substrate per minute.

Solid phase analysis

The pretreated and untreated solid samples were analyzed using the Fourier Transform InfraRed (FT-IR) spectroscopy, and the ultimate analysis. The FT-IR (Shimadzu, IR Affinity–1 with a MIRacle universal sampling accessory) was used to evaluate the structural properties of the biochar with and without pretreatments. The infrared spectra collected range from 4000 to 700 cm^{-1} with a resolution of 4 cm^{-1}.

Liquid phase analysis

The liquid phase was analyzed using the FT-IR and the UV-Vis spectroscopy. The FT-IR (Shimadzu, IR Affinity–1 with a MIRacle universal sampling accessory) was used to evaluate the biochar depolymerization by following the production of new signals in the liquid phase's spectrum compared with the controls. The UV-Vis (Perking Elmer) analyses were measurements at specific wavelengths that allowed the evaluation of the biochar's depolymerization degree and some chemical properties of the compounds in the liquid. The degree of depolymerization was measured by the increment in the absorbance at A450 nm (Selvi et al., 2009; Jiang et al., 2013). The

$E_{270/400}$, $E_{465/665}$, $E_{250/365}$, $E_{280/472}$, $E_{280/664}$, $E_{472/664}$, coefficients were calculated to identify some characteristics of the compounds found in the liquid phase (Timofeevna Shirshova et al., 2006). The glucose content was evaluated using High performance liquid chromatography (Waters 2690, Separations Module, Waters Corporation, Milford, MA) equipped with auto sampler, Shodex SP 810 packed column and a Refractive Index (RI) detector. The samples were centrifuged and filter before injection, each sample ran for 20 minutes at a flow rate of 1 mL/min, 60°C using HPLC water as mobile phase.

RESULTS AND DISCUSSION

Biochar biodepolymerization

Experiment optimization

The original experiment design had a solution of 2% of biochar, and the addition of biochar at the beginning of the experiment. However, under these conditions the microorganisms did not growth or showed any modifications to the liquid medium. To overcome the growth inhibition the biochar loading was reduced to 1%; however, at 1% the microbes still exhibited growth inhibition. To favor the fungi growth and biochar depolymerization two modifications were done. First, the biochar loading was reduced to 0.5%, and second, the biochar addition time was modified (10^{th} day). The first modification wanted to reduce the inhibitors in the biochar and the second modification wanted to increase the biomass quantity and the content of cellular metabolites before

the biochar addition. In that way, the fungi can reduce the negative effects of the biochar's presence. These modifications have been used in other applications of ligninolytic fungus with compounds with high level of recalcitrance. Böhemer employed a 10 day spam previous the addition of textile industry wastewater, this approach improved the effluent discoloration and the microbes' strength (Böhmer et al., 2010). Additionally, in the depolymerization of low-rank coal, the coal samples were added within five days of fungal growth (Selvi et al., 2009). Using the above mentioned modifications, the microorganisms produced biomass and/or modifications in the liquid media. The inhibition generated by the biochar concentrations of 1 and 2% was related with the medium's pH after the biochar addition. The Kirk's medium has a pH around 4–4.5; nevertheless, it increased to 9–10 after the biochar addition (1 and 2 %). The modifications performed in the experiment, helped the microorganisms to manage in a better way the changes generated by the biochar.

The microorganisms exhibited clear differences in their growth. On one hand, *C. subvermispora* and *P. chrysosporium* showed low biomass. This low biomass production was related with an inhibition caused by the agitation and the inoculum preparation. When these microbes were not agitated they exhibited large quantities of biomass (data not shown). For that reason, the depolymerization experiment with *P. chrysosporium* was performed under static conditions to avoid the inhibition. This condition is the most favorable for this microbe and has been tested by different authors (Kirby et al., 2000). Although, *C. subvermispora* evidenced an inhibition in the biomass production; it did not show an inhibition in the ligninolytic enzymes production, reason why, the

depolymerization experiment was done under agitation conditions. The agitated conditions were preferred to increase the contact between the biochar particles, the fungi, and their enzymes. The growth inhibition exhibited by *C. subvermispora* under agitated conditions has not been explicit reported by any other studies; however, all the researches using *C. subvermispora* ATCC 90466 (also known as *C. subvermispora* FP 105752-Sp) in agitated cultures, used as inoculum previously prepared homogenized mycelium. This previous preparation consisted in growing mycelial mats during 10 to 15 days under stationary conditions and later breaking the mycelium using a blender (Ruttimann-Johnson et al., 1993).

On the other hand, *B. adusta* and *P. placenta* formed more biomass than the other two fungi. Even though, they have more biomass; the biomass was developed different in both microbes. *B. adusta* grew in a single biomass core from the inoculum plugs. In this case, the inoculum plugs got together in the first days of the treatment and from there a large piece of biomass was formed. Opposite to *B. adusta, P. placenta* developed several pellets from the inoculum plugs; the pellet's size increased with the days, but around day 15 the growth stopped. The microorganisms that produced more biomass were more likely to attach the biochar on the surface of the biomass. The largest adsorption was observed in *B. adusta*. In fact, this fungus was able to remove all the observable particles of biochar from the liquid medium. *P. placenta* adsorbed biochar; however, this microbe had a biochar concentration in the liquid medium greater than *B. adusta*. The ability to absorb aromatic molecules by fungus has been observed in smaller

aromatic compounds such as polycyclic aromatic hydrocarbons, polychlorinated biphenyls, and different types of dyes (Russo et al., 2010).

Ligninolytic enzymes analysis

At the end of the depolymerization experiment, the ligninolytic activities were measured. In this experiment, three microorganisms evidenced at least one type of the ligninolytic enzymes. *P. chrysosporium* was the only microorganism that did not exhibit the production of enzymes. An inhibition of the production of ligninolytic enzymes under static conditions using Kirk's media with low nitrogen media has not been reported for *P. chrysosporium.* The only modification between the depolymerization experiment and other works using *P. chrysosporium* was the presence of biochar. That leads to think in a negative effect created by biochar in the enzymatic production of *P. chrysosporium*. Similar to this experiment, the presence of biochar has been reported to reduce the growth and enzymatic production in different microorganisms (Chen et al., 2013). This inhibition can be related with substances in the biochar that reduced the ability of the fungi to produce enzymes (Ascough et al., 2010). *C. subvermispora* produced laccase and MnP, and the laccase activity was larger than the MnP activity. The production of large quantities of MnP than laccase is an uncommon situation for *C. subvermispora*, which generally produce large quantities of MnP than laccase. However, a significant production of laccase than MnP has been found in cultures of *C. subvermispora* when this microbe is degrading wood particles (Tanaka et al., 2009). *C. subvermispora* exhibited the greatest laccase production (47 U/L) and the second

production of MnP (1.1 U/L). Similar to *C. subvermispora,* the strain RBSlb exhibited an association between the production of laccase and MnP and the depolymerization of low-rank coal. However, the strain RBSlb obtained similar levels of laccase and MnP during the depolymerization (Willmann and Fakoussa, 1997).

Differently to *C. subvermispora*, *P. placenta* only produced laccase, and *B. adusta* just produced MnP. On one hand, the production of laccase from *P. placenta* has been reported in the depolymerization of lignocellulosic structures (Wei et al., 2010). The presence of a like-laccase enzyme was reported by Alfredsen and Fossdal (2010); in this case, the laccase activity was only expressed when the wood was furfurylated (addition of furfuryl alcohol) (Alfredsen and Fossdal, 2010). Similar to that, the production of laccase by *P. placenta* can be associated with furfurals or other compounds attached into the biochar's surface that could activate the laccase's production. Additionally, is important to describe that these activities were just observed under alkaline pH (8–9). *P. placenta* has laccase activity (28U/L) lower than *C. subvermispora*. The production of laccase has been associated with the depolymerization of low-rank coal (Willmann and Fakoussa, 1997); however, the majority of papers report a requirement of LiP or MnP to achieve the depolymerization. On the other hand, the production of MnP by *B. adusta* has been described in the discoloration and detoxification of different dyes and textile wastewaters. The greatest production of MnP was achieved by *B. adusta* (3.4 U/L). Similar to the depolymerization experiment; in these cultures of *B. adusta* the principal enzyme found was MnP (Eichlerová et al., 2007).

UV-Vis and FT-IR analysis

The level of biochar biodepolymerization was measured by the absorbance at 450 nm (Figure 22).

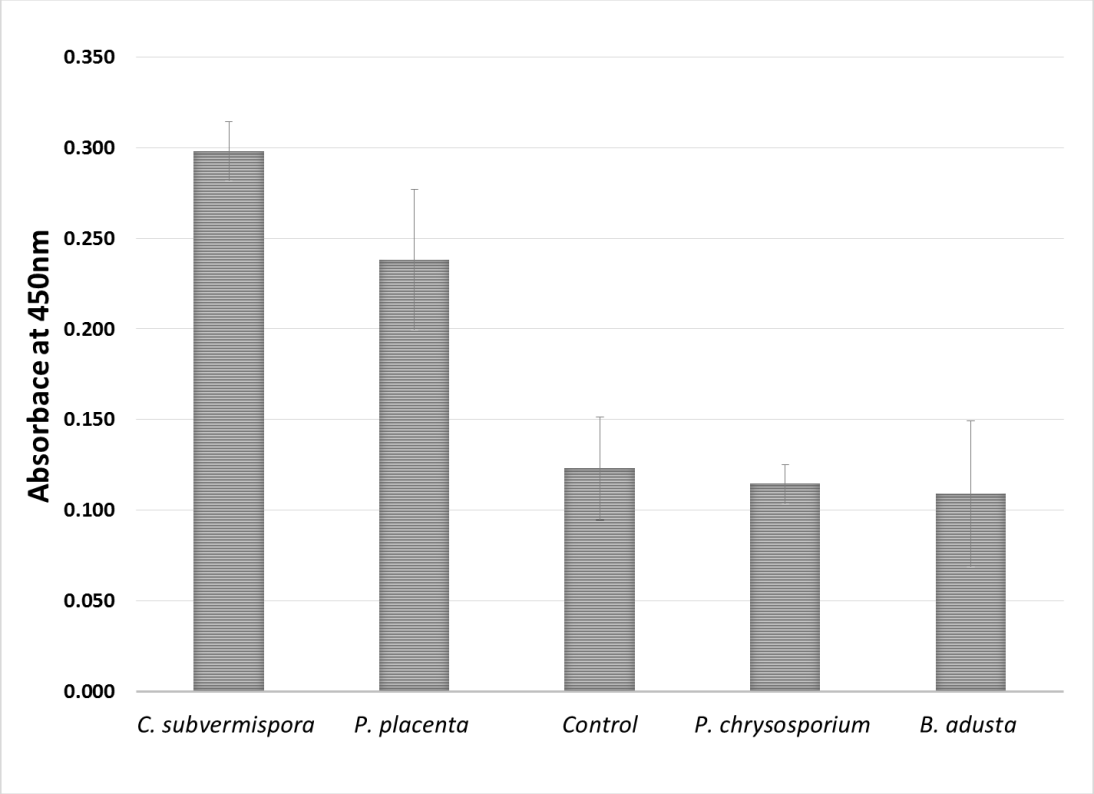

Figure 22. Effect of selected fungal species on biodepolymerization of cotton wastes biochar.

The microorganisms that exhibited the depolymerization were *C. subvermispora* and *P. placenta.* These two treatments had absorbances greater than the control. In fact, *C. subvermispora* incremented the absorbance more than two fold compared with the

control. In contrast, *P. chrysosporium* and *B. adusta* exhibited absorbances lower than the control; however, their differences were not representative.

Table 11. Duncan's multiple range test for the biochar depolymerization at 450 nm

Microorganism	Duncan Grouping[1]	Mean (Abs)	N
Ceriporiopsis subvermispora	A	0.29800	3
Postia placenta	B	0.23833	3
Phanerochaete chrysosporium	C	0.11433	3
Bjerkandera adusta	C	0.10900	3

1. **Means with the same letter are not significantly different**

The differences observed in the Figure 19 were supported statistically using a one way Anova and the Duncan's test (Table 11). This statistical test confirmed *C. subvermispora* as the microorganism that achieved the greatest depolymerization; this can be said because it has significant differences against all the other microorganisms. *C. subvermispora* exhibited the largest production of laccase and MnP, and the largest depolymerization. This correlation between depolymerization and enzymatic activity evidenced the production of laccase and MnP as the most important factor for the biochar depolymerization. This correlation between enzymes production and

depolymerization has been found in low-rank coal and humic substances. However, in these molecules the principal responsible of the catalysis was the MnP. Opposite to low-rank coal, the production of MnP by *B. adusta* did not reflected a high increment in the absorbance at 450 nm. This result can be explained by the lack of production of laccase activity and by the biochar adsorption evidenced in this microbe. The adsorption of the biochar allowed more contact between the microbe and the biochar, which could generated an easier consumption of the depolymerized molecules. The structural differences between low-rank coal and biochar could lead to the necessity of large quantities of laccase for the depolymerization of biochar than low-rank coal. Some of the differences between low-rank coal and biochar are the presence of a large number of substituents in the biochar's aromatic rings. The existence of substituents helps the laccase's catalysis which needs activated substituents to be more effective (Medina et al., 2013). One of the reasons of the depolymerization difference between *C. subvermispora* and the other fungi is probably generated by the simultaneous production of laccase and MnP. In other substances, the synergic effect of both enzymes achieved a greater degradation than the treatments or microorganisms that just have one type of enzyme (Rodrigues et al., 2008).

In addition to the 450 mn absorbance; other significant signals were measured. These absorbances are shown in Table 12. *P. chrysosporium* has the smallest absorbances in the wavelengths below 450 nm; in contrast, *B. adusta* had the lowest absorbances above 450 nm. Different to the absorbances above 450 nm, at 280 and 340 nm, *B. adusta* obtained the largest absorbances of all the fungi. This is an evidence of

aromatic compounds and depolymerization; however, the low absorbance in the other wavelengths indicates the absence of large aromatic compounds like fulvic or humic acids.

Table 12. Absorbances at specific wavelengths for the biodepolymerization experiment's liquid phase.

Wavelength	*P. placenta*	*B. adusta*	*C. subvermispora*	*P. chrysosporium*	*Control*
280 nm	2.928	3.792	3.443	2.405	2.551
340 nm	2.094	2.642	1.343	0.752	0.547
360 nm	1.262	0.893	0.691	0.494	0.371
400 nm	0.488	0.302	0.39	0.2	0.211
436 nm	0.295	0.137	0.316	0.125	0.172
465 nm	0.23	0.089	0.281	0.105	0.155
472nm	0.221	0.067	0.273	0.102	0.152
600 nm	0.105	0.015	0.193	0.07	0.119
664 nm	0.074	0.008	0.164	0.062	0.111

The production of aromatic compounds evidenced by the absorbance at 280 nm was observed in the treatments with high depolymerization. However, the absorbance at 280 nm was associated with increments in the other wavelengths analyzed. The relation

between $E_{280/472}$ describes the presence of aromatic groups in the compounds obtained by the depolymerization such as humic or fulvic acids. *P. placenta* and *C. subvermispora* showed a smaller proportion between these absorbances, different to *B. adusta* which had a greater relation. In that way, *P. placenta* and *C. subvermispora* generated molecules with more aromatic compounds in their structure; opposite to *B. adusta* where the aromatic compounds are not together in a bigger molecule (Uyguner and Bekbolet, 2005). A low absorbance at 436 nm indicates molecules with more aliphatic, carbohydrates or nitriles compounds; whereas high absorbance indicates carboxylic and phenolic groups (Timofeevna Shirshova et al., 2006). The absorbance obtained by *P. placenta* and *C. subvermispora* suggest the presence of carboxylic and phenolic groups in the molecules formed. The coefficient $E_{472/664}$ is associated with the level of condensation of the chain of aromatic carbons. In this coefficient, *P. placenta* and *C. subvermispora* exhibited different behaviors. On one hand, *P. placenta* had a high value, which indicates more aliphatic structures and less condensed aromatic structures. On the other hand, *C. subvermispora* obtained a low value. It indicates large degree of condensation in the chain of aromatic carbons.

The FT-IR analysis of the liquid phase after the depolymerization analysis is shown in the Figure 23. The spectra of the liquid phase exhibited a characteristic band between 950 and 1200 cm^{-1}; this band was observed in all the treatments. However, each treatment exhibited different peaks or intensities in there. The treatments that achieved low depolymerization (*P. chrysosporium* and *B. adusta*) exhibited some similar signals with the controls; however, these signals were shorter than the controls. *P. placenta* and

C. subvermispora exhibited the presence of a new band between 1300 and 1500 cm^{-1}; this band has been associated with C–H bonds (Wolfe et al., 2009). Additionally to this band, *C. subvermispora* generated other band at 1500–1700 cm^{-1}, signals at this position have been associated with compounds with aromatic rings and double bonds.

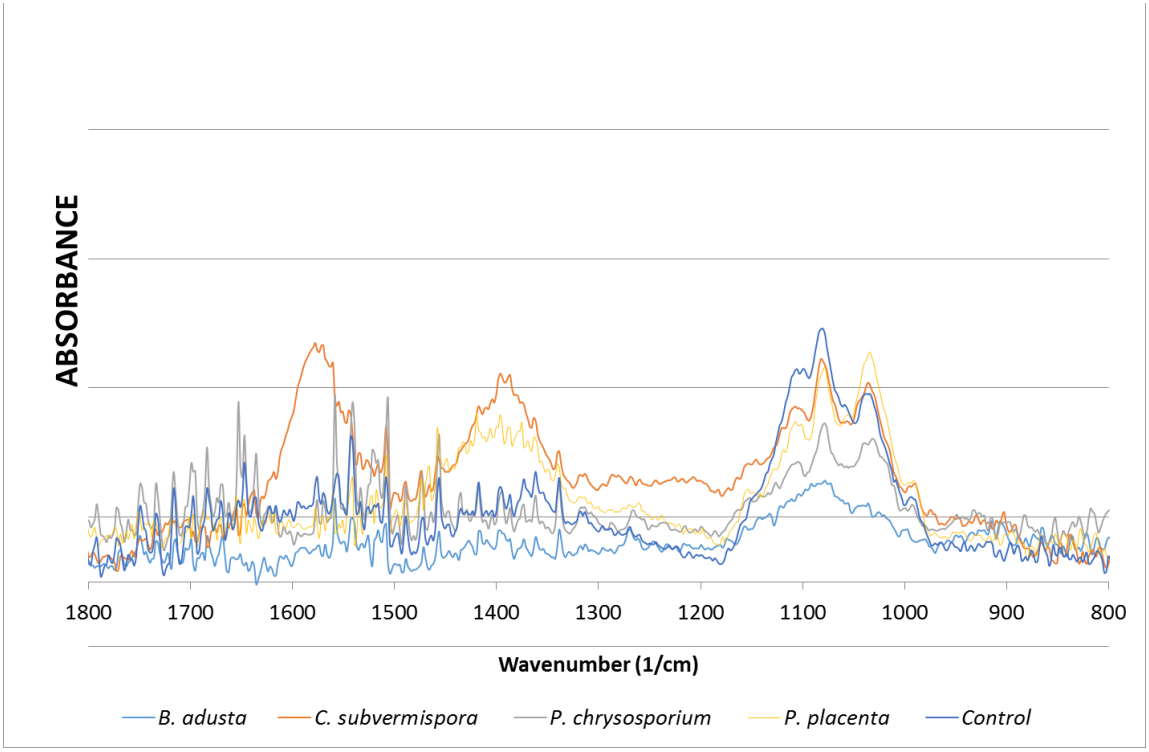

Figure 23. FT-IR spectra of the liquid phase after biochar biodepolymerization by selected fungal species

The FT-IR analysis of the solid phase (Figure 24) detected some changes in the biochar's structure after the biological treatment. The biochar control with the Kirk's

medium evidenced three significant signals 872 cm^{-1}, 900–1200 cm^{-1}, and 1200–1700 cm^{-1}.

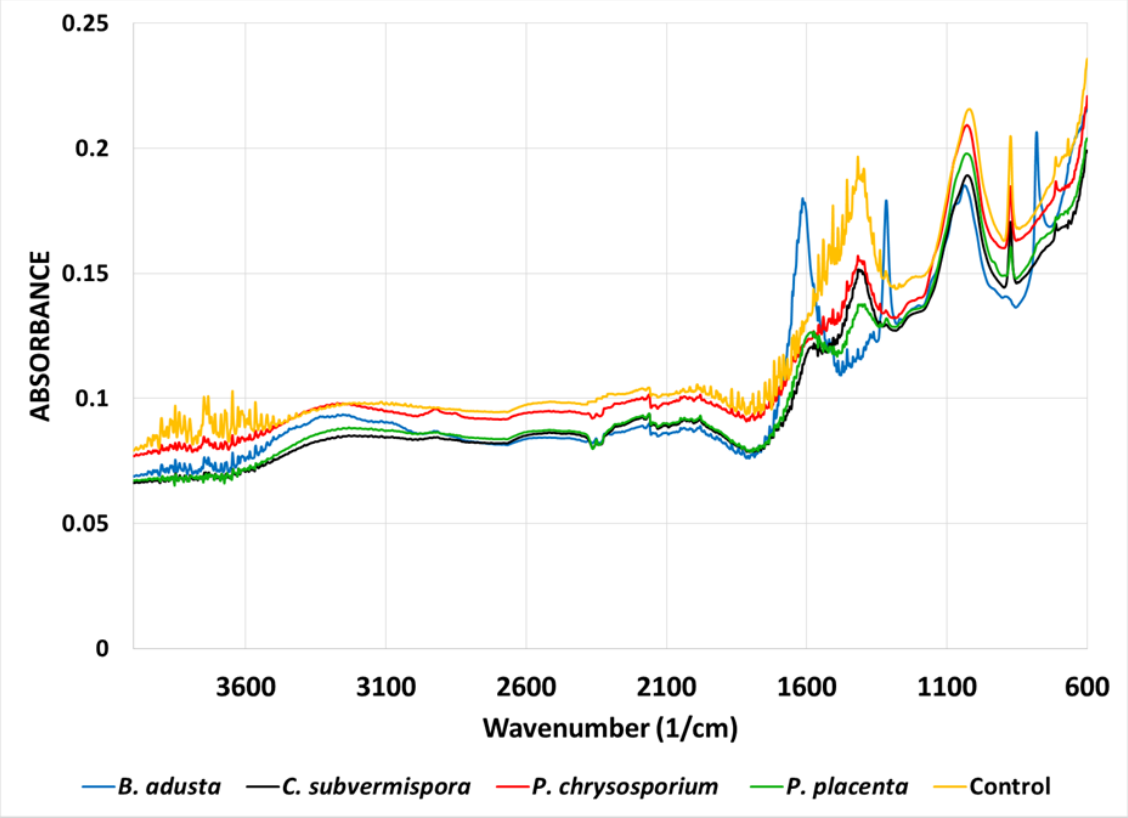

Figure 24. FT-IR spectra of the biochar solid phase biodepolymerization by selected fungal species

The 872 cm^{-1} signal is associated with lone aromatic C–H wag which indicates aromatic hydrogens (Kaal et al., 2012). The band between 900 and 1200 cm^{-1} has the maximum point at 1030 cm^{-1}, and is correlated with the Si–O stretching. Silica

compounds make part of biochar because they are part of the gasification system's bed material. Finally, the band between 1200 and 1700 cm^{-1} has the highest peak at 1396 cm^{-1}. This peak is associated with the $–COO^-$ symmetric stretching (Xu et al., 2011). The solid phase after the *B. adusta* treatment exhibited the most significant modifications in the FT-IR spectrum. The biochar in this case exhibited three new bands, two narrow peaks at 783 and 1311 cm–1 and a broad band between 1500 and 1700 cm^{-1}. Additionally, the biochar from this treatment evidence the disappearance of the signals at 872 cm^{-1} and the 1200–1700 cm^{-1}.The band at 900–1200 cm^{-1} did not showed significant modifications compared with the control's biochar. The strong difference between the control and this treatment is related with the large biochar adsorption in the biomass. This adsorption produced a solid phase with biochar and biomass particles together, union that created a substantial change in the FT-IR spectra. *P. chrysosporium* exhibited a peak profile with three signals, 872, 900–1200, and 1300–1500 cm^{-1}. The first two signals were observed in the control; however, in this treatment the absorbances were slightly lower. The greatest change was at 1300–1500 cm^{-1}, which is a new band that replaced the 1500–1700 cm^{-1} band. Additionally, this new band has a significant reduction in absorbance versus the control. *P. placenta* and *C. subvermispora* exhibited similar signals at 872, 900–1200, 1300–1500, and 1500–1700 cm^{-1}. The differences between both treatments were the signal's intensity. *P. placenta* has higher absorbances at 900–1200 and 1500–1700 cm^{-1}, and *C. subvermispora* exhibited stronger signals at 872 and 1300–1500 cm^{-1}. The most substantial differences between both treatments and the control were observed at 872 cm^{-1}. In this signal both treatments significantly

reduced the signal's intensity. This peak is related with aromatic carbons (Kaal et al., 2012). The reduction in these signals and the increment in the 450 nm absorbance can be associated with the biochar biodepolymerization because the enzymes found in these microbes (laccase and MnP) catalyze reactions with this type of compounds. Another important change between these two treatments and the control occurred at 1200–1700 cm^{-1}. The treatments transformed the large band at 1200–1700 cm^{-1} in two bands at 1300–1500 and 1500–1700 cm^{-1}. These two bands are associated with aromatic compounds and C–H bonds.

Depolymerization kinetic

The depolymerization kinetic evaluated the changes in the liquid phase of *P. placenta* and *C. subvermispora* cultures through time. The experiment employed a destructive sampling methodology for 35 days and followed the next variables, enzymatic activities, depolymerization at 450 nm, glucose concentration, UV-Vis spectra and FT-IR spectra. Figure 25 shows the depolymerization kinetic of *C. subvermispora.* Similar to the previous observation this fungus did not showed a significant increment in its biomass, this low quantity of biomass can be related with an inhibition by the agitation. Similar to the previous experiment, this microbe exhibited two types of ligninolytic enzymes through the kinetic; laccase and MnP. This microbe did not produce LiP. Laccase was the enzyme greatest produced followed by MnP, Figure 25 shows two production peaks, a small one during days 8 and 10 and a large peak during days 24 to 27.

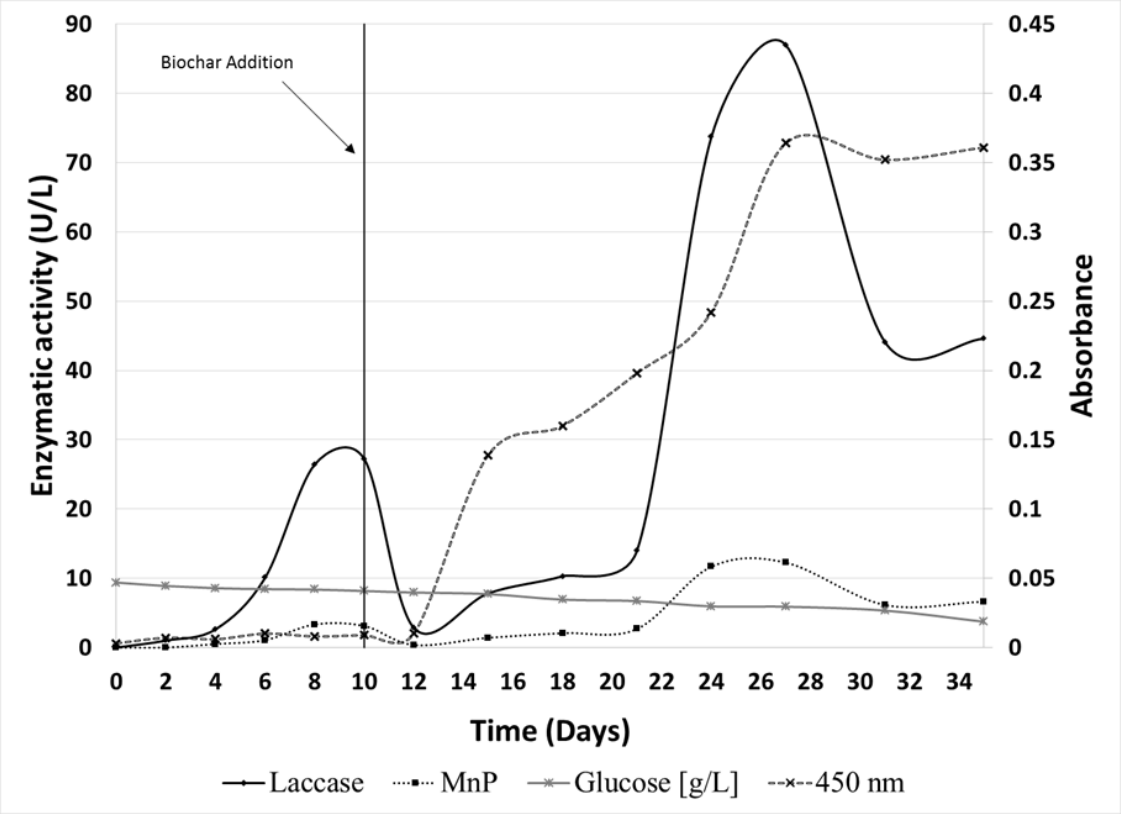

Figure 25. Cotton wastes biochar depolymerization in relation to the production of ligninolytic enzymes by *C. subvermispora*

The initial increment in the laccase production dropped after the biochar addition. However, after that drop, the laccase production achieved its maximum at day 27 (87 U/L). The MnP production had the same production profile than laccase activity, with two production peaks. Similar to laccase, the maximum activity obtained by MnP was achieved at day 27 (12 U/L). These results evidence that the ligninolytic enzymes production by *C. subvermispora* was not associated with the secondary metabolism. In fact, the microorganism was capable to produce enzymes in every stage of the kinetic. This finding coincides with other studies with *C. subvermispora;* where laccase and

MnP were secreted during the growing and stationary phase (Catcheside and Ralph, 1999).

The biochar was added at day 10; however, the absorbance at 450 nm kept low values until day 12. After day 12, the absorbance constantly increased until day 27 when the depolymerization achieved a stationary phase. The absorbance increment coincides with the production of the enzymatic activities; this association confirms the relationship between biochar depolymerization and the production of laccase and MnP. This relation between depolymerization and enzyme production was reported in the depolymerization of low-rank coal by *Nematoloma frowardii b19.* This fungus showed large quantities of MnP which allowed the increment of the 450 nm absorbance by the production of fulvic and humic acids (Hofrichter et al., 1999). The glucose consumption by *C. subvermispora* was small (Figure 25). In fact, at the end of the kinetic (day 35) was possible to detect significant glucose remaining (4g/L). Glucose concentration reduced following a linear pattern during the kinetic; however, this linear patter evidenced two different slopes one between days 0 and 12, and other between day 15 and 35. The first one was around 0.11 g/day; whereas the second was around 0.15g/d. This augment in glucose consumption correlates with the days with the largest enzymes production; in that way, the increment in enzyme production increased the fungus' glucose needs. The UV-Vis spectra at different days are in Figure 26.

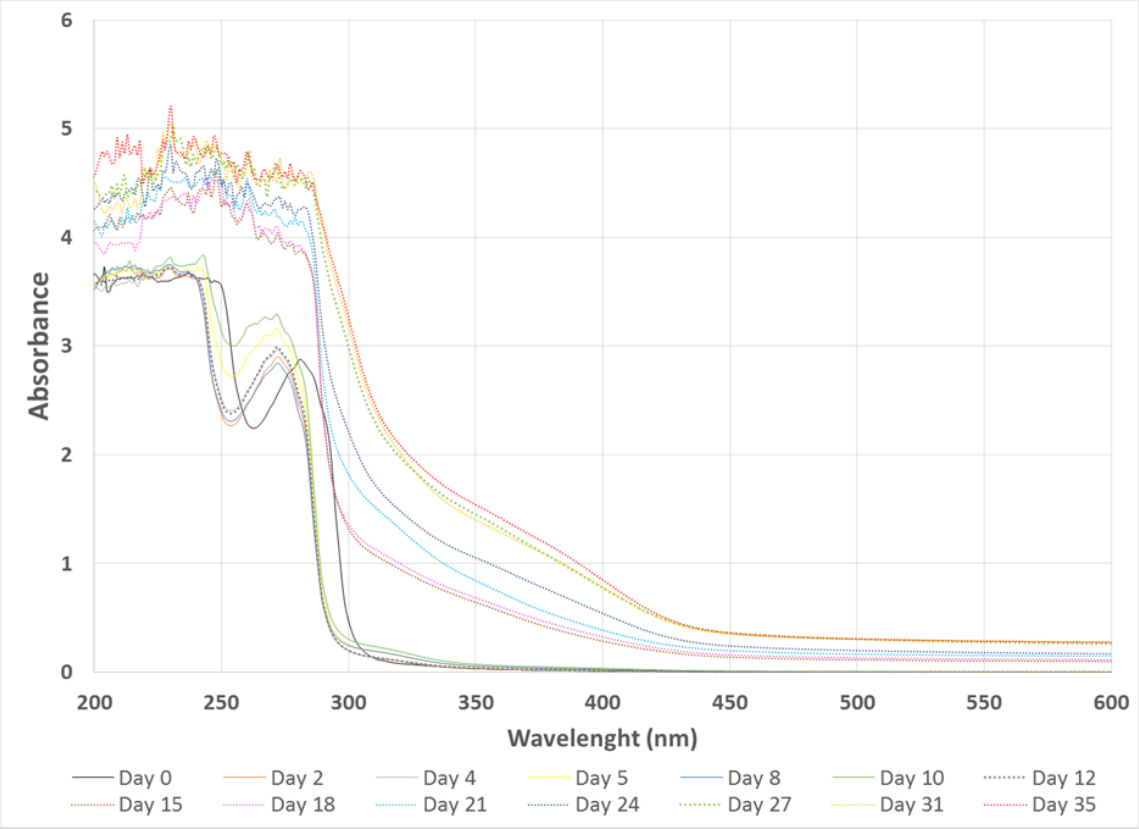

Figure 26. UV-Vis spectra of the liquid phase of the depolymerization kinetic of experiment *C. subvermispora***.**

The UV-Vis spectra exhibited the most considerable variations after day 15 and were detected between 450 nm and 300 nm. This spectrum zone is associated with the fulvic and humic acids production. Additionally, the spectrum evidenced an increment in this band from day 15 to 27; after day 27 the increments in the absorbance were smaller. This behavior agrees with the observed in the 450 nm absorbance. The absorbance at 436 nm increased with the days, specially the last 10 days. The augment in this wavelength evidenced an increment in the compounds with carboxylic and phenolic

groups (Timofeevna Shirshova et al., 2006). The relation between $E_{280/472}$ decreased when the days pass by and principally when the ligninolytic enzymes were formed. This relation evidence an increment with time in the compounds with large number of aromatic compounds in their structures (Uyguner and Bekbolet, 2005). The increment in the UV-Vis signals at 450 nm and the variations obtained in the other wavelengths have been related with the production of fulvic a humic substances from low-rank coal. This relationship indicates that fulvic and humic acids were produced from the biochar.

The FT-IR analysis (Figure 27) exhibited three significant bands similar as the previous experiment (900–1200, 1300–1500, and 1500–1700 cm^{-1}). The largest modifications were observed at the 1300–1500, and 1500–1700 cm^{-1} bands. In the initial days several signals at these wavenumbers are observed; however, after day 15, these signals start to get together forming a broad band. On one hand, the broad band at 1300–1500 cm^{-1} has its maximum at 1395 cm^{-1} and 1390 cm^{-1}. The first signal is associated with acid groups; whereas the second corresponds to C–H bending vibrations. On the other hand, 1500–1700 cm^{-1} band exhibited its maximum at 1575 cm^{-1}; signal associated with aromatic rings and carboxylic acids.

The depolymerization of biochar using *C. subvermispora* is explained by the production of ligninolytic enzymes. The two ligninolytic enzymes generated by this microbe were laccase and MnP. On one hand, Laccases are principally associated with the catalysis of phenolic aromatics. However, these types of enzymes are known for their lack of specificity; which allows them to catalysis different type of molecules.

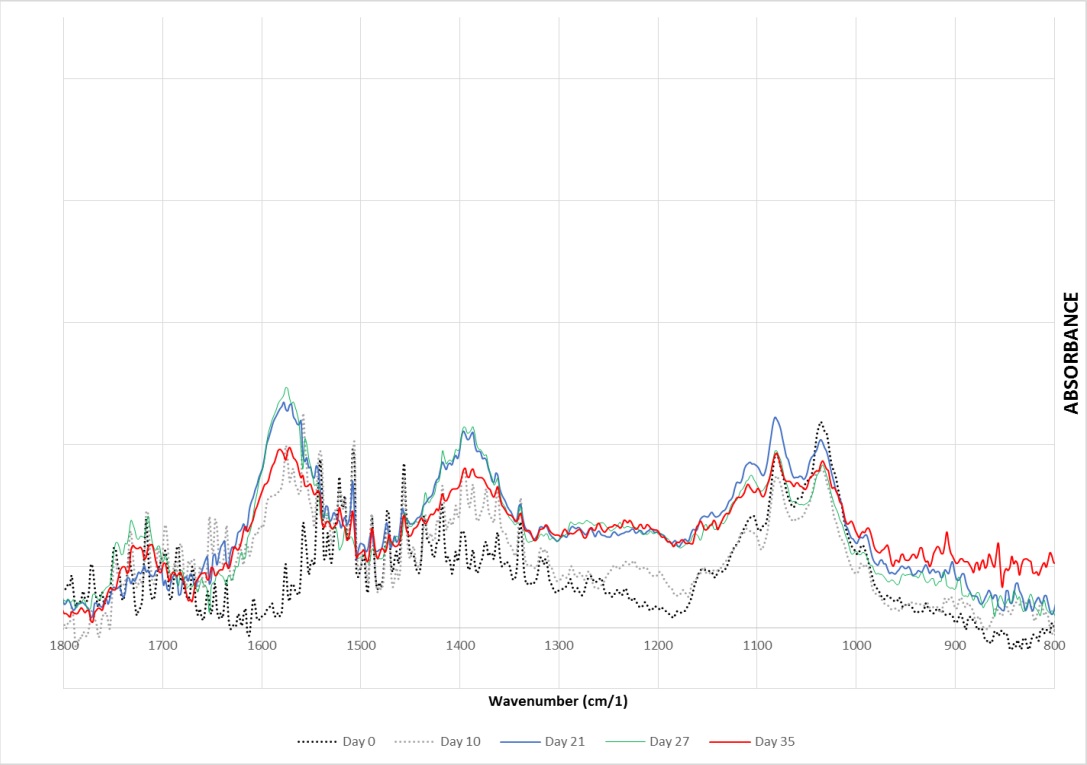

Figure 27. FT-IR spectra of the liquid phase of the depolymerization kinetic of experiment *C. subvermispora.*

On the other hand, MnP is associated with the cleavage of aromatic structures with or without phenols. This ability is associated with the production of Mn(III), a low size and high oxidative power ion, that ion attack molecules like phenols, some methoxylated aromatics, chloroaromatics, and organic acids (Fakoussa and Hofrichter, 1999). The research of Keiluweit et al, (2010) separated the gasification biochar in fourth groups, transition chars, amorphous chars, composite chars and turbostratic chars. The cotton wastes biochar can be described as a composite biochar, because the temperature at which the gasification process was performed. This type of biochar is

composed by phenols, quinones, pyrroles and small polyaromatic units linked with graphitic crystallites. The ligninolytic enzymes can attack some of the amorphous structures and initiate the degradation of other molecules inside the biochar. Additionally, Similar as observed in nature, MnP and laccases can act synergistically to depolymerize the biochar structure. As mentioned before, the biodepolymerization of low-rank coal is associated with the MnP catalysis and in minor level with the laccase activity. In biochar biodepolymerization using *C. subvermispora*, the laccase activity exhibited the largest production. This increment in the laccase activity can be related with the structural differences evidenced by biochar and the low-rank coal. The biochar has more substituents in the aromatic structures which facilitate the laccase's catalysis and production. Further studies need to evaluate in-vitro the capacity of laccase and MnP to depolymerize biochar structures. It is necessary to screen a great number of microorganisms to guarantee the most effective process to depolymerize biochar. Additionally, it will be necessary to evaluate the effect of other types of biochar to find if it is an association between the biochar's origin and the level of depolymerization.

CONCLUSIONS

Gasification biochar can be solubilized when is treated with adequate microorganisms. *C. subvermispora* was the most efficient strain to depolymerize the gasification biochar compared with the other fungus tested. The catalysis by laccase and

MnP was the principal factor in the depolymerization of biochar. The greatest depolymerization with *C. subvermispora* was obtained after 27days of culture and an association between the increment in the depolymerization and the increment in the ligninolytic enzymes was found. The UV-Vis and FT-IR analyses exhibited that substances with chemical similitude to humic substances were formed from biochar. These results pave a way in the development of a biological process that can transform biochar in other compounds using ligninolytic fungus.

CHAPTER VI

CONCLUSIONS

The use of ligninolytic enzymes have been proved as an option in the production of biofuels from cotton wastes. Ligninolytic enzymes can be useful in the transformation of cotton gin trash in ethanol and the ligninolytic fungus can be used to transform the cotton wastes biochar in other substances.

The best pretreatment combination was the sequential use of ultrasonication, hot water and ligninolytic enzymes (U+HW+E). The use of U+HW+E pretreatment combination released high amounts of sugars increased delignification and modified the cellulose structure of the CGT confirmed by the FT-IR spectrum.

The addition of alkali-ultrasonication pretreatment to hot liquid water and ligninolytic enzyme pretreatments increased the cellulose conversion in 9–18% and the ethanol yield in 16-35% versus the treatment without alkali-ultrasonication. The U-NaOH15%+HW+E pretreatment exhibited the highest cellulose conversion (41%) and ethanol yield (64%).

It is necessary to improve the hot liquid water conditions to achieve a more significant increment in the production of ethanol from cotton gin trash using the combination of pretreatments selected in this dissertation.

FT-IR and principal components were effective methodologies to identify the variations in the signal of the cellulose, hemicellulose, and lignin from CGT after the different pretreatments.

The PCA of the FT-IR spectra could separate and identify the CGT biomass from different types of pretreatments and identify the signals with the most variation inside the spectra. In the future, this type of discrimination technique can be used in the bioethanol industry for quality control and prediction analysis.

The chemical treatments depolymerized the biochar in other components. The ATC- H_2SO_4 [10%] treatment produced the greatest modifications in the biochar solid phase and the ATC-$KMnO_4$ [10%] generated the largest depolymerization in the liquid phase. ATC-$KMnO_4$ [10%] reduced the carbon content (7%) in the solid phase versus the original biochar, and had the greatest absorbance at 450 nm in the liquid phase.

The biochar can be recycled using the ATC-$KMnO_4$ [10%] treatment until the carbon content is depleted; in that way, the recycling will allow a complete use of the biochar produced in the gasification of cotton wastes.

It was possible to separate some of the compounds produced from ATC-$KMnO_4$ [10%] by methanol precipitation and rotovaporation. With this methodology, two types of silicon related compounds and a brown liquid associated with fulvic acids were obtained.

C. subvermispora was the most efficient strain to depolymerize the gasification biochar compared with the other fungus tested. The catalysis by laccase and MnP was the principal factor in the depolymerization of biochar.

The biochar depolymerization was associated with the production of laccase and manganese peroxidase by *C. subvermispora*; this is an evidence of the possibility of use biological treatments to produce chemical substances from the biochar.

Chemical depolymerization using ATC-$KMnO_4$ is a more efficient technology than biological depolymerization using *C. subvermispora* to produce modifications in the biochar liquid and solid phases, and to generate a large number and quantity of compounds.

Further studies should evaluate the effect of biochar from other feedstocks and from other thermal conditions in the chemical and biological depolymerization. Additionally, further investigations should focus in the complete identification of the depolymerization products and to improve the purification technologies.

REFERENCES

1. Agblevor, F.A., Cundiff, J.S., Mingle, C., Li, W., 2006. Storage and characterization of cotton gin waste for ethanol production, Resour. Conserv. Recycling. 46, 198-216.

2. Agblevor, F., Batz, S., Trumbo, J., 2003. Composition and ethanol production potential of cotton gin residues, Appl. Biochem. Biotechnol. 105, 219-230.

3. Ait Baddi, G., Hafidi, M., Cegarra, J., Alburquerque, J.A., Gonzálvez, J., Gilard, V., Revel, J., 2004. Characterization of fulvic acids by elemental and spectroscopic (FTIR and 13C-NMR) analyses during composting of olive mill wastes plus straw, Bioresour. Technol. 93, 285-290.

4. Akpinar, O., Ak, O., Kavas, A., Bakir, U., Yilmaz, L., 2007. Enzymatic production of xylooligosaccharides from cotton stalks, J. Agric. Food Chem. 55, 5544-5551.

5. Albrecht, R., Le Petit, J., Terrom, G., Périssol, C., 2011. Comparison between UV spectroscopy and nirs to assess humification process during sewage sludge and green wastes co-composting, Bioresour. Technol. 102, 4495-4500.

6. Alfredsen, G., Fossdal, C.G., 2010. *Postia placenta* gene expression during growth in furfurylated wood, Proceedings of The International Research Group On Wood Protection, 41th Annual Conference, Biarritz, France. IRG/WP 10-10734: 1-9.

7. Angel T., M., 2002. Molecular biology and structure-function of lignin-degrading heme peroxidases, Enzyme Microb. Technol. 30, 425-444.

8. Angın, D., Köse, T.E., Selengil, U., 2013. Production and characterization of activated carbon prepared from safflower seed cake biochar and its ability to absorb reactive dyestuff, Appl. Surf. Sci. 280, 705-710.

9. Aquino, F.L., Capareda, S.C., Parnell Jr., C.B., 2010. Elucidating the solid, liquid, and gaseous products from batch pyrolysis of cotton gin trash, Transactions of the ASABE. 53, 651-658.

10. Archibald, F.S., Bourbonnais, R., Jurasek, L., Paice, M.G., Reid, I.D., 1997. Kraft pulp bleaching and delignification by Trametes versicolor, J. Biotechnol. 53, 215-236.

11. Ascough, P.L., Sturrock, C.J., Bird, M.I., 2010. Investigation of growth responses in saprophytic fungi to charred biomass, Isotopes Environ. Health Stud. 46, 64-77.

12. Babot, E.D., Rico, A., Rencoret, J., Kalum, L., Lund, H., Romero, J., del Río, J.C., Martínez, ÁT., Gutiérrez, A., 2011. Towards industrially-feasible delignification and

pitch removal by treating paper pulp with *Myceliophthora thermophila* laccase and a phenolic mediator, Bioresour. Technol. 102, 6717-6722.

13. Bajwa, S.G., Bajwa, D.S., Holt, G., Coffelt, T., Nakayama, F., 2011. Properties of thermoplastic composites with cotton and guayule biomass residues as fiber fillers, Industrial Crops and Products. 33, 747-755.

14. Böhmer, U., Kirsten, C., Bley, T., Noack, M., 2010. White-rot fungi combined with lignite granules and lignitic xylite to decolorize textile industry wastewater, Engineering in Life Sciences. 10, 26-34.

15. Butler, E., Devlin, G., Meier, D., McDonnell, K., 2011. A review of recent laboratory research and commercial developments in fast pyrolysis and upgrading, Renewable and Sustainable Energy Reviews. 15, 4171-4186.

16. Capareda, S., Parnell, C., 2007. Fluidized bed gasification of cotton gin trash for liquid fuel production, Proceedings of the Beltwide cotton conferences, New Orleans, Louisiana, 2097-2105.

17. Catcheside, D.E.A., Ralph, J.P., 1999. Biological processing of coal, Appl. Microbiol. Biotechnol. 52, 16-24.

18. Chandel, A.K., Kapoor, R.K., Singh, A., Kuhad, R.C., 2007. Detoxification of sugarcane bagasse hydrolysate improves ethanol production by *Candida shehatae* NCIM 3501, Bioresour. Technol. 98, 1947–1950.

19. Chaudhary, G., Singh, L.K., Ghosh, S., 2012. Alkaline pretreatment methods followed by acid hydrolysis of *Saccharum spontaneum* for bioethanol production, Bioresour. Technol. 124, 111–118.

20. Chen, J., Liu, X., Zheng, J., Zhang, B., Lu, H., Chi, Z., Pan, G., Li, L., Zheng, J., Zhang, X., Wang, J., Yu, X., 2013. Biochar soil amendment increased bacterial but decreased fungal gene abundance with shifts in community structure in a slightly acid rice paddy from Southwest China, Applied Soil Ecology. 71, 33-44.

21. Chen, M., Zhao, J., Xia, L., 2009. Comparison of four different chemical pretreatments of corn stover for enhancing enzymatic digestibility, Biomass Bioenergy. 33, 1381–1385.

22. Chen, Q., Marshall, M.N., Geib, S.M., Tien, M., Richard, T.L., 2012. Effects of laccase on lignin depolymerization and enzymatic hydrolysis of ensiled corn stover, Bioresour. Technol. 117, 186–192.

23. Chen, W., Yu, H., Liu, Y., Chen, P., Zhang, M., Hai, Y., 2011. Individualization of cellulose nanofibers from wood using high-intensity ultrasonication combined with chemical pretreatments, Carbohydr. Polym. 83, 1804–1811.

24. Claus, H., Filip, Z., 1998. Degradation and transformation of aquatic humic substances by laccase-producing fungi *Cladosporium cladosporioides* and *Polyporus versicolor*, Acta Hydrochim. Hydrobiol. 26, 180–185.

25. Corvini, P., Schäffer, A., Schlosser, D., 2006. Microbial degradation of nonylphenol and other alkylphenols—our evolving view, Appl. Microbiol. Biotechnol. 72, 223-243.

26. Costa, S.M., Goncalves, A.R., Esposito, E., 2005. *Ceriporiopsis subvermispota* used in delignification of sugarcane bagasse prior to soda/anthraquinone pulping, Davison, B.H., Evans, B.R., Finkelstein, M., McMillan, J.D. (Eds.), Twenty-Sixth Symposium on Biotechnology for Fuels and Chemicals. Humana Press, pp. 695-706.

27. Couto, S., Toca-Herrera, J., 2006. Lacasses in the textile industry, Biotechnol. Mol. Biol. Rev. 115–120.

28. Deal, C., Brewer, C.E., Brown, R.C., Okure, M.A.E., Amoding, A., 2012. Comparison of kiln-derived and gasifier-derived biochars as soil amendments in the humid tropics, Biomass Bioenergy. 37, 161–168.

29. Dias, A., Sampaio, A., Bezerra, R., 2007. Environmental applications of fungal and plant systems: decolourisation of textile wastewater and related dyestuffs, Singh, S., Tripathi, R. (Eds.), Environmental Bioremediation Technologies. Springer Berlin Heidelberg, pp. 445-463.

30. Dong, X., Ma, L.Q., Zhu, Y., Li, Y., Gu, B., 2013. Mechanistic investigation of mercury sorption by brazilian pepper biochars of different pyrolytic temperatures based on x-ray photoelectron spectroscopy and flow calorimetry, Environ. Sci. Technol. 47, 12156–12164.

31. Eichlerová, I., Homolka, L., Nerud, F., 2007. Decolorization of high concentrations of synthetic dyes by the white rot fungus *Bjerkandera adusta* strain CCBAS 232, Dyes and Pigments. 75, 38-44.

32. Elisashvili, V., Kachlishvili, E., Khardziani, T., Agathos, S., 2010. Effect of aromatic compounds on the production of laccase and manganese peroxidase by white-rot basidiomycetes, J. Ind. Microbiol. Biotechnol. 37, 1091–1096.

33. Elkins, K.M., Nelson, D.J., 2001. Fluorescence and FT-IR spectroscopic studies of Suwannee river fulvic acid complexation with aluminum, terbium and calcium, J. Inorg. Biochem. 87, 81-96.

34. Fakoussa, R.M., Hofrichter, M., 1999. Biotechnology and microbiology of coal degradation, Appl. Microbiol. Biotechnol. 52, 25-40.

35. Ferreira, D., Barros, A., Coimbra, M.A., Delgadillo, I., 2001. Use of FT-IR spectroscopy to follow the effect of processing in cell wall polysaccharide extracts of a sun-dried pear, Carbohydr. Polym. 45, 175–182.

36. Gessa, C., Cabras, M., Micera, G., Polemio, M., Testini, C., 1983. Spectroscopic characterization of extracts from humic and fulvic fractions: IR and1H NMR spectra, Plant Soil. 75, 169–177.

37. Goshadrou, A., Karimi, K., Taherzadeh, M.J., 2011. Bioethanol production from sweet sorghum bagasse by *Mucor hiemalis*, Industrial Crops and Products. 34, 1219–1225.

38. Grimes, J., Carter, T., Godwin, J., 2006 Mar. Use of a litter material made from cotton waste, gypsum, and old newsprint for rearing broiler chickens, Poultry Science. 85, 563-568.

39. Guler, C., Ozen, R., 2004. Some properties of particleboards made from cotton stalks (*Gossypium hirsitum* L.), European Journal of Wood and Wood Products. 62, 40-43.

40. Gutiérrez, A., Rencoret, J., Cadena, E.M., Rico, A., Barth, D., del Río, J.C., Martínez, ÁT., 2012. Demonstration of laccase-based removal of lignin from wood and non-wood plant feedstocks, Bioresour. Technol. 119, 114–122.

41. Hammel, K.E., Cullen, D., 2008. Role of fungal peroxidases in biological ligninolysis, Curr. Opin. Plant Biol. 11, 349-355.

42. Hina, K., Bishop, P., Arbestain, M.C., Calvelo-Pereira, R., Macias-Agulla, J.A., Hindmarsh, J., Hanly, J.A., MacÃas, F., Hedley, M.J., 2010. Producing biochars with enhanced surface activity through alkaline pretreatment of feedstocks, Aust. J. Soil Res. 48, 606-617.

43. Hofrichter, M., Bublitz, F., Fritsche, W., 1997. Fungal attack on coal II. Solubilization of low-rank coal by filamentous fungi, Fuel Process Technol. 52, 55-64.

44. Hofrichter, M., Ziegenhagen, D., Sorge, S., Ullrich, R., Bublitz, F., Fritsche, W., 1999. Degradation of lignite (low-rank coal) by ligninolytic basidiomycetes and their manganese peroxidase system, Appl. Microbiol. Biotechnol. 52, 78-84.

45. Huang, Z., Liers, C., Ullrich, R., Hofrichter, M., Urynowicz, M.A., 2013a. Depolymerization and solubilization of chemically pretreated powder river basin

subbituminous coal by manganese peroxidase (MnP) from *Bjerkandera adusta*, Fuel. 112, 295-301.

46. Huang, Z., Urynowicz, M.A., Colberg, P.J.S., 2013b. Stimulation of biogenic methane generation in coal samples following chemical treatment with potassium permanganate, Fuel. 111, 813-819.

47. Imai, M., Ikari, K., Suzuki, I., 2004. High-performance hydrolysis of cellulose using mixed cellulase species and ultrasonication pretreatment, Biochem. Eng. J. 17, 79-83.

48. Javed, S., Naveed, S., Feroze, N., Zafar, M., Shafaq, M., 2010. Crystal and amorphous silica from KMnO4 treated and untreated rice husk, Journal of quality and technology management. 6,.

49. Jeihanipour, A., Taherzadeh, M.J., 2009. Ethanol production from cotton-based waste textiles, Bioresour. Technol. 100, 1007–1010.

50. Jeoh, T., Agblevor, F.A., 2001. Characterization and fermentation of steam exploded cotton gin waste, Biomass Bioenergy. 21, 109–120.

51. Jiang, F., Li, Z., Lv, Z., Gao, T., Yang, J., Qin, Z., Yuan, H., 2013. The biosolubilization of lignite by *Bacillus sp*. Y7 and characterization of the soluble products, Fuel. 103, 639-645.

52. Joan, R.H., Froilan, L.A., Sergio, C.C., 2007. Activated carbon production from pyrolysis and steam activation of cotton gin trash. Proceedings of the Beltwide cotton conferences, New Orleans, Louisiana, 1494-1499.

53. Jönsson, L.J., Palmqvist, E., Nilvebrant, N.-., Hahn-Hägerdal, B., 1998. Detoxification of wood hydrolysates with laccase and peroxidase from the white-rot fungus *Trametes versicolor*, Appl. Microbiol. Biotechnol. 49, 691-697.

54. Jurado, M., Prieto, A., Martínez-Alcalá, Á, Martínez, ÁT., Martínez, M.J., 2009. Laccase detoxification of steam-exploded wheat straw for second generation bioethanol, Bioresour. Technol. 100, 6378-6384.

55. Kaal, J., Martínez Cortizas, A., Reyes, O., Soliño, M., 2012. Molecular characterization of Ulex europaeus biochar obtained from laboratory heat treatment experiments – A pyrolysis–GC/MS study, J. Anal. Appl. Pyrolysis. 95, 205-212.

56. Kantarelis, E., Zabaniotou, A., 2009. Valorization of cotton stalks by fast pyrolysis and fixed bed air gasification for syngas production as precursor of second generation biofuels and sustainable agriculture, Bioresour. Technol. 100, 942-947.

57. Karatas, H., Olgun, H., Akgun, F., 2013. Experimental results of gasification of cotton stalk and hazelnut shell in a bubbling fluidized bed gasifier under air and steam atmospheres, Fuel. 112, 494-501.

58. Kaur, U., Oberoi, H.S., Bhargav, V.K., Sharma-Shivappa, R., Dhaliwal, S.S., 2012. Ethanol production from alkali- and ozone-treated cotton stalks using thermotolerant *Pichia kudriavzevii* HOP–1, Industrial Crops and Products. 37, 219-226.

59. Khindaria, A., Yamazaki, I., Aust, S.D., 1996. Stabilization of the veratryl alcohol cation radical by lignin peroxidase, Biochemistry (N. Y.). 35, 6418-6424.

60. Kim, I., Han, J., 2012. Optimization of alkaline pretreatment conditions for enhancing glucose yield of rice straw by response surface methodology, Biomass Bioenergy. 46, 210-217.

61. Kirby, N., Marchant, R., McMullan, G., 2000. Decolourisation of synthetic textile dyes by *Phlebia tremellosa*, FEMS Microbiol. Lett. 188, 93-96.

62. Klasson, K.T., Wartelle, L.H., Lima, I.M., Marshall, W.E., Akin, D.E., 2009. Activated carbons from flax shive and cotton gin waste as environmental adsorbents for the chlorinated hydrocarbon trichloroethylene, Bioresour. Technol. 100, 5045-5050.

63. Kolb, M., Sieber, V., Amann, M., Faulstich, M., Schieder, D., 2012. Removal of monomer delignification products by laccase from *Trametes versicolor*, Bioresour. Technol. 104, 298-304.

64. Krasznai, D.J., Champagne, P., Cunningham, M.F., 2012. Quantitative characterization of lignocellulosic biomass using surrogate mixtures and multivariate techniques, Bioresour. Technol. 110, 652-661.

65. Kuwata, K., Saito, Y., Shida, S., Ohta, M., 2009. Intercalation of wood charcoal with sulfuric acid, Journal of Wood Science. 55, 154–158.

66. Larsson, S., Reimann, A., Nilvebrant, N., Jönsson, L., 1999. Comparison of different methods for the detoxification of lignocellulose hydrolyzates of spruce, Appl. Biochem. Biotechnol. 77, 91–103.

67. Laser, M., Schulman, D., Allen, S.G., Lichwa, J., Antal Jr., M.J., Lynd, L.R., 2002. A comparison of liquid hot water and steam pretreatments of sugar cane bagasse for bioconversion to ethanol, Bioresour. Technol. 81, 33-44.

68. Lee, J.M., Jameel, H., Venditti, R.A., 2010. A comparison of the autohydrolysis and ammonia fiber explosion (AFEX) pretreatments on the subsequent enzymatic hydrolysis of coastal Bermuda grass, Bioresour. Technol. 101, 5449-5458.

69. Leibbrandt, N.H., Aboyade, A.O., Knoetze, J.H., Görgens, J.F., 2013. Process efficiency of biofuel production via gasification and Fischer–Tropsch synthesis, Fuel. 109, 484-492.

70. Li, L., Li, X.-., Tang, W.-., Zhao, J., Qu, Y.-., 2008. Screening of a fungus capable of powerful and selective delignification on wheat straw, Lett. Appl. Microbiol. 47, 415-420.

71. Li, Y., Wang, X., Zhu, Y., Wang, L., Wang, Z., 2012. In situ preparation of biochar coated silica material from rice husk, Colloids Surf. Physicochem. Eng. Aspects. 395, 157–160.

72. Lin, Y., Munroe, P., Joseph, S., Henderson, R., Ziolkowski, A., 2012. Water extractable organic carbon in untreated and chemical treated biochars, Chemosphere. 87, 151–157.

73. Lu, C., Wang, H., Luo, Y., Guo, L., 2010. An efficient system for pre-delignification of gramineous biofuel feedstock in vitro: Application of a laccase from *Pycnoporus sanguineus* H275, Process Biochemistry. 45, 1141–1147.

74. M. A. Macias-Corral, Z. A. Samani, A. T. Hanson, R. DelaVega, P. A. Funk, 2005. Producing energy and soil amendment from dairy manure and cotton gin waste, Transactions of the ASAE. 48, 1521–1526.

75. Maglinao Jr., A.L., Capareda, S.C., 2010. Development of computer control system for the pilot scale fluidized bed biomass gasification system, American Society of Agricultural and Biological Engineers Annual International Meeting 2010. 7, 5733-5747.

76. Maglinao, A.L., Capareda, S.C., 2008. Operation of the TAMU fluidized bed gasifier using different biomass feedstock, American Society of Agricultural and Biological Engineers Annual International Meeting 2008. 11, 6734-6743.

77. Maiti, S., Purakayastha, S., Ghosh, B., 2007. Production of low-cost carbon adsorbents from agricultural wastes and their impact on dye adsorption, Chem. Eng. Commun. 195, 386-403.

78. Martin, H., 2002. Review: lignin conversion by manganese peroxidase (MnP), Enzyme Microb. Technol. 30, 454-466.

79. Martín-Sampedro, R., Eugenio, M.E., Carbajo, J.M., Villar, J.C., 2011. Combination of steam explosion and laccase-mediator treatments prior to *Eucalyptus globulus* kraft pulping, Bioresour. Technol. 102, 7183-7189.

80. Martín-Sampedro, R., Eugenio, M.E., Villar, J.C., 2012. Effect of steam explosion and enzymatic pre-treatments on pulping and bleaching of *Hesperaloe funifera*, Bioresour. Technol. 111, 460-467.

81. Martín, C., Galbe, M., Wahlbom, C.F., Hahn-Hägerdal, B., Jönsson, L.J., 2002. Ethanol production from enzymatic hydrolysates of sugarcane bagasse using recombinant xylose-utilising *Saccharomyces cerevisiae*, Enzyme Microb. Technol. 31, 274-282.

82. Mattinen, M., Maijala, P., Nousiainen, P., Smeds, A., Kontro, J., Sipilä, J., Tamminen, T., Willför, S., Viikari, L., 2011. Oxidation of lignans and lignin model compounds by laccase in aqueous solvent systems, J Molec Catal B. 72, 122–129.

83. Medina, F., Aguila, S., Baratto, M.C., Martorana, A., Basosi, R., Alderete, J.B., Vazquez-Duhalt, R., 2013. Prediction model based on decision tree analysis for laccase mediators, Enzyme Microb. Technol. 52, 68-76.

84. Mohorčič, M., Teodorovič, S., Golob, V., Friedrich, J., 2006. Fungal and enzymatic decolourisation of artificial textile dye baths, Chemosphere. 63, 1709–1717.

85. Monti, F., Dell'Anna, R., Sanson, A., Fasoli, M., Pezzotti, M., Zenoni, S., 2013. A multivariate statistical analysis approach to highlight molecular processes in plant cell walls through ATR FT-IR microspectroscopy: The role of the α-expansin PhEXPA1 in Petunia hybrida, Vibrational Spectroscopy. 65, 36-43.

86. Moreno, A.D., Ibarra, D., Fernández, J.L., Ballesteros, M., 2012. Different laccase detoxification strategies for ethanol production from lignocellulosic biomass by the thermotolerant yeast *Kluyveromyces marxianus* CECT 10875, Bioresour. Technol. 106, 101–109.

87. Mukome, F.N.D., Six, J., Parikh, S.J., 2013. The effects of walnut shell and wood feedstock biochar amendments on greenhouse gas emissions from a fertile soil, Geoderma. 200–201, 90-98.

88. Nigam, P., Gupta, N., Anthwal, A., 2009. Pre-treatment of Agro-Industrial Residues, Nigam, P., Pandey, A. (Eds.), Biotechnology for Agro-Industrial Residues Utilisation. Springer Netherlands, pp. 13-33.

89. Oboirien, B.O., Ojumu, T.V., Obayopo, S.O., 2013. Fungi solubilisation of low rank coal: Performances of stirred tank, fluidised bed and packed bed reactors, Fuel Process Technol. 106, 295-302.

90. Olofsson, K., Rudolf, A., Lidén, G., 2008. Designing simultaneous saccharification and fermentation for improved xylose conversion by a recombinant strain of *Saccharomyces cerevisiae*, J. Biotechnol. 134, 112–120.

91. Palmqvist, E., Hahn-Hägerdal, B., 2000. Fermentation of lignocellulosic hydrolysates. I: inhibition and detoxification, Bioresour. Technol. 74, 17-24.

92. Park, J., Hung, I., Gan, Z., Rojas, O.J., Lim, K.H., Park, S., 2013. Activated carbon from biochar: Influence of its physicochemical properties on the sorption characteristics of phenanthrene, Bioresour. Technol. 149, 383-389.

93. Peuravuori, J., Pihlaja, K., 1997. Molecular size distribution and spectroscopic properties of aquatic humic substances, Anal. Chim. Acta. 337, 133–149.

94. Philippoussis, A., Zervakis, G., Diamantopoulou, P., 2001. Bioconversion of agricultural lignocellulosic wastes through the cultivation of the edible mushrooms *Agrocybe aegerita, Volvariella volvacea and Pleurotus spp*. World Journal of Microbiology and Biotechnology. 17, 191-200.

95. Piontek, K., Glumoff, T., Winterhalter, K., 1993. Low pH crystal structure of glycosylated lignin peroxidase from *Phanerochaete chrysosporium* at 2.5 Å resolution, FEBS Lett. 315, 119–124.

96. Plácido, J., Imam, T., Capareda, S., 2013. Evaluation of ligninolytic enzymes, ultrasonication and liquid hot water as pretreatments for bioethanol production from cotton gin trash, Bioresour. Technol. 139, 203-208.

97. Popescu, M., Simionescu, B.C., 2012. Multivariate statistical analysis of mid-infrared spectra for a G1 allyl-terminated carbosilane dendrimer, Spectrochimica Acta Part A: Molecular and Biomolecular Spectroscopy. 92, 398-405.

98. Pütün, A.E., Özbay, N., Önal, E.P., Pütün, E., 2005. Fixed-bed pyrolysis of cotton stalk for liquid and solid products, Fuel Process Technol. 86, 1207–1219.

99. Qiu, W., Chen, H., 2012. Enhanced the enzymatic hydrolysis efficiency of wheat straw after combined steam explosion and laccase pretreatment, Bioresour. Technol. 118, 8–12.

100. Quigley, D.R., Wey, J.E., Breckenridge, C.R., Stoner, D.L., 1988. The influence of pH on biological solubulization of oxidized, low-rank coal, Resour. Conserv. Recycling. 1, 163–174.

101. Ralph, J.P., Catcheside, D.E.A., 1994. Decolourisation and depolymerisation of solubilised low-rank coal by the white-rot basidiomycete *Phanerochaete chrysosporium*, Appl. Microbiol. Biotechnol. 42, 536-542.

102. Reig, F.B., Adelantado, J.V.G., Moya Moreno, M.C.M., 2002. FTIR quantitative analysis of calcium carbonate (calcite) and silica (quartz) mixtures using the constant ratio method. Application to geological samples, Talanta. 58, 811-821.

103. Robinson, T., Chandran, B., Nigam, P., 2001. Studies on the production of enzymes by white-rot fungi for the decolourisation of textile dyes, Enzyme Microb. Technol. 29, 575-579.

104. Rodrigues, M.A.M., Pinto, P., Bezerra, R.M.F., Dias, A.A., Guedes, C.V.M., Cardoso, V.M.G., Cone, J.W., Ferreira, L.M.M., Colaço, J., Sequeira, C.A., 2008. Effect of enzyme extracts isolated from white-rot fungi on chemical composition and in vitro digestibility of wheat straw, Anim. Feed Sci. Technol. 141, 326-338.

105. Rogers, G.M., Poore, M.H., Paschal, J.C., 2002. Feeding cotton products to cattle, Veterinary Clinics of North America: Food Animal Practice. 18, 267-294.

106. Russo, M.E., Di Natale, F., Prigione, V., Tigini, V., Marzocchella, A., Varese, G.C., 2010. Adsorption of acid dyes on fungal biomass: Equilibrium and kinetics characterization, Chem. Eng. J. 162, 537-545.

107. Ruttimann-Johnson, C., Salas, L., Vicuna, R., Kirk, T.K., 1993. Extracellular enzyme production and synthetic lignin mineralization by *Ceriporiopsis subvermispora*, Appl. Environ. Microbiol. 59, 1792–1797.

108. Sadaka, S., Sharara, M.A., Ashworth, A., Keyser, P., Allen, F., Wright, A., 2014. Characterization of biochar from switchgrass carbonization, Energies. 7, 548-567.

109. Sadaka, S., 2013. Gasification of raw and torrefied cotton gin wastes in an auger system, Appl. Eng. Agric. 29, 405-414.

110. Salvachúa, D., Prieto, A., López-Abelairas, M., Lu-Chau, T., Martínez, ÁT., Martínez, M.J., 2011. Fungal pretreatment: An alternative in second-generation ethanol from wheat straw, Bioresour. Technol. 102, 7500-7506.

111. Sarkar, N., Ghosh, S.K., Bannerjee, S., Aikat, K., 2012. Bioethanol production from agricultural wastes: An overview, Renewable Energy. 37, 19-27.

112. Selvi, A.V., Banerjee, R., Ram, L.C., Singh, G., 2009. Biodepolymerization studies of low rank Indian coals, World Journal of Microbiology and Biotechnology. 25, 1713–1720.

113. Semenova, Z.V., Kushnarev, D.F., Litvintseva, M.A., Rokhin, A.V., 2007. Humic acids from the sapropel of Lake Ochaul, Solid Fuel Chemistry. 41, 129–133.

114. Sergio, R., 2006. Laccases: blue enzymes for green chemistry, Trends Biotechnol. 24, 219-226.

115. Sharma-Shivappa, R.R., Chen, Y., 2008. Conversion of cotton wastes to bioenergy and value-added products, Transactions of the ASABE. 51, 2239-2246.

116. Shen, J., Agblevor, F., 2011. Ethanol production of semi-simultaneous saccharification and fermentation from mixture of cotton gin waste and recycled paper sludge, Bioprocess and Biosystems Engineering. 34, 33-43.

117. Shen, J., Agblevor, F.A., 2008a. Kinetics of enzymatic hydrolysis of steam-exploded cotton gin waste, Chem. Eng. Commun. 195, 1107–1121.

118. Shen, J., Agblevor, F.A., 2008b. Optimization of enzyme loading and hydrolytic time in the hydrolysis of mixtures of cotton gin waste and recycled paper sludge for the maximum profit rate, Biochem. Eng. J. 41, 241-250.

119. Shen, Y., Zhao, P., Shao, Q., 2014. Porous silica and carbon derived materials from rice husk pyrolysis char, Microporous and Mesoporous Materials. 188, 46-76.

120. Shi, J., Chinn, M.S., Sharma-Shivappa, R.R., 2008. Microbial pretreatment of cotton stalks by solid state cultivation of *Phanerochaete chrysosporium*, Bioresour. Technol. 99, 6556-6564.

121. Shi, J., Sharma-Shivappa, R.R., Chinn, M., Howell, N., 2009. Effect of microbial pretreatment on enzymatic hydrolysis and fermentation of cotton stalks for ethanol production, Biomass Bioenergy. 33, 88-96.

122. Silverstein, R.A., Chen, Y., Sharma-Shivappa, R.R., Boyette, M.D., Osborne, J., 2007. A comparison of chemical pretreatment methods for improving saccharification of cotton stalks, Bioresour. Technol. 98, 3000-3011.

123. Sissine, F., 2007. Energy Independence and Security Act of 2007: A summary of major provisions, 2011, https://wiki.umn.edu/pub/ESPM3241W/S09TopicSummaryTeamFourteen/CRS_Report_for_Congress.pdf.

124. Sluiter, A., Hames, B., Ruiz, R., Scarlata, C., Sluiter, J., Templeton, D., and Crocker, D., 2011. Determination of structural carbohydrates and lignin in biomass, technical report. National Renewable Energy Laboratory/TP-510-42618. 2011, 15.

125. Smith, J.W., Tollner, E.W., Eiteman, M.A., 1999. Microbial gum formation from the decomposition of cotton gin trash, Bioresour. Technol. 69, 215-222.

126. Sundaramoorthy, M., Kishi, K., Gold, M.H., Poulos, T.L., 1994. The crystal structure of manganese peroxidase from *Phanerochaete chrysosporium* at 2.06-A resolution. Journal of Biological Chemistry. 269, 32759-32767.

127. Tan, Y.H., Wahab, M.N., 1997. Extracellular enzyme production during anamorphic growth in the edible mushroom, *Pleurotus sajor-caju*, World Journal of Microbiology and Biotechnology. 13, 613-617.

128. Tanaka, H., Koike, K., Itakura, S., Enoki, A., 2009. Degradation of wood and enzyme production by *Ceriporiopsis subvermispora*, Enzyme Microb. Technol. 45, 384-390.

129. Timofeevna Shirshova, L., Ghabbour, E.A., Davies, G., 2006. Spectroscopic characterization of humic acid fractions isolated from soil using different extraction procedures, Geoderma. 133, 204-216.

130. USDA, 2008. Crop production Report 2007 summary, http://www.usda.gov/nass/PUBS/TODAYRPT/crop1113.pdf. Visited in 2011,.

131. Uyguner, C.S., Bekbolet, M., 2005. Evaluation of humic acid photocatalytic degradation by UV-vis and fluorescence spectroscopy, Catalysis Today. 101, 267-274.

132. Velmurugan, R., Muthukumar, K., 2012. Sono-assisted enzymatic saccharification of sugarcane bagasse for bioethanol production, Biochem. Eng. J. 63, 1-9.

133. Vivekanand, V., Dwivedi, P., Sharma, A., Sabharwal, N., Singh, R., 2008. Enhanced delignification of mixed wood pulp by *Aspergillus fumigatus* laccase mediator system, World Journal of Microbiology and Biotechnology. 24, 2799-2804.

134. Wan, C., Li, Y., 2010. Microbial delignification of corn stover by *Ceriporiopsis subvermispora* for improving cellulose digestibility, Enzyme Microb. Technol. 47, 31-36.

135. Wan, C., Li, Y., 2011. Effectiveness of microbial pretreatment by *Ceriporiopsis subvermispora* on different biomass feedstocks, Bioresour. Technol. 102, 7507-7512.

136. Wang, Z., C. Pant, B., H. Langford, C., 1990. Spectroscopic and structural characterization of a Laurentian fulvic acid: notes on the origin of the color, Anal. Chim. Acta. 232, 43-49.

137. Wei, D., Houtman, C.J., Kapich, A.N., Hunt, C.G., Cullen, D., Hammel, K.E., 2010. Lacease and its role in production of extracellular reactive oxygen species during wood decay by the brown rot basidiomycete *Postia placenta*, Appl. Environ. Microbiol. 76, 2091-2097.

138. White, D.H., Coates, W.E., Wolf, D., 1996. Conversion of cotton plant and cotton gin residues to fuels by the extruder 'feeder liquefaction process, Bioresour. Technol. 56, 117–123.

139. Willmann, G., Fakoussa, R., 1997. Extracellular oxidative enzymes of coal-attacking fungi, Fuel Process Technol. 52, 27-41.

140. Wolfe, A.P., Tappert, R., Muehlenbachs, K., Boudreau, M., McKellar, R.C., Basinger, J.F., Garrett, A., 2009. A new proposal concerning the botanical origin of Baltic amber, Proceedings of the Royal Society B: Biological Sciences. 276, 3403-3412.

141. Wu, W., Yang, M., Feng, Q., McGrouther, K., Wang, H., Lu, H., Chen, Y., 2012. Chemical characterization of rice straw-derived biochar for soil amendment, Biomass Bioenergy. 47, 268-276.

142. Xu, R., Xiao, S., Yuan, J., Zhao, A., 2011. Adsorption of methyl violet from aqueous solutions by the biochars derived from crop residues, Bioresour. Technol. 102, 10293–10298.

143. Yu, J.T., Dehkhoda, A.M., Ellis, N., 2011. Development of biochar-based catalyst for transesterification of canola oil, Energy and Fuels. 25, 337-344.

144. Yuan, J., Xu, R., Zhang, H., 2011. The forms of alkalis in the biochar produced from crop residues at different temperatures, Bioresour. Technol. 102, 3488-3497.

145. Zabaniotou, A.A., Roussos, A.I., Koroneos, C.J., 2000. A laboratory study of cotton gin waste pyrolysis, J. Anal. Appl. Pyrolysis. 56, 47-59.

146. Zervakis, G., Philippoussis, A., Ioannidou, S., Diamantopoulou, P., 2001. Mycelium growth kinetics and optimal temperature conditions for the cultivation of edible mushroom species on lignocellulosic substrates, Folia Microbiol. (Praha). 46, 231-234.

147. Ziegenhagen, D., Hofrichter, M., 1998. Degradation of humic acids by manganese peroxidase from the white-rot fungus *Clitocybula dusenii*, J. Basic Microbiol. 38, 289-299.

148. Zouari-Mechichi, H., Mechichi, T., Dhouib, A., Sayadi, S., Martínez, A.T., Martínez, M.J., 2006. Laccase purification and characterization from *Trametes trogii*

isolated in Tunisia: decolorization of textile dyes by the purified enzyme, Enzyme Microb. Technol. 39, 141–148.